



---

# Transport of Ions Through Clays of the Peize and Waalre Formation

*MASTER OF SCIENCE THESIS*

---

*Author*

Beer van Esser

*Under the supervision of*

Dr. P.J. (Phil) Vardon

Dr. E.A.C. (Erika) Neeft

Dr. A.A.M. (Anne-Catherine) Dieudonné

Dr. H.A. (Hemmo) Abels

DEPARTMENT OF GEOSCIENCE AND ENGINEERING

Publicly defended the 15th of July, 2022

Copyright 2022 TU Delft & COVRA NV

## Abstract

High-level waste can be radiotoxic for thousands of years and should be carefully handled to prevent accidents. The research for geological disposal of radioactive waste focuses on the construction and durability of a geologic disposal facility in Dutch clays or salts. One of the challenges is assessing these host rocks' capability to retard radionuclides and prevent them from entering the biosphere. This research focuses on disposal in clay. Because of clay's low permeability, water movements are slow, and radionuclides transport is expected to occur predominantly by diffusion. The Peize and Waalre formations, situated on the interface between brackish and salt groundwater, serve as a natural analogue for targeted deeper, poorly indurated host rocks. The known disparity in chlorine levels between the aquifers adjacent to these clays qualify these formations for *NaCl*-tracer research. A cutting sampling study determined the conductivity of these clays' porewater. Combining this with a one-dimensional modelling study, the saline history of this formation has been simulated. *NaCl* gradients were demonstrated at different drilling locations. The most manifested gradient is attempted to fit in the one-dimensional model. The model results suggest that this gradient originates from adjacent aquifer salinity, the clays' physical properties and the difference in hydraulic head. The observed salinity discrepancy between aquifers and ion concentration gradient in the first Waalre Clay confirm the assumption that the member can be a natural analogue. Uncertainty on the continuity of the total system prohibits concluding that diffusion-dominated transport in Dutch poorly indurated clays can be assumed. The best fitting scenario this research found fitting the empirical Waalre clay salinity curve is combined transport by diffusion and advection. The finding of diffusion-advection transport implies that the Waalre clay shows more complexity than initially expected.

## Preface

While writing this thesis the relevance of research into nuclear waste disposal was emphasised again. A devastating war in Ukraine resulted in a European energy crisis reviving a decades old discussion on nuclear energy and the accompanying waste. Providing Europe's people and policymakers with solid, trustworthy and unbiased data on the options for nuclear waste disposal is key to having this discussion with an open mind. Independent of the outcome of that debate the currently stored waste is awaiting long-term disposal. The people I got to know during this eight month thesis firmly established my trust in this process.

First and foremost I want to thank Erika for her contribution to this research. Your devotion, patience and kindness made me feel free to ask any question. I'd like to thank you, Phil, for your support and guidance through this project, your experience shielded me from a lot of mistakes. Anne-Catherine, I'd like to thank you for the abundance of ideas you put up to help my research. Unfortunately I was not able to work them all out. Hemmo, your feedback was most straightforward which certainly led to a better and more academic report, I am grateful for that. Thanks to all four for your elaborate feedback and the time you took to steer this research in the right direction. The frequent meetings we had were energising and it felt great to be backed by so much knowledge.

I'd like to thank COVRA for the opportunity to be part of their research team for eight months. I've felt welcome the first time I walked in and the company's people, goals, and impressive location left a lasting impression. Thank you for allowing me to present my work at the annual EURAD conference and introducing me there. I'd like to express my gratitude to the people at RCSG, Frank, thank you for your enthusiasm and helping me initiate my research. Drillers Wessel, Johan and Wiese, you really enhanced my graduation experience by showing me around at the drilling rig and contributed to the research by taking the push core. I'd like to thank Mark for inviting me to the drilling site in Rotterdam which proved to contain the most valuable cuttings. I'm thankful that at the Delft location Pieter was so welcoming and bettered my understanding of the sampling process.

Starting at Mechanical Engineering led me to Delft, Mijnbouw thereafter proved to be a better fit as it showed me a field in which I experience great interest. I have always felt supported by my parents and brother to choose my own way. Attempting to become a TU Delft graduate proved to be a nine-year undertaking on which I look back in great joy. The friends I made at the Oude Delft are for a lifetime and make me want to do it all over again.

Beer van Esser  
30th June 2022, Delft

# Contents

Abstract . . . . .	ii
Preface . . . . .	iii
List of Figures . . . . .	vii
List of Tables . . . . .	viii
<b>1 Introduction and Problem Description</b>	<b>1</b>
1.1 Research Question . . . . .	3
1.2 Sub-Questions . . . . .	3
<b>2 Literature and Knowledge</b>	<b>4</b>
2.1 Deep Geological Disposal . . . . .	4
2.2 Transport Processes . . . . .	5
2.2.1 Diffusion . . . . .	5
2.2.2 Advection . . . . .	7
2.3 Geology . . . . .	7
2.3.1 Geology of the Netherlands . . . . .	7
2.3.2 Rupel formation . . . . .	7
2.3.3 Peize and Waalre Formations . . . . .	9
2.3.4 Present subsurface models . . . . .	10
2.3.5 Geochemistry and hydrogeology . . . . .	11
2.3.6 Sea level . . . . .	13
2.3.7 Sampling locations . . . . .	14
2.4 Drill Cuttings . . . . .	14
2.4.1 Jet drilling . . . . .	15
2.4.2 Suction drilling . . . . .	15
2.5 Natural Analogues . . . . .	15
<b>3 Hydrogeology Analyses</b>	<b>18</b>
3.1 Methodology . . . . .	18
3.1.1 Locations and collection . . . . .	19

3.1.2	Storage . . . . .	20
3.1.3	Preparation . . . . .	21
3.1.4	Conductivity . . . . .	21
3.2	Results . . . . .	23
3.2.1	Rijswijk . . . . .	23
3.2.2	Rotterdam . . . . .	24
3.2.3	Delft . . . . .	26
3.2.4	Results interpretation . . . . .	26
<b>4</b>	<b>Model</b>	<b>30</b>
4.1	Methodology . . . . .	30
4.1.1	Modelling method . . . . .	30
4.1.2	Base model . . . . .	30
4.1.3	Boundary conditions and input values . . . . .	31
4.1.4	Model variances . . . . .	31
4.1.5	Bottom salt concentration . . . . .	32
4.1.6	Vertical advection . . . . .	33
4.1.7	Diffusion coefficient . . . . .	34
4.1.8	Scenario study . . . . .	34
4.1.9	Lab-testing diffusion coefficient and sensitivity study . . . . .	35
4.2	Results . . . . .	38
4.2.1	Base model results . . . . .	38
4.2.2	Bottom salt concentration . . . . .	38
4.2.3	Vertical advection . . . . .	39
4.2.4	Diffusion coefficient . . . . .	40
4.2.5	Scenario study . . . . .	40
4.2.6	Model Results Interpretation . . . . .	42
<b>5</b>	<b>Discussion</b>	<b>44</b>
5.1	Hydrogeology Analysis . . . . .	44
5.1.1	Continuity . . . . .	44

5.1.2	Location differences . . . . .	45
5.1.3	Data acquisition . . . . .	46
5.1.4	Laboratory observations . . . . .	46
5.1.5	Data possibilities . . . . .	47
5.1.6	Conductivity sample handling . . . . .	48
5.1.7	pXRF . . . . .	48
5.2	Hydrogeology Modelling . . . . .	49
5.3	Research Footprint . . . . .	50
<b>6</b>	<b>Conclusions and Outlook</b>	<b>51</b>
6.1	Research Question . . . . .	51
6.2	Sub-questions . . . . .	52
6.3	Outlook . . . . .	54
	<b>Appendix</b>	<b>60</b>
	<b>A Graphs</b>	<b>60</b>
	<b>B Images</b>	<b>65</b>
	<b>C Data</b>	<b>67</b>
	<b>D Code</b>	<b>73</b>

# List of Figures

1	Artist impression of a GDF in the Netherlands (Verhoef et al., 2020) . . .	4
2	Formations of interest in red squares - Timescale not linear - (TNO, 2019)	8
3	Left: thickness of Boom clay and faulting   right: top-depth of Boom clay (Vis & Verweij, 2014) . . . . .	9
4	Lower Pleistocene fluvial sediments showing interfingering Eridanos and Rhine-Meuse sediments (Somsen, 2015) . . . . .	10
5	Eridanos prograding environment towards Northwest during middle Quaternary (Knox et al., 2010) . . . . .	12
6	Cyclicality of global sea level according to NOAA (2016) . . . . .	13
7	Suction drilling with drag-drill bit (Smet Group, 2022) . . . . .	14
8	Jet drilling with PDC-bit (Smet Group, 2022) . . . . .	14
9	Expected interface between brackish and salt groundwater (TNO DINOloket, 2022) . . . . .	16
10	Process diagram, Table 3 links to the steps respective sections . . . . .	18
11	Locations of sampling listed in Table 4 . . . . .	19
12	REGIS II V2.2 model formation continuity (TNO DINOloket, 2022) . . .	19
13	Obtained values for the Rijswijk samples . . . . .	24
14	Obtained values Rotterdam samples with numbered Waalre clays (WC#)	25
15	Obtained values for the Delft samples . . . . .	27
16	Calculated sample porosity per site . . . . .	28
17	Electrical conductivity of laboratory pore water   <i>Please note different x-axis scales</i> . . . . .	29
18	Peize Sand 1 fluctuating NaCl concentration over 1Ma . . . . .	33
19	Lab setup modelled . . . . .	36
20	Result and sensitivity . . . . .	37
21	Model porewater conductivity   Total time 1My, showing five moments in time   Waalre clay 1 (WC1) aquitard between Kreftenheye (KH) and Peize Sand 1 (PS1)   $D_c = 7.5E-12 \text{ m}^2/\text{s}$ , no advection, no sea level cycle . . . .	38
22	Model porewater conductivity   Total time 1My, showing four moments in time   Waalre clay 1 (WC1) aquitard between Kreftenheye (KH) and Peize Sand 1 (PS1)   $D_c = 7.5E-12 \text{ m}^2/\text{s}$ , no advection, including sea level cycle from Table 7 . . . . .	39

23	WC1 base model (Figure 21) + advection . . . . .	40
24	WC1 base model (Figure 21) with varying $D_c$ . . . . .	40
25	Laboratory conductivity measurements including fit compared to scenario R	41
26	Laboratory conductivity measurements including fit compared to best fitting model . . . . .	42
27	Rotterdam samples increase of conductivity over 2months time . . . . .	48
A.1	Rijswijk conductivity with focus on first drilling session with tapwater as drilling fluid . . . . .	60
B.1	RCSG facilities . . . . .	65
B.2	Push core used at the RCSG location . . . . .	66
B.3	Sample bin in Rotterdam showing big clay lumbs . . . . .	66
D.1	code to plot Figure 18 . . . . .	73

## List of Tables

1	Ion conductivity (Vanýsek, 2012) . . . . .	5
2	Water type qualification according to thresholds set up by the TNO GDN (2022) . . . . .	13
3	Sections linked to Figure 10 . . . . .	18
4	Sampled locations . . . . .	19
5	RCSG batches . . . . .	20
6	Base model boundary conditions and input . . . . .	31
7	WC1 bottom concentration sinusoid . . . . .	32
8	Minimum and maximum values Rotterdam WC1 Darcy’s law . . . . .	33
9	Model input values advection . . . . .	33
10	Correlation scenarios . . . . .	35
11	Diffusion coefficient lab model dimensions . . . . .	36
12	Model dimensions that achieve best fit on laboratory measurements . . . . .	42
13	Material consumption and waste mitigation . . . . .	50



# 1 Introduction and Problem Description

Hospitals, nuclear power plants, industry, and research organisations produce radioactive waste. High-level waste can be radiotoxic for thousands of years and should be carefully handled to prevent any accidents, now or in the future (Alexander et al., 2015). In every European country, an institute or government agency is investigating or executing the final disposal of this waste. In the Netherlands, COVRA is responsible for collecting, processing, storage and long-term disposal of radioactive waste (Schultz van Haegen, 2017). It's Long-term Research Programme for geological disposal of radioactive waste focuses on the construction and durability of a geologic disposal facility (GDF) in Dutch clays or salts. For this particular research, the focus is on the potential of clay as host rock for waste disposal. As part of this long-term research programme, Verhoef et al. (2020) have outlined the work to be done, including the core of this research: "Task 4A.2 Diffusion-dominated transport in poorly indurated clays".

Spent reactor fuel and vitrified waste classify as High-Level radioactive waste (HLW) due to their high longevity and radiotoxicity. HLW will be encapsulated in super containers designed to contain the waste for thousands of years. Despite these precautions, it is expected that some radionuclides will leak from degrading waste packages into the surrounding natural clay barrier after tens of thousands of years (Verhoef et al., 2017). That clay barrier, e.g., Paleogene clays, was deposited millions of years ago and will exist for millions to come (Griffioen, 2015). Radiotoxicity levels must stay below limits to ensure the safety of a deep geologic disposal facility is accepted. One of the challenges is to assess the capability of these host rocks to retard radionuclides (Mazurek et al., 2008). If a formation cannot contain radionuclides nor prevent significant contamination of the biosphere, it is not suited to be a host rock. Natural analogues are a method to gather information on a system that cannot be directly addressed in a laboratory or model. The key factors here are the heterogeneity and complexity of natural systems and, in particular, the vast dimensions and long timescales over which safety must be assured (NAWG, 2021). Natural tracer studies offer such understanding.

Tracers offer unique possibilities for analysing flow and transport processes over large scales of time and space (Gimmi, 2010). (Isotope) tracers considered by most research are halogens ( $Cl^-$ ,  $Br^-$ ,  $I^-$ ,  $\delta^{37}Cl$ ), water isotopes and noble gases ( $He$ ,  $^3He/^4He$ ,  $Ar$ , etc.) (Mazurek et al., 2009). These tracers are considered because they do not sorb on mineral surfaces, do not undergo chemical reactions with minerals and do not fractionate into the liquid phase. Borehole data from research sites, e.g. Mont Terri in Switzerland, show that chlorine, in formation pore-waters, displays smooth, regular profiles with depth (Alexander et al., 2015). The CLAYTRAC project, conducted specifically to ensure the long-term safety of deep geologic disposal, by Mazurek et al. (2009) combines results of several tracer studies that indicate diffusion-dominated transport processes through clay formations. Gimmi and Waber (2004) show that formations as Malm, Keuper, Muschelkalk and Bundsandstein show diffusion-dominated transport.

Because of clay's low permeability, water movements are slow, Verhoef et al. (2020) expect transport of radionuclides to take place predominantly by diffusion. However, there is insufficient evidence for diffusion-dominated transport for poorly hardened clays

in the Netherlands. For every geologic disposal facility, the safety case needs to assure people that their models can adequately predict the long-term behaviour of its repository. Targeted Dutch clays at a suitable depth, such as the Boom clay, are known to be confined in saline aquifers. Therefore, it is impossible to assess the diffusion by natural tracer chlorine. There are poorly indurated clays at shallower depths, the Peize and Waalre formations, situated on the interface between brackish and salt groundwater (TNO GDN, 2022). These clays are known to have experienced little mineralogical alteration since deposition which contributes to their potential to be a natural analogue. This research focuses on the pore-water ion concentration of these two fluvial sediments present in the West-Netherlands (TNO DINOloket, 2022).

The known disparity in chlorine levels between the aquifers confining these poorly indurated clays qualify these formations for tracer research. Salts dissolved in the pore-water migrate through the clays via diffusion and other transport processes such as advection. This research will attempt to measure a chloride gradient, if present, and investigate what its origin is. This is summarised in the research question: *Is there an ion concentration gradient in the Peize-Waalre Formation that confirms the assumption that transport of radionuclides in poorly indurated clays in the Netherlands takes place predominantly by diffusion?*

To answer the research question, there are several topics to address. The actual concentration gradient needs to be demonstrated. Literature could show whether this ion concentration gradient could originate from other mechanisms than diffusion. The location and properties indicate a good chance that the Peize and Waalre formation can be a natural analogue for radionuclide retardation in clays. A decision will be made on the comparability between the targeted host rock and these shallower, poorly indurated Dutch clays by thoroughly investigating its characteristics. To present a broader and more versatile research range, a model of the investigated formation will simulate the past to recreate the empirical findings. The model allows for exploring different scenarios and understanding the formation's pore-water past.

As this diffusion process is known to be slow in clays (Verhoef et al., 2017) and the clays are about one million years old, the hypothesis is that there is a measurable gradient in these clays. Depending on the curve observed, conclusions can be drawn on the system's (steady) state and diffusion or advection velocities. Currently, the assumption is that these radionuclides will mainly be transported by diffusion.

First, a literature study is conducted to determine the present knowledge of the targeted formations, including geohydrology, depositional environment and logging data. Next, an empirical study is conducted on live drilling cuttings that have been sampled for analysis in a laboratory. The results of these laboratory measurements are subsequently incorporated into the formation model construction. This model calculates the influence of different variables over one million years on the present chloride concentration gradient. By fitting the model outcome to the laboratory results, conclusions are drawn on the history of the formation and its suitability to be a natural analogue for deeper, poorly indurated Dutch clays.

## 1.1 Research Question

---

*Is there an ion concentration gradient in the Peize-Waalre Formation that confirms the assumption that transport of radionuclides in poorly indurated clays in the Netherlands takes place predominantly by diffusion?*

---

## 1.2 Sub-Questions

To process of answering the research question is guided by subdividing it. First the ion gradient will be tried to be demonstrated in the field. Literature and field findings should prove whether this gradient originates from transport processes. The option that any other type of transport or origin has resulted in a gradient is investigated. Any properties found in this literature study that prevent the Formation from being a natural analogue will be highlighted. The results of the field and literature study will be combined in an attempt to accurately model the Peize and Waalre Formation's porewater history.

1. *Is there an ion concentration gradient in the Peize-Waalre formation?*
2. *Could an ion concentration gradient originate from another mechanism than transport processes?*
3. *Are there properties or characteristics that prevent the Peize-Waalre from being a natural analogue of a Paleogene Clay?*
4. *Is it possible to model the measured ion profiles and apply that to different poorly indurated clays in the Netherlands?*

## 2 Literature and Knowledge

### 2.1 Deep Geological Disposal

The research on deep geologic disposal in the Netherlands focuses on two types of subsurface rocks, poorly indurated clays and rock salts. The host rock forms the main barrier in their disposal concepts (Verhoef et al., 2020). Both poorly indurated clays and rock salts feature properties that are found to be suitable for geologic disposal. As this research focuses on clays, salts will not be further discussed.

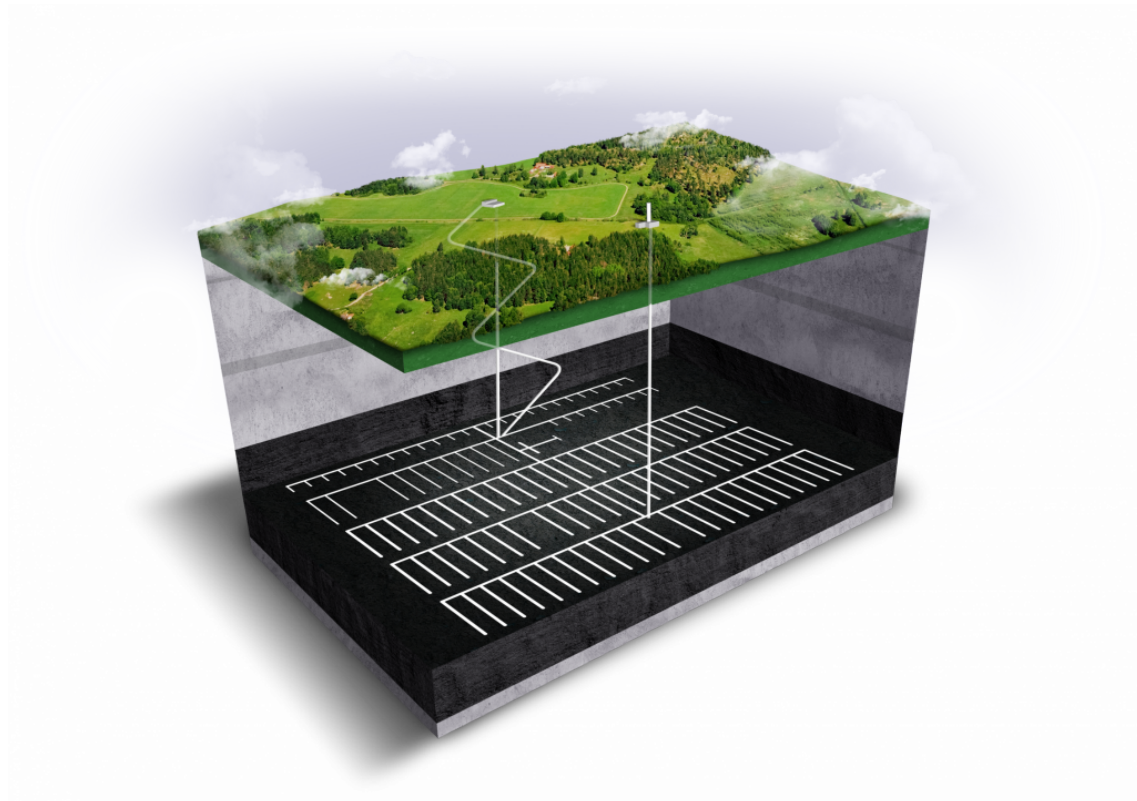


Figure 1: Artist impression of a GDF in the Netherlands (Verhoef et al., 2020)

Figure 1 shows a geologic disposal facility that could be designed for the Dutch radioactive waste, a ramp or shaft to a suitable clay, in which corridors are drilled with a tunnel boring machine to dispose of waste. More in-depth information on the nature of radionuclides and expected waste volumes produced can be found in Appendix A. Vis and Verweij (2014) describe that clay layers suited for radioactive-waste disposal preferably have the following properties contributing to isolation:

1. Low permeability and low hydraulic gradients.
2. Tendency for plastic deformation and self-sealing of fractures. Research on this has been done at Mont Terri, an international research project for, amongst others, hydrogeological characterisation of the Opalinus clay formation. Even though the tectonic regime at Mont Terri, near Basel, Switzerland, includes fractures and faults, these do not contribute significantly to the overall permeability due to the self-sealing properties of the clays (Croisé et al., 2004)

3. Chemical buffering capacity
4. Geochemical characteristics favouring low solubility of radionuclides
5. High capacity to retard the migration of radionuclides towards the accessible environment (biosphere), e.g. through sorption capacity and diffusion-dominated transport. (Vis & Verweij, 2014).

This research will focus on the clay’s capacity to retard the mitigation of radionuclides towards the biosphere. Retardation of radionuclides is key to ensuring the long-term safety of any GDF.

## 2.2 Transport Processes

### 2.2.1 Diffusion

Diffusion is the net movement of energy, atoms, and molecules from locations with high concentrations to locations with lower concentrations. This fundamental physical property is based on the random directions of particles that distribute evenly over that given space when present in a volume. There are many similarities in the mathematical approach to the conduction of heat in solids and the diffusion of matter (Carslaw & Jaeger, 1946). This was written into law by Adolf Fick as the first law for diffusion (Equation 2.1).

$$J_D = -D \cdot \frac{\partial c}{\partial x} \quad (2.1)$$

where  $J$  is the diffusion flux in the amount of substance per unit time,  $D$  is the diffusion coefficient measured in area per unit time,  $c$  is the mass concentration of solute based on the volume of solution in soil and  $x$  the direction of transport (Shackelford, 1991). The diffusion coefficient ( $D$ ) and conductivity ( $\lambda$ ) are linearly related (Vanýsek, 2012). Dissolved salts in (pore)water are subject to diffusion, and the ions act as diluted species for which their transport properties depend on several parameters (COMSOL, 2017). Temperature highly influences the diffusion constant and is stated to increase  $D$  on average by 2 to 3% for every degree Celsius above standard 25°C.

Table 1: Ion conductivity (Vanýsek, 2012)

Ion	$\Lambda_{\pm}$ ( $10^{-4}m^2Smol^{-1}$ )	$D$ ( $10^{-9}m^2s^{-1}$ )
Na <sup>+</sup>	50,08	1,334
Cl <sup>-</sup>	76,31	2,032
NaCl	126,39 ( $\Lambda^{\circ}$ )	1,2 - 1,8 (Nimdeo et al., 2014)

At standard conditions Vanýsek (2012) lists the diffusion coefficient of  $Na^+$  and  $Cl^-$  in aqueous solution (Table 1). For solutions of simple salts such as  $NaCl$ , it can be assumed that they diffuse together due to the net charge they carry. This so-called Equivalent Ionic Conductivity  $\Lambda^{\circ}$ , which is the molar conductivity per unit charge concentration, is defined as Equation 2.2.

$$\Lambda^\circ = \Lambda_+ + \Lambda_- \quad (2.2)$$

where  $\Lambda_-$  and  $\Lambda_+$  are equivalent ionic conductivities of the cation and anion (Vanýsek, 2012). Even though the ions are diluted in the water and physically separated, their opposing charges force them to stick together. This implies that while  $Cl^-$  its conductivity/diffusion coefficient is higher than  $Na^+$ , they diffuse faster into the water without creating a charge concentration when together. This is crucial to the conductivity and diffusion rate of  $NaCl$  in any medium and, in this research, its soils.

The diffusion coefficient of both the sands and clays greatly influences any of the results. The unit of this coefficient, area/time, is displayed as  $m^2/second$ . The diffusion coefficient of  $NaCl$  in clays differs per clay. As described in Nimdeo et al. (2014) the diffusion coefficient for  $NaCl$  in demineralized water is about  $1,2 - 1,8 * 10^{-9} m^2/s$ . This is the highest diffusion observed in any soil and is known as the free water diffusion ( $D_o$ ). Sands and clays retard this diffusion due to their tortuosity and constrictivity as they described the apparent diffusion coefficient ( $D_a$ ) by Pearson et al. (2003) in Equation 2.3.

$$D_a = \frac{\chi}{\tau^2} \frac{D_o}{R} \quad (2.3)$$

where the apparent diffusion ( $D_a$ ) is based on the free water diffusion, the tortuosity squared ( $\tau$ ), the constrictivity ( $\chi$ ) and the retardation factor ( $R$ ). *tortuosity*, the number and amount of curving any matter experiences when travelling through a soil. (Hasenpatt et al., 1989), (Thomas et al., 2012), (Millington & Quirk, 1961). The tortuosity factor, varying between 0 and 1, negatively influences soil permeability and diffusion. *Constrictivity* is a dimensionless factor between 0 and 1 that is used to quantify the influence of pores diameter on physical phenomena (Bini et al., 2019). For diffusion of helium Pearson et al. (2003) concluded that the tortuosity and constrictivity combined ( $\chi/\tau^2$ ), the 'geometric factor', accounts for a 0,00625 diffusion reduction through Opalinus clay. The helium diffuses 160x more slowly through Opalinus clay than through free water. Experiments need to be done to determine the geometric factor for  $NaCl$  in the Peize and Waalre clays. The process of determining the apparent Diffusion coefficient of the Peize and Waalre will be described in Lab-testing diffusion coefficient and sensitivity study.

Fick's law (Equation 2.1) can be expanded with the apparent diffusion coefficient  $D_a$ . This law will determine the flux based on distance, concentration and the Diffusion coefficient.

$$J = -D_a \cdot \frac{\partial c}{\partial x} \quad (2.4)$$

A partial differential equation is needed to determine the change of concentration to time, known as Fick's second law (Equation 2.5).

$$\frac{\partial C}{\partial t} = D \frac{\partial^2 C}{\partial x^2} \quad (2.5)$$

where  $C$  is the concentration in given dimension ( $C = C(x, t)$ ),  $t$  is time,  $D$  is the diffusion coefficient, from now on  $D_a$ , and  $x$  is the position.

Poorly indurated clays have been investigated for their diffusion properties. A good example is the Boom Clay Formation in Belgium which has been extensively researched for its diffusion properties (Leupin et al., 2017). In those experiments tracers (Super-heavy water and Iodine isotopes) are injected in a borehole interval and their concentrations monitored. The pressure head of the fluid is maintained at values close to zero to avoid any advective transport.

### 2.2.2 Advection

Advection is the mechanical transport of solutes along with the bulk flux of the water, driven by the gradient in gravitational potential energy. In most cases, this means the gradient in gravitational potential energy (Phillips & Castro, 2014). Darcy's law (Equation 2.6) describes the flux through a porous medium.

$$q = -\frac{k}{\mu L} \Delta p \quad (2.6)$$

where the flux  $q$  is a one-dimensional variable in  $m/s$ ,  $k$  the permeability of the medium in  $m^2$ ,  $\mu$  the dynamic viscosity of the fluid in  $Pa \cdot s$ ,  $L$  a given distance in meters and  $\delta P$  the pressure difference over  $L$  in  $Pa$ . (Griffioen et al., 2016) states that advection may cause transport into or out of clays on a geological timescale. If advection rates in certain formations, either upwards or downwards, are of too high levels, radionuclides may enter the biosphere. Advection rates in aquifers are, by definition, higher than in the neighbouring aquitard. If radionuclides escape this aquitard, their dispersion will increase significantly.

## 2.3 Geology

### 2.3.1 Geology of the Netherlands

At the present-day Holocene Netherlands location, for millions of years, a wide variety of climates are acknowledged (Wong et al., 2007). In this report, two ages are of particular interest as clays have been deposited that might either be suitable for geological disposal or can be used as a natural analogue during these times. Figure 2 shows the stratigraphic units that are observed in the Dutch subsoil according to TNO. The Peize and Waalre members (NUPZ and NUWA) and Rupel member (NMRU) are discussed below.

### 2.3.2 Rupel formation

Between 33,9 and 27,8 million years ago, the geologic Rupelian stage took place (Faul, 2018), which coincides with the start of the Oligocene (Vis & Verweij, 2014). The Rupel

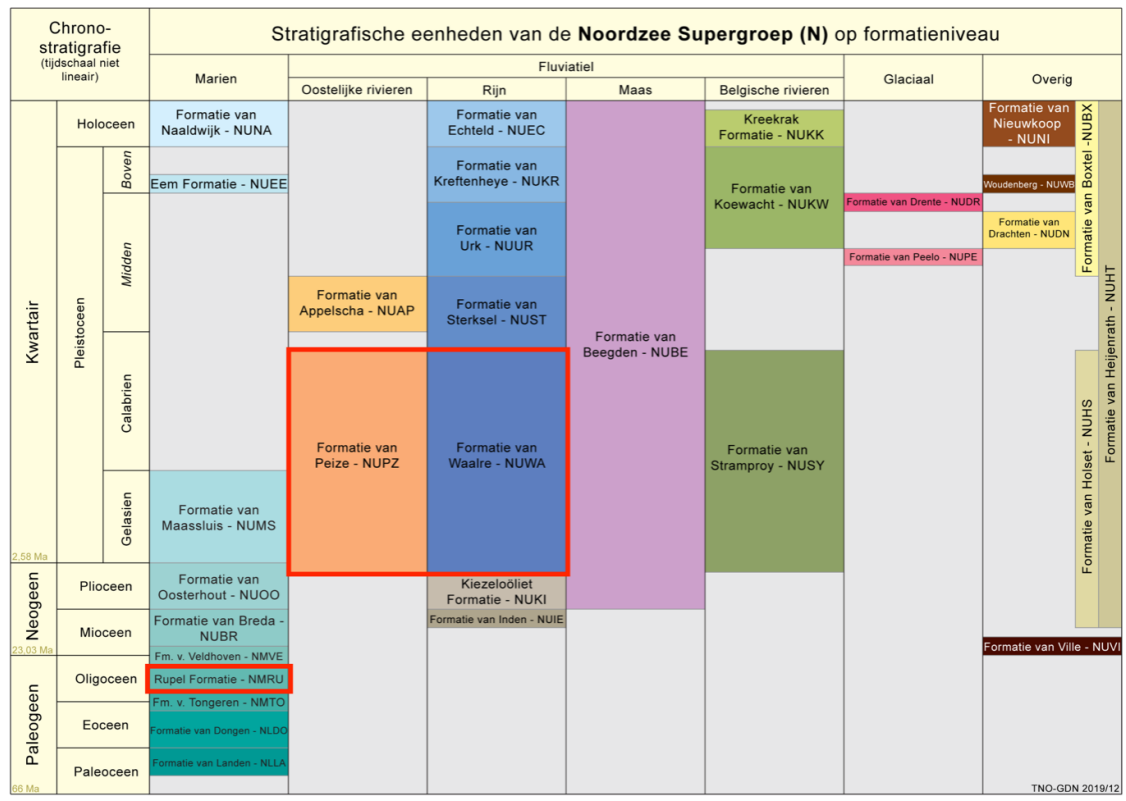


Figure 2: Formations of interest in red squares - Timescale not linear - (TNO, 2019)

Formation's depositional setting was a middle to outer neritic (continental) marine setting with waters up to 500 meters deep. The formation's thickness varies up to 250 meters; its geographical distribution is across the entire Netherlands with regional correlation in the UK, Germany and Belgium (TNO – GDN, 2021). Within the Rupel Formation, clays and sands are described, towards both top and base, the clays grade into silts and rather abruptly into sands (Vis et al., 2016). Within the Rupel Formation, several members are observed, of which the Boom- and the Berg-member are the only two geographically distributed over the entire Netherlands. The Berg member, formerly Vessem Member, underlies the Boom Member (Vis et al., 2016). The Boom member has been extensively analysed by Vis et al. (2016) as a part of the programme into geological disposal of geologic waste, OPERA. They describe the Boom clay as a marine clay which was deposited in a time when the global climate shifted from a greenhouse world to a glaciated one. TNO DINOloket (2022) describes clays that become siltier towards the base and top. Abels et al. (2007) describe rhythmic variations in the silts and clays resistivity measured using spectral analysis of borehole records. These successions are primarily driven by the 41 kyear obliquity cycle, also known as the Milankovitch cycle. On top of that, 100- and 405-kyear cycles have been identified that reflect changes in Antarctic ice volume. The depth, thickness and presence have been calculated by Vis et al. (2016) by analysing borehole data from boreholes registered in the DINOloket database. Figure 3 shows two essential conclusions of that report that drastically increased the knowledge and filled white spots on the Boom clay in the Netherlands. For the potential geologic disposal of radioactive

waste, the OPERA-report follows the same points of departure for thickness and depth as were used in a past disposal programme, CORA.

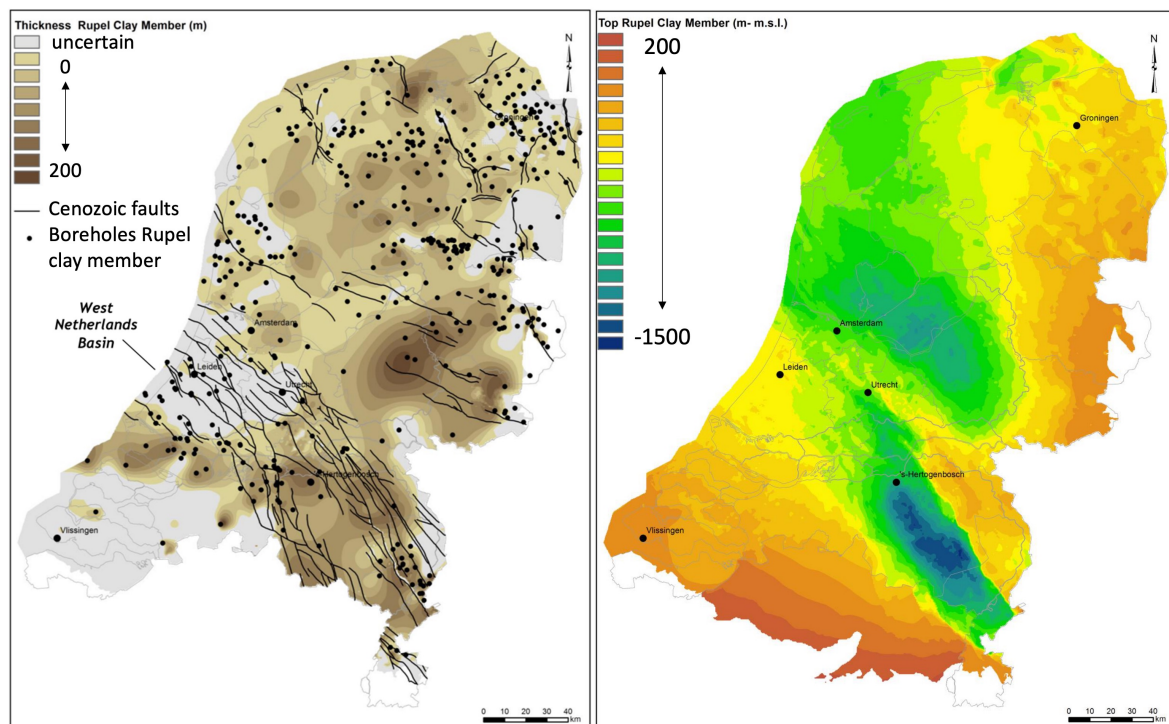


Figure 3: Left: thickness of Boom clay and faulting | right: top-depth of Boom clay (Vis & Verweij, 2014)

### 2.3.3 Peize and Waalre Formations

The Peize and Waalre formations are both fluvial sediments deposited simultaneously in the middle of the Netherlands (Figure 4). The Peize formation origin is Eridanos (Baltic River system) delta deposits during the late Pliocene – early Pleistocene, 2,8Ma to 1,0Ma (Overeem et al., 2003). The Waalre formation consists of Rhine-Meuse sediments, a low-gradient meandering fluvial system including estuarine conditions (Wong et al., 2007).

The Waalre formation shows grey-coloured fine to medium sand, alternating with clay deposited in flood basins and oxbow lakes. The Peize formation shows fine sands to clay layers at the delta top (TNO DINoloket, 2022). On top of the Waalre and Peize formations in the west Netherlands, the Urk and Kreftenheye Formations are present. The Urk Formation is fluvial Rhine sediment consisting of coarse sands with occasional gravel. Towards the North, it transitions into estuarine, tidal, and shallow marine sediments. The Kreftenheye is a medium to coarse sand from a fluvio-glacial system. Both formations will show good permeability and freshwater influx in the next paragraph (2.3.5). The Peize and Waalre formation are known to have experienced little mineralogical alteration since deposition.

In the past century, the West-Netherlands have been perforated countless times, either deep-drilling for hydrocarbons or shallower to depths of a few hundred meters for groundwater extraction and heat-storage systems (“WKOtool”, 2022). These wells all pierce the

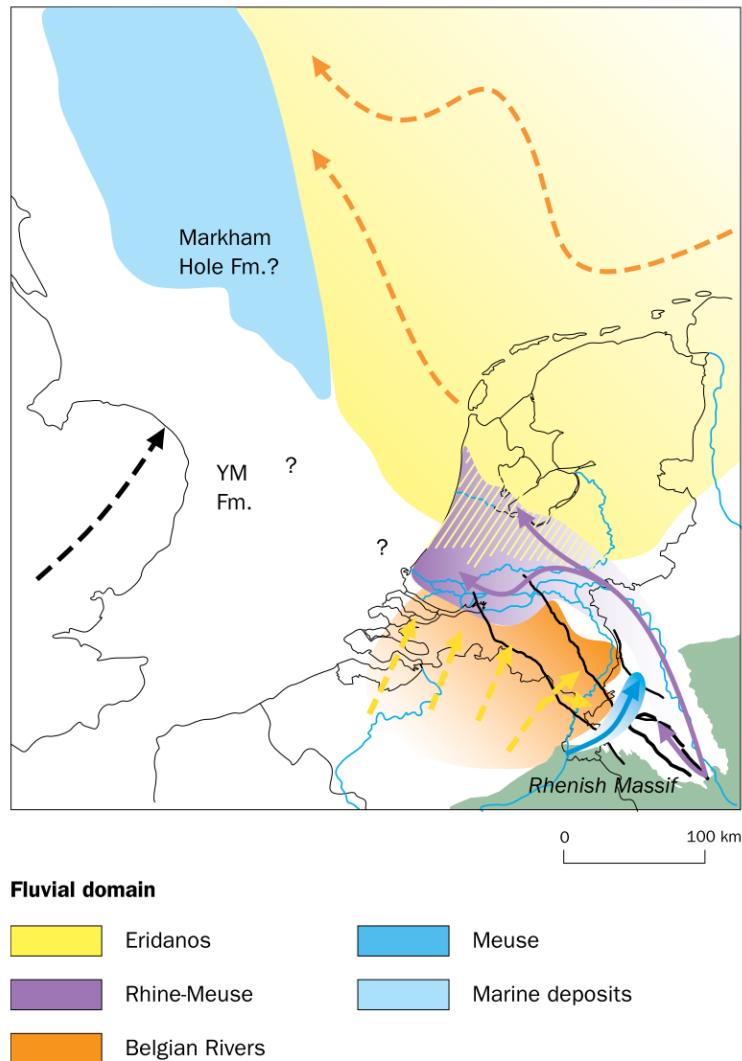


Figure 4: Lower Pleistocene fluvial sediments showing interfingering Eridanos and Rhine-Meuse sediments (Somsen, 2015)

formations of interest, the Peize and Waalre formations, at depths of 50 to 100 meters. Every year new hydrocarbon exploration, heat-storage systems and water wells are drilled, granting the opportunity to collect fresh, unweathered clays and sands. All three locations feature Waalre clays at about 50 meters depth. At greater depths, between 80 and 100 meters, two more sequences of the Waalre formation show. These clays will be referred to as WC1 (Waalre clay 1, youngest / top), WC2 (older, below WC1), and WC3. The same system counting WS1, WS2, ... is applied for the sands. As shown in Figure 9 the saltwater interface is expected at or near the top of the Peize/Waalre-formation, more on that in 2.5 Natural Analogues.

### 2.3.4 Present subsurface models

Subsurface models made available by TNO allow for a preliminary check on the expected present formations. REGIS II v2.2 is a TNO model that is based on a data found in

the *BasisRegistratie Ondergrond*, BRO (Subsurface Key Register). The model is built on top of the already existing *Digitaal Geologisch Model*, DGM (Digital Geologic Model), which uses 26.500 high-quality borehole logs selected from the vast DINOloket database of 430.000 logs. This data is processed and interpolated (Hummelman et al., 2019) to form DGM. This model acts as a framework for REGIS II, which uses additional data from pumping tests and hydraulic heads to create a hydrogeological model (TNO DINOloket, 2019). The resolution of 100x100m, aquifer-focus and shallow depths target made this model favourable over other TNO models. From their quality assessment, no artefacts were observed that show significant influence on the Peize and Waalre Formation model (TNO DINOloket, 2022).

### 2.3.5 Geochemistry and hydrogeology

Past research on the geochemistry of the Waalre clays concluded that they are mostly unaltered since deposition. Based on that, any alteration found in the clays can be appointed to external factors such as groundwater. Groundwater in the region contains numerous elements and minerals of which at least 44 tracer elements have been demonstrated by Stuyfzand (1991). This research focuses on the transport of salt ions through clay strata. The elements Sodium (*Na*) and Chlorine (*Cl*) make up over 90% of the solutes in shallow groundwater by weight (Griffioen et al., 2016). Therefore we assume the conductivity measured in pore water is mostly induced by the *NaCl*-ions, which allows for coupling conductivity measurements to NaCl-concentration in pore water. These measurements are further described in 3.1.4 Conductivity.

Sodium chloride's molar weight is 58,44 g/mol of which 22,99 g/mol Na (about 40 wt%) and 35,45 g/mol (about 60 wt%). North-sea salinity averages at 34000 mg/l which translates to 19000 mgCl/l (Safetyatsea, 2008) (Quante & Colijin, 2016). In literature, salinity and chloride content are used both. When salinity is mentioned in this research, it is based on total dissolved solids (TDS). North-sea chloride concentration is > 100 times more saline than the maximum allowed chloride content (150 mg/l) in Dutch drinking water (Inspectie Leefomgeving en Transport, 2013). In shallow aquifers in the Netherlands, salinity is determined by the ratio between seawater and meteoric water influx. Deeper reservoirs with halite or other rock salts can become hypersaline by dissolving the salt into the groundwater. Hypersaline groundwater measures about 70-150.000 mgCl/l or a salinity of 110-250.000 mg/l (Griffioen et al., 2016)

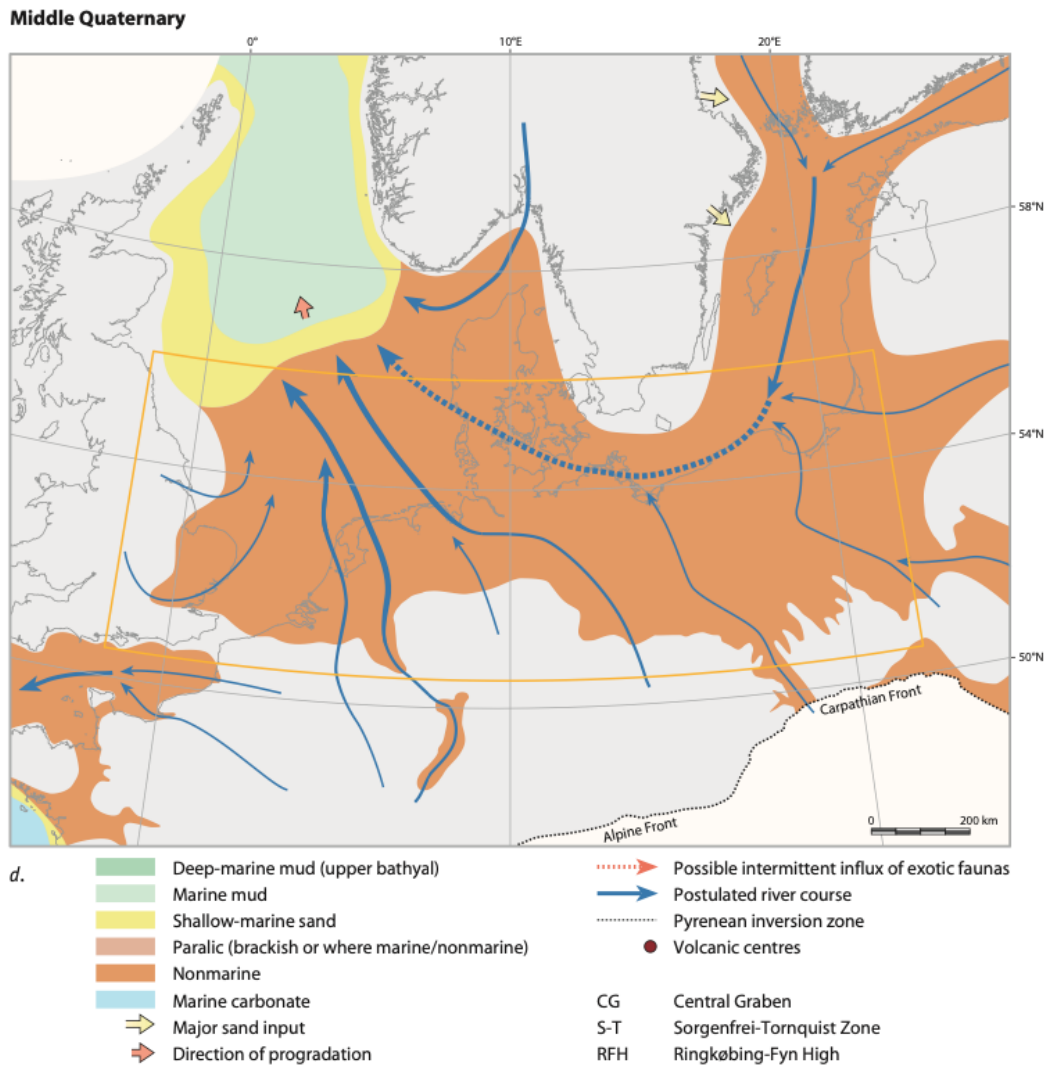


Figure 5: Eridanos prograding environment towards Northwest during middle Quaternary (Knox et al., 2010)

Fluvial sedimentary systems deposited the Peize and Waalre formations during the middle Quaternary (1Ma). Figure 5 shows research by Knox et al. (2010) in which they map the combined Eridanos/Meuse/Rhine delta that progrades towards the Northwest, filling the basin. The West Netherlands are part of nonmarine sediments, which confirms the non-saline origin of the pore fluids. The salinity of the Baltic and Alpine rivers during the middle Quaternary is unknown, except that their sediments are still flowing through our rivers today. Vreedenburg and van Zanten (1991) state that the natural chloride load of the Rhine is  $40 \text{ kg Cl}^-/s$  over an average discharge of  $2.200 \text{ m}^3/s$ , or  $18 \text{ mg Cl}^-/l$ . Any river deposits by the current (unpolluted) Rhine on floodplains or in river banks will therefore contain pore water with this salinity of  $30 \text{ mg NaCl}/l$ . There is no reason in literature (Niedrist et al., 2021) to assume that the salinity of the influx of fresh sediments from the Alps and Baltics changed over the last million years. Therefore the salinity of the river Rhine,  $30 \text{ mg NaCl}/l$ , will be used in the model as the initial value for the fluvial sediments (see 4 Model).

Table 2: Water type qualification according to thresholds set up by the TNO GDN (2022)

Qualification	mg Cl <sup>-</sup> /l	derived mg NaCl/l
Fresh	0-150	0-250
Brackish	150-1000	250-1660
Salt	>1000	> 1660

TNO’s Geological Service determined standards to qualify groundwater based on its chloride content listed in Table 2. These standard maps can be constructed to visualise the Dutch subsurface salinity. A depth map of the brackish to salt interface can be consulted at TNO – GDN (2021).

### 2.3.6 Sea level

Sea level does affect the salinity of subsurface aquifers as described by Canul-Macario et al. (2020). Therefore, the measurements done by this research and others such as KWR, TNO and water supply companies cannot be taken as a static value. The current sea level is high compared to the past 100ky (Figure 6). When looking at the timespan this research focuses on,  $\approx 1\text{My}$ , a cyclic sea level rise and fall can be observed. This cyclicity of 100 to 150 ky results in an average sea level of 60 meter below today’s level and 120 meter lower than today’s during an ice age.

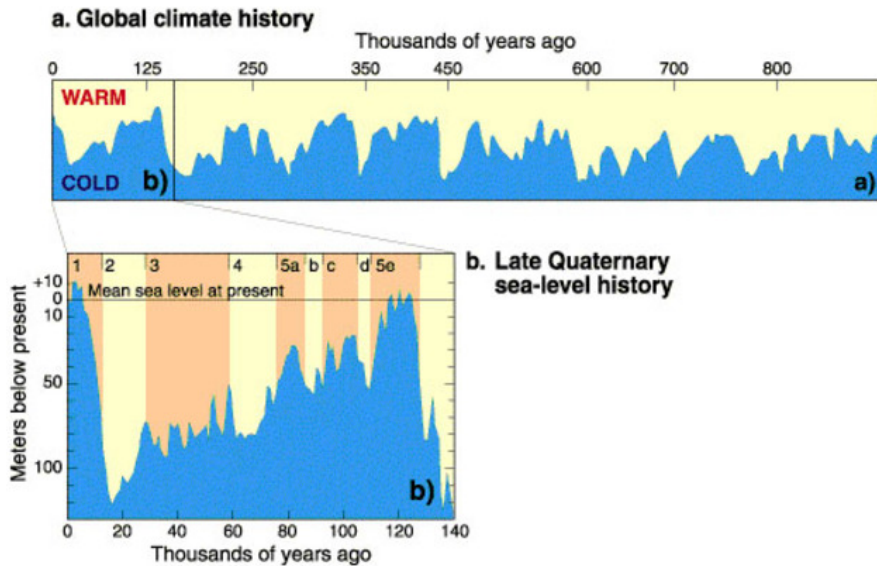


Figure 6: Cyclicity of global sea level according to NOAA (2016)

When the sea level is that low, there cannot be an influx of salt water into deeper aquifers of the Peize and Waalre sands. Meteoric water will push the saline water out, resulting in Peize and Waalre clays enclosed both on the top and the bottom by relatively fresh water. Depending on the diffusion velocity, this cyclicity might be observed in the clays better than in the sands.

### 2.3.7 Sampling locations

- RCSG, Rijswijk This facility, the Rijswijk Centre for Sustainable Geo-Energy, is located at a former Shell research laboratory. Currently, TNO operates this facility to improve geo-energy-related technologies and accelerate the energy transition. Their focus lies on geothermal energy and subsurface storage of heat, hydrogen and  $CO_2$ . The Rijswijk samples were taken during a commercial drilling related to research at RCSG (see Figure B.1 in Images for facilities).
- Meent, Rotterdam At this location in the centre of Rotterdam, a new warmte koude opslag (WKO) is drilled. Office buildings and high-density residential buildings use shallow reservoirs to store excess heat or cold to use months later seasonally. De Ruiter Grondwatertechniek BV, a company involved in the RCSG drilling, is the operator on this drill site. Drilling occurred at the end of January, and the cuttings were sampled in early February 2022.
- DAPGEO-02, Delft The last sampled location is related to the TU Delft campus geothermal project. For this project, in March 2022, a heavily cored and measured monitoring well was drilled about 3km north of the primary well location.

## 2.4 Drill Cuttings

When drilling a borehole, the excavated soil is transported upwards from the drilling bit to a separator at the surface. This separator sieves the drilling mud and removes cuttings by particle size, the drilling mud is subsequently recirculated, and the cuttings are disposed of. One of the problems experienced during sampling these cuttings is the influence of the drilling method on the cutting quality. Two standard drilling methods, jet drilling and suction drilling, are observed during this research and displayed in Figure 7 and 8.

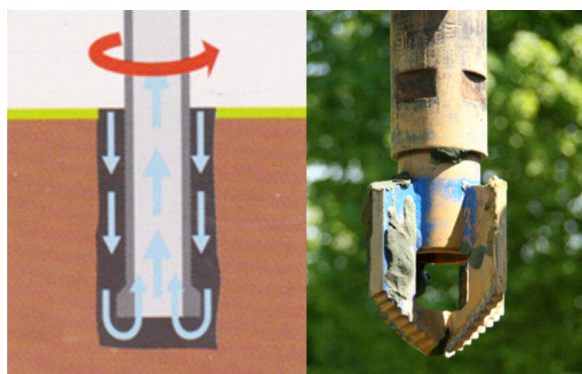


Figure 7: Suction drilling with drag-drill bit (Smet Group, 2022)

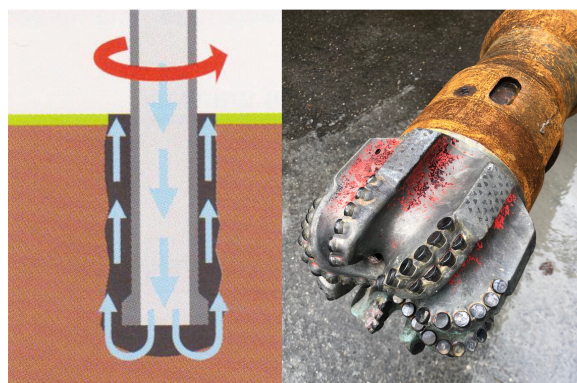


Figure 8: Jet drilling with PDC-bit (Smet Group, 2022)

### 2.4.1 Jet drilling

This is a relatively simple technique used extensively in water extraction, sampling wells and deep geological exploration (Smet Group, 2022). Water is pumped down through stems (pipes) and transports the spoil (cuttings) to the surface outside the drill stem. The advantage is that there is no depth restriction for this method. However, the diameter of the borehole is maxed at around 500mm.

As accessible drilling operations through the Peize and Waalre within the timeframe of this research were scarce, every occasion had to be taken to acquire data. For cutting gathering, jet drilling is not preferred due to three disadvantages;

1. The drill bit grinds the clays to minuscule particles to a point there is no recognition of the original form;
2. The risk of the open borehole wall crumbling into the upwards transported drilling fluid contaminating the sample;
3. The volume of upwards transported drilling mud is much higher than when it would have been when transported up through the smaller diameter stem. This higher volume results in a lower transport speed allowing for lower accuracy by delay and more time for dilution of the samples.

### 2.4.2 Suction drilling

This technique also involves a drill stem bored into the ground. It differs from jet drilling in that the drilling fluid flows downward through the borehole, and the cuttings are sucked up through the drill stem (Smet Group, 2022). Suction drilling is used to drill wells in coarse fractions and for large-diameter boreholes. This method has cutting collection advantages, roughly the opposite of the disadvantages listed in 2.4.1 Jet drilling. Especially the small diameter upflow and, therefore, minimal feedback time between the actual soil disturbance and the surface sampling has advantages. The drill bit shown in Figure 7 creates scraped clay lumps with a diameter up to a few centimetres which is essential when the goal is sampling undisturbed soil.

## 2.5 Natural Analogues

Mazurek et al. (2008) describe the transferability of certain parameters between different research sites and formations. Under certain circumstances, information or results can be transferable when the original setting was not a test setup. It is impossible to do research on the timescale a GDF has to operate. Therefore, it is crucial to predict what interactions and processes occur at a timescale of hundreds of thousands of years. Using processes that take place in nature as an analogue for processes, one is planning to comprehend one can predict the subject's response. In this research, different clay formations in the Dutch subsurface are expected to be a possible natural analogue for radionuclide transport through Paleogene clays. The Peize and Waalre formations, around Delft at about 50-100 meters deep, are topped by a fresh aquifer and underlain by a salt aquifer.

Figure 9 shows the interpolated brackish to salt interface at the sampling locations. Salt diffusion systems can be analogous to radionuclide contaminants. (Shackelford, 1991)

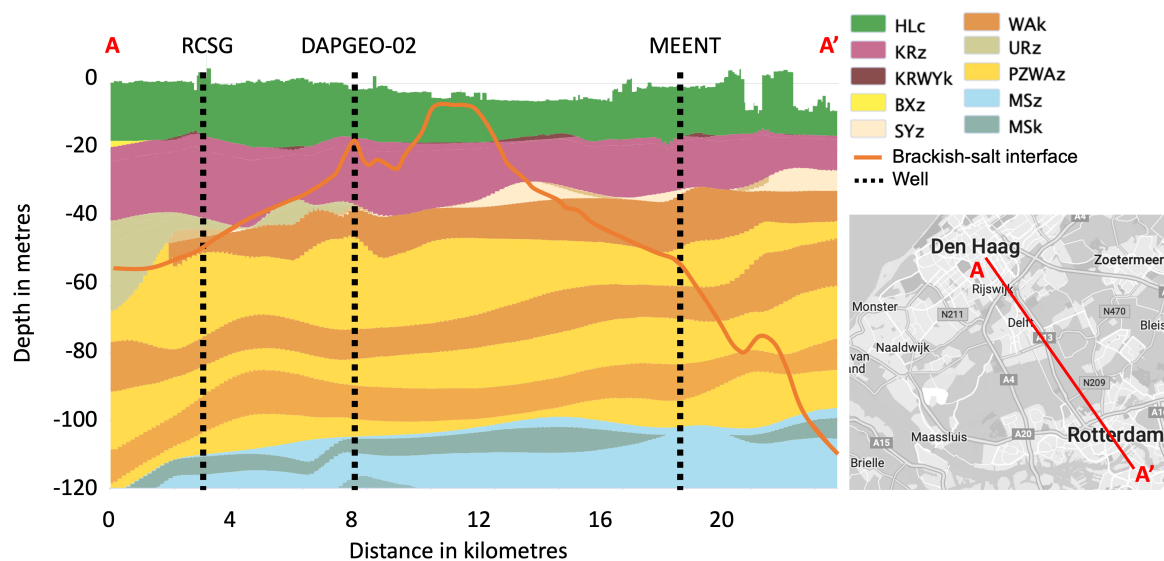


Figure 9: Expected interface between brackish and salt groundwater (TNO DINOloket, 2022)

Both locations show the transfer from fresh ( $<150$  mg/l) to brackish ( $>150$  mg/l) (Table 2) at the interface between the Urk-formation and the Peize-Waalre Formation. The nearest measurements are in Rotterdam, so this might not be as accurate as desired. A report by Hydreco on the construction of the Delft Campus monitoring well does expect the brackish / salt interface to be at the top of the clay layers (Hydreco, 2014). From the GrondwaterAtlas by TNO, it is extracted that the freshwater reaching the Waalre-clay travelled 200 years to reach the interface (TNO – GDN, 2021).

Mazurek et al. (2008) shows in his research on the transferability of information between different clay research facilities that there are properties that fall within a certain margin. This report concludes that compaction decreases porosity and increases tortuosity, enhancing the effect. Every researched clay falls within a small band allowing researchers to estimate diffusion rates without knowing the exact tortuosity or other specifics.

The specific inaccessible features that concern radioactive waste disposal is described by the Natural Analogue Working Group (NAWG) as:

- The very long time it will take for long-lived waste to decay to safe levels
- The large spatial scales which cannot be directly addressed in a laboratory
- The heterogeneity and structural complexity of the geological environment which will host the repository

These three features will be addressed in this research. Alexander et al. (2015) describe how  $Cl^-$  concentration in pore waters displays smooth, regular profiles with depth. These sodium and chloride ions serve as a natural tracer as described in by Gimmi (2010) and Mazurek et al. (2009). A tracer is a substance used to trace the course of a chemical or biological process. Tracers can be either natural or artificial; nature provided a concentration deviation in this case.

The expected difference in chloride ion concentration described in Sea level will result in flux through the clay. The speed at which the salt ions diffuse through the clay quantify the retardation capability of the investigated formation. This way, poorly indurated Dutch clay, the shallower Peize and Waalre formation functions as a natural analogue for deeper situated clays.

### 3 Hydrogeology Analyses

#### 3.1 Methodology

The Peize and Waalre formation has been selected as a potential natural analogue. Several drilling sites in the West Netherlands allowed for sampling their cuttings while drilling through the formations of interest. After that, every single sample goes through the same set of proceedings. The Drill-cutting analysis is done in three consecutive steps visualised in Figure 10; Collection, Processing and Analysis. It is read from left to right; when an arrow continues in two follow-up stages, this describes the splitting of a physical sample. These actions are listed and linked with their respective paragraph in Table 3.

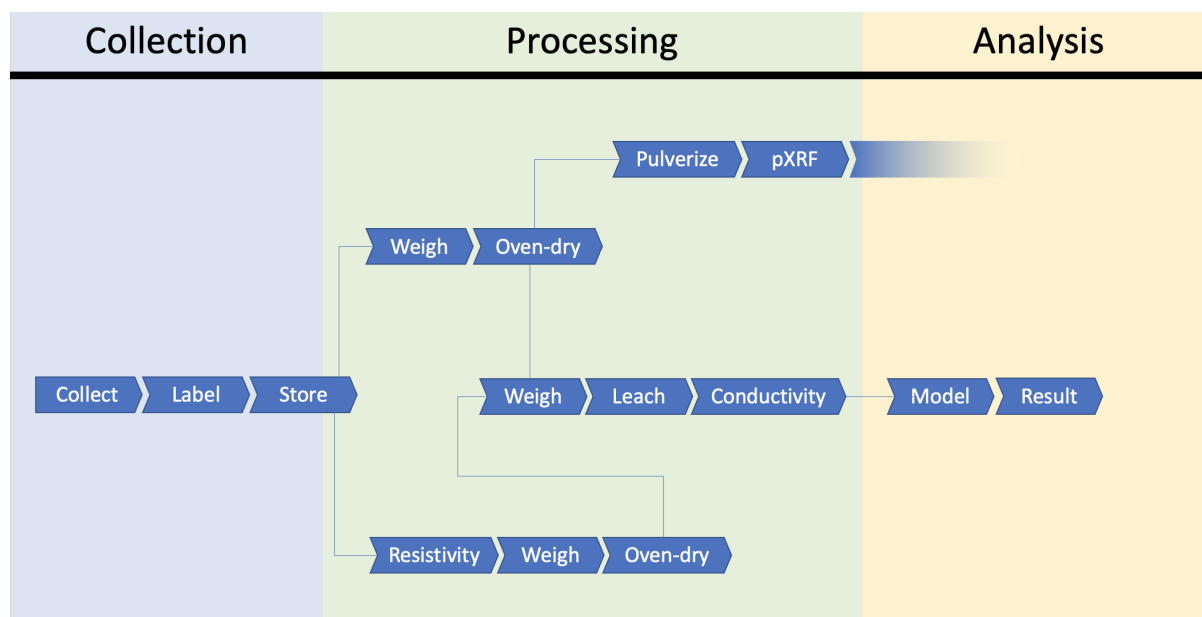


Figure 10: Process diagram, Table 3 links to the steps respective sections

Table 3: Sections linked to Figure 10

Action	report section
Collect	3.1.1
Label	3.1.1
Store	3.1.2
Weigh	3.1.3
Oven-dry	3.1.3
Pulverize	3.1.3
pXRF	5.1.7
Leach	3.1.4
Conductivity	3.1.4
Model	4
Result	3.2

### 3.1.1 Locations and collection

Three different drill sites are sampled for this research, chronologically; RCSG, W1 and DAPGEO-02. They have been listed in 4, the working name in the table is how these locations will be referred to.

Table 4: Sampled locations

Well name	Working name	Well type	GPS Location
RCSG	Rijswijk	Research	N52,03627 E4,32725
W1	Rotterdam	Water production	N51,92158 E4,48115
DAPGEO-02	Delft	Monitoring	N52,02557 E4,37940

Figure 11 shows the GPS locations projected on a map with The Hague in the north-west and Rotterdam in the south-east. Figure 12 is a REGIS II V2.2 model (see subsection 2.3.4 visualisation of the present formations and their expected continuity. The sampling method for the three locations differs slightly and is therefore described per location below. The influence of these different sampling methods is elaborated on in section 5 Discussion. To accurately analyse soil samples, it is important to acquire, sample, transport and measure while preventing contamination or dilution. Since the drilling process is not purposed for soil collection, this will be the sampling step where contamination and dilution are expected to be most severe. Research on pore-water and clay contents has been done before by numerous researchers. Gimmi and Waber (2004) describes the difficulties experienced when measuring clay pore-water contents due to local heterogeneity. In 2.4 Drill Cuttings a more elaborate description has been given on the drilling methods.

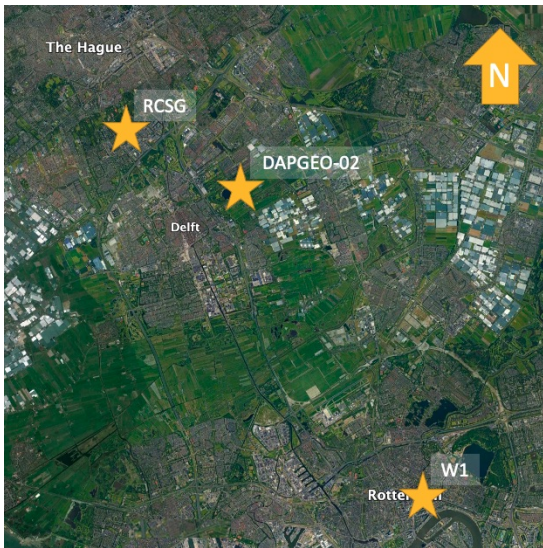


Figure 11: Locations of sampling listed in Table 4

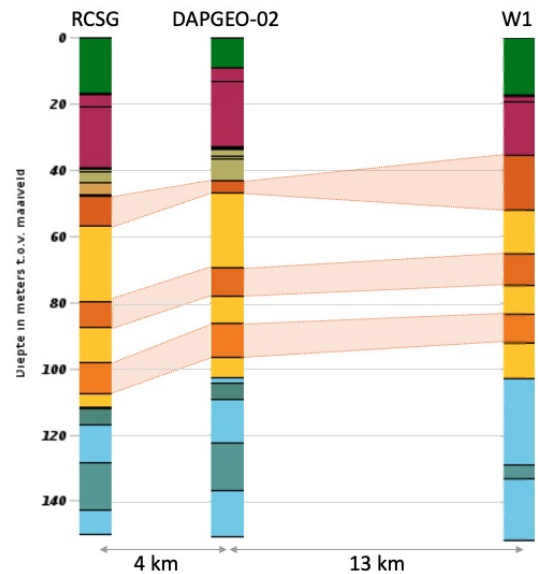


Figure 12: REGIS II V2.2 model formation continuity (TNO DINOloket, 2022)

- RCSG, Rijswijk During their activities there was time to take a one-meter push core at a depth of 36 meter (see Figure B.2 in Images for the push core). Compared to cuttings, (push) cores contain more information about the subsurface as they are relatively unaltered, and the depositional sequence is preserved. This sampling location can be divided into three separate sample batches listed in Table 5. Drilling took place in January 2022, and the technique used throughout this process was jet drilling (see 2.4 Drill Cuttings). Cuttings will therefore have mixed extensively with the drilling fluid and might not be sampled with a significant delay (minutes).

Table 5: RCSG batches

Depth	Process	Drilling fluid
36-37m	Push core	-
36-48m	Create space for BHA (Bottom Hole Assembly)	Tap water
48-180m	Actual drilling operation	KCl-mixture

The drilling operator expected the push core to be taken from the top of WC1. The second batch was gathered manually with a highly irregular vertical speed. Sample depth has therefore been corrected for the travel time of the cuttings. The samples have been collected at the drilling mud screen, separating the fluids from the solid cuttings. The third batch was gathered by shift personnel as part of their regular sampling protocol. The researcher subsequently sampled these samples on an interval of 1 meter.

- W1, Rotterdam At this location, a small amount of salt has been dissolved in the drilling mud to enhance the particle settling speed. The results will show whether this salt significantly influences the measurements. As this site makes use of suction drilling (see 2.4 Drill Cuttings), the cuttings are expected to be less influenced and contaminated by the drilling mud. See Figure B.3 in Images for a sampling bin with visible clay lumps. The samples are sampled with a resolution of 1 meter in the clay sections and larger intervals towards the deeper (>100m) parts.
- DAPGEO-02, Delft This monitoring well was sampled every meter by the drilling engineers as part of the protocol the researcher sampled. At this location jet drilling is the operators method of choice. Lessons have been learned from the past two locations as sand samples proved to less valuable. As the differences measured between sand bodies are very small the sampling frequency is increased to every 5 metre. Clay sampling is done the smallest resolution possible, 1 metre at this location.

### 3.1.2 Storage

Several types of containers are used to store the cuttings: plastic zipper bags by Toppits, plastic sampling jars and smaller laboratory jars. Every sample taken or split is (re) labelled and documented on paper and in a digital file system. This is to prevent mixing up or losing any valuable information. To provide the opportunity to redo inaccurate measurements, no sample container is emptied for experiments. By following this ap-

proach, several process errors have been corrected.

The sampling jars potentially contain chlorinated polyethylene (CPE); the risk of contamination of the sample is expected to be very low as the containers are food-grade and will not be damaged. The bags and containers are stored in labelled crates and then stored in a climate room.

### 3.1.3 Preparation

Weighing The first step on both the conductivity- and pXRF-branch of the diagram in Figure 10 is weighing the sample by placing a spoonful (10ml) of a sample from the container into a labelled aluminium disposable dish. This dish its weight is noted and, in the further calculation, subtracted from the sample weight.

Drying Every sample that needed to be dried has been dried in soil drying ovens. At 105 °C the water is forced to evaporate out of the clays, which is a standard procedure in clay handling (Department of Sustainable Natural Resources, 1990). This relatively low temperature does not affect its mineral composition. After >24h drying, a few samples are picked randomly to be weighed another time. This process continues until no weighed sample shows a different weight than the day before. All water has been evaporated. Dried samples are handled directly or stored in the storage room. If stored and re-handled, they are oven-dried for 24h to prevent re-hydration.

Calculation Porosity is a property of any porous medium which is described by Equation 3.1

$$\Phi = V_w/V_t \quad (3.1)$$

where  $V_w$  is the volume of the water and  $V_t$  is the total volume. The literature shows that the density of clay solids ( $\rho_s$ ) is about 2,65 g/cm<sup>3</sup>; this is therefore assumed in this calculation. The density of water ( $\rho_w$ ) is 1,0 g/cm<sup>3</sup>. From the measurements taken, both the solid mass ( $M_s$ ) and the mass of the evaporated water ( $M_w$ ) are known. From there on, it is possible to calculate the water and solid volumes (Equation 3.2) respectively. The sum of these volumes is the total volume of the pre-oven sample (Equation 3.3); now, the porosity can be calculated Equation 3.1.

$$V_w = M_w/\rho_w \quad \text{and} \quad V_s = M_s/\rho_s \quad (3.2)$$

$$V_t = V_s + V_w \quad (3.3)$$

### 3.1.4 Conductivity

The conductivity of the pore water is chosen to be the main figure to measure its salinity. Several assumptions and simplifications have to be made;

- Available pore space is at 100%, all pore water can be intruded by diffusing NaCl, and there are no pockets.
- The amount of dissolved NaCl accounts for such a high percentage of the total ion concentration (>90%, see Geochemistry and hydrogeology) that it solely contributes to the pore water conductivity
- The sample temperature during all measurements is 20°C

The approach is a standard protocol for the device that is used to measure conductivity. The Consort C6010 is a multi-parameter analyser. This research is equipped with a conductivity probe calibrated to a 0,1M KCl solution every measurement day. Five gram of dried sample are weighed in a marked plastic test tube, and after that, 25 millilitres of demineralised water is added. This water's conductivity is <2 microS/cm and, therefore, has minimal influence on the result. All samples are shaken extensively for approximately 1 minute to ensure complete wetting of the sample. The wetted 'mud' is then set aside for a few days to allow the solid particles to settle. The NaCl ions in the sample leach into the water, increasing its conductivity. The measurements are done on all the samples on the same day to ensure they have undergone the same treatment and leaching time. The conductivity of the pore water is calculated by working backwards from the observed reading on the analyser (Equation 3.4).

$$\kappa_{pore} = \kappa_{lab} \cdot \frac{W_{dw} W_s}{W_w W_{dry}} \quad (3.4)$$

where  $\kappa_{pore}$  is the original pore water conductivity,  $\kappa_{lab}$  is the analyser result and the  $W$ 's are the weights of the 'demineralised water', 'Sample (before oven)', 'Water (in sample)' and 'Dry sample (after oven)'. To translate any measured pore water conductivity in Siemens per meter to either  $TDS$  (total dissolved solids) or  $mol/m^3$  Equation 3.5 has been extracted from Niedrist et al. (2021) which is transliterated in Equation 3.6. The *molar ionic conductivity* has been determined in 2.2.1 Diffusion.

$$\kappa\left(\frac{mS}{cm}\right) = 10 * \frac{C_{salt}\left(\frac{g}{L}\right) \cdot \Lambda\left(\frac{S}{m \cdot mol}\right)}{M\left(\frac{g}{mol}\right)} \quad (3.5)$$

$$\text{Conductivity} = \frac{\text{Concentration salt} \cdot \text{molar ionic conductivity}}{\text{molar mass}} \quad (3.6)$$

where the temperature to which this molar ionic conductivity is calibrated is crucial. For this research, the table provided by Vanýsek (2012) lists the ionic conductivities at 25°C. To compensate for the 5°C lower lab temperature standard, the numbers provided by this table are lowered by 5°C · 3% = 15% as the ionic conductivity is lower at lower temperatures. A measured conductivity of 1mS/cm can now be interpreted as a NaCl concentration of 0,0540g/l. This equation (3.5) provides a linear ratio, which is not an exact representation of empirical research. Castellazzi et al. (2012) show a NaCl conductivity curve that is exponential. However, due to the measurement results being of the same order of magnitude, this curve effect is not taken into account in this research. The focus lies on the conductivity ratio between the different samples, and there is no need to compare the separate locations.

## 3.2 Results

150 Documented samples have been taken from the three locations. All sampling and laboratory notes alongside direct measurement results can be found per sample in Data. The described labwork methodology has been undertaken for each of the three sampling locations. This results in both a sample porosity ( $\lambda$ ) and a pore water electrical conductivity ( $EC_{pw}$ ). Using these two figures, interpretations can be made and measurements verified. On the y-axis, the depth is shown from 0 to 150 meters, the x-axis shows the electrical conductivity in miliSiemens per centimetre. Please note that the x-axis values differ per sampling location. The graphs are shown feature black and red dots. Black dots are measurements that have been marked as valid in the process. Red dot data points are shown but have, somewhere along the sampling, processing and measuring process, been marked as potentially compromised, e.g., spillage, open container, organics. These interpretations are formed based on literature and discussion with experts. Experts have analysed all samples at the drilling site, which resulted in a rough distinction between clays and sands. Every result graph features a yellow-red background indicative of the soil present at depth, yellow for sand and red for clays.

### 3.2.1 Rijswijk

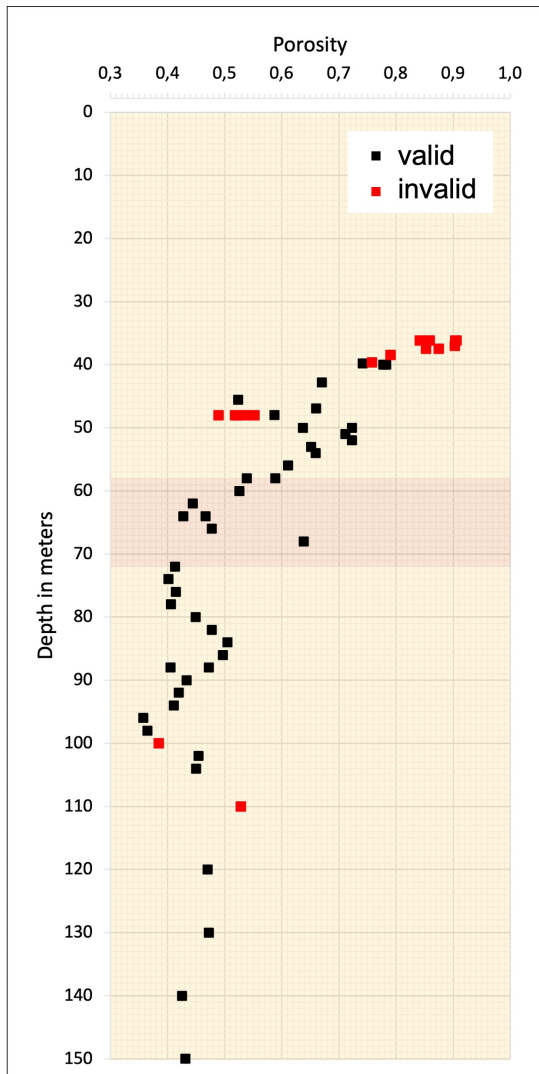
Figure 13a and 13b show the results from both the porosity calculations and the electrical conductivity measurements. This sampling location has been divided into three separate sample batches as elaborated on in 3.1.1 Locations and collection;

1. Push core [36-37m];
2. Preparation drilling to create space for BHA (Bottom Hole Assembly), drilling fluid tap water [36-48m];
3. Actual drilling operation, drilling fluid KCl-mixture [48-180m]

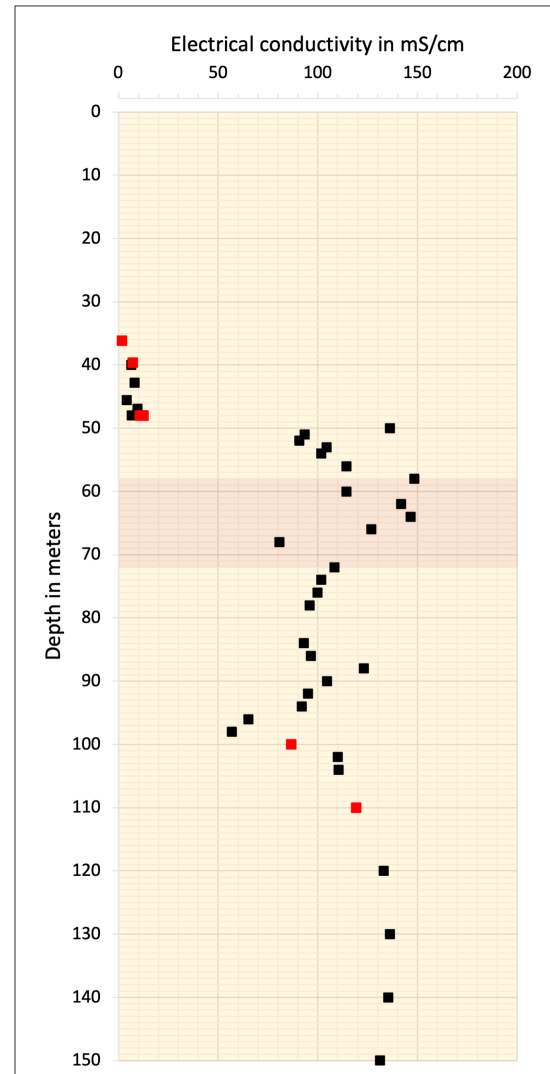
The push core was taken at a depth of 36 meter; unfortunately, it showed very few original clays and sands. The drilling tower has been present since the 1980s, and significant debris has fallen into the open borehole. The one-meter push core sequence smelled oily, contained plastics and discoloured within days. After oven-drying, little matter remained to confirm the suspicion of it not being natural soil. The push core data is shown in Figure 13a as very high porosity red dots; no EC measurements have been done on these samples.

The second batch of Rijswijk samples has been collected while drilling with tap water. These cuttings, collected from drilling depths of 36 to 48 meter, appendix figure Figure A.1 shows a cutout of the complete electrical conductivity graph. The average pore-water conductivity measured in this batch is seven mS/cm, which translates to 4g/l NaCl using Equation 3.5.

The third and final batch encompasses the most measurements and presents the best visible porosity gradient. The porosity steadily decreases from about .7 at 50-meter depth to .4 at 100-meter depth. The electrical conductivity measured in the pore water averages at >100 mS/cm, which translates to a 1M KCl solution (Handbook of Chemistry &



(a) Porosity in samples



(b) Porewater electrical conductivity

Figure 13: Obtained values for the Rijswijk samples

Physics, 2001). 1 Mol of KCl weighs 74,5g, implying that vast amounts of KCl have been soluted in the drilling fluid. Measuring pore-water NaCl-salinity cannot occur because the drilling fluid contamination increases the salinity  $>10$  times. This location does not provide enough reliable data for this research, examining the transport of ions through clays.

### 3.2.2 Rotterdam

The Rotterdam location clays and sands have been taken from the samples by the geologist at the location. A single batch of samples is from the same moment, of the same age, and in the same container. These parallels are good for the reliability of the data. The clay lumps described in the methodology prove the samples taken at this location to be the least disturbed by external influences. Figure 14a and 14b respectively show the

porosity and electrical conductivity measured in the Rotterdam samples. Underlain by the geologist's interpretation of clays (red) and sands (yellow).

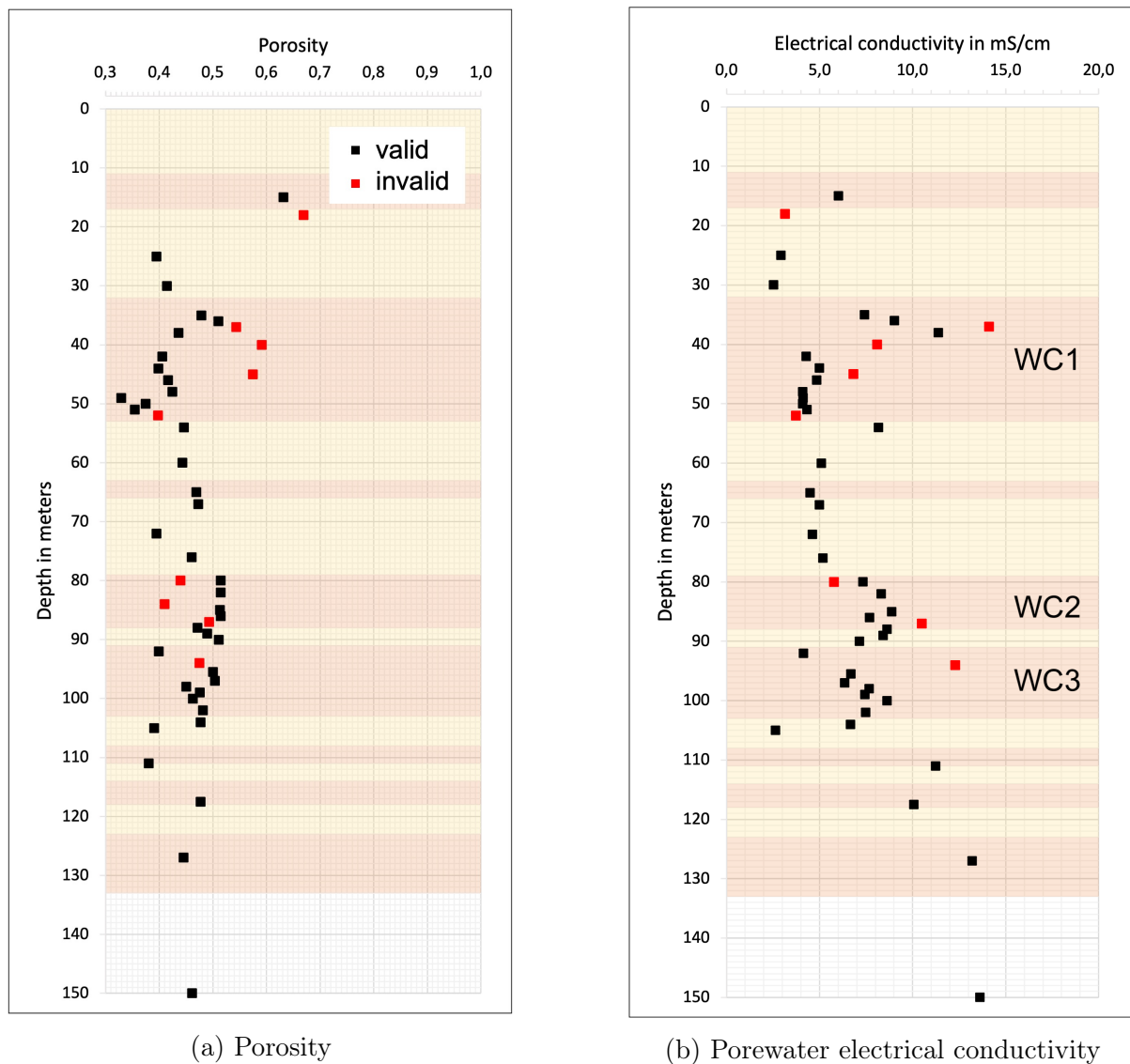


Figure 14: Obtained values Rotterdam samples with numbered Waalre clays (WC#)

The samples show a porosity between .3 and .6, although mainly between .4 and .5. There is no visible compaction trend in deeper soils; the deepest taken sample at 150 meters still shows a porosity of .45. Average clay porosity (.47) is higher than the sands (.41). Three measurements in the second clay layer show high porosity due to organic contents and are therefore considered invalid. The complete table of measurements and anomalies can be consulted in Data.

The brackish-salt interface (at 1000mgCl/l) observed in the Grondwatertool is found at a depth of 70 meters. 1 gCl/l corresponds to about 1,6gNaCl/l, leading to a pore water conductivity of 3mS/cm. The Peize sand aquifer is measured to be more saline than the model by TNO indicates. The sands are generally less conductive than the clays, indicating flushing by the aquifer. The found conductivity of the bottom saline aquifer and accompanying molarity (0,027M) will be used as an input for the model. Pore water

conductivity gradually increases towards about 15 mS/cm, corresponding to about 8 g/l or 150 mol/m<sup>3</sup>.

The curve observed in WC1 does not show the typical bell curve that is seen in research by Gimmi (2010). This suggests that there are more transport processes influencing the pore water salinity. The model designed in the second part of this research will try to identify these processes. WC2 and WC3 show a small bell curved salinity profile indicating a less complicated transport history. The scatter of WC2 and WC3 is of such a level that a higher resolution is necessary to draw conclusions. What can be observed is the slight drop in salinity between WC2 and WC3 indicates flushing by the thin sand layer in between.

### **3.2.3 Delft**

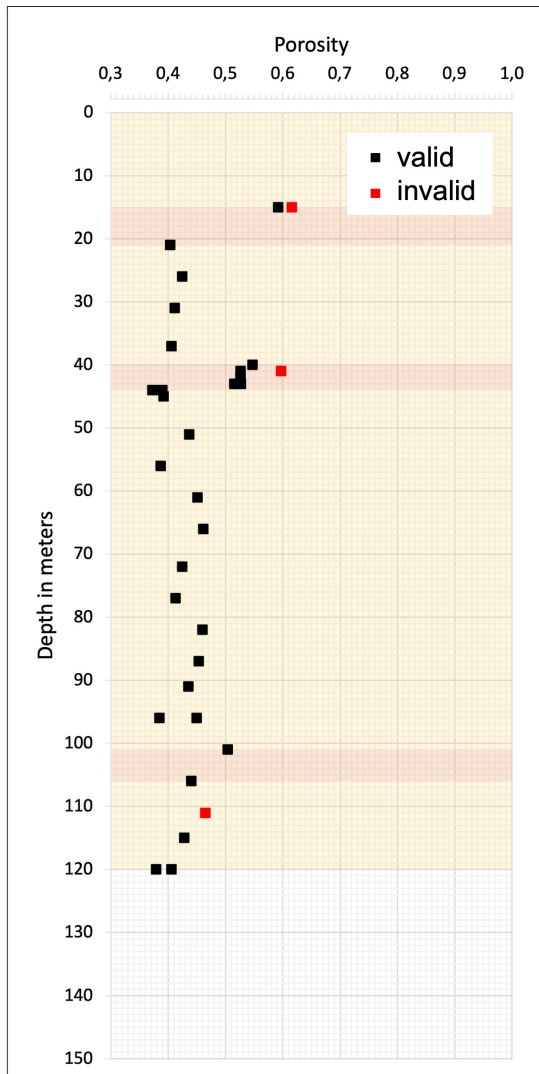
The Delft location has been sampled significantly later than the other two; the sampling sequence has therefore been refined. Sands have proven to be of less interest and are therefore sampled on a lower frequency, clays on the contrary are sampled every available metre, this is explained in subsection 3.1.1. All measurements done in sands show comparable results in pore water electrical conductivity. This is expected due to the high diffusion coefficient and the present subsurface flow of groundwater (described in 4.1.3). The mixing and distribution of the salt ions result in homogeneous results. At the sampling location, clays and sands are distinguished. The clays are sampled with a resolution of 1m, and the sands at 5m. Figure 15a & 15b show both the porosity and conductivity measured in the lab.

The constant porosity in the sands and clays stands out compared to the other two locations. The sand porosity shows minimum and maximum numbers between 0,4 and 0,5, whereas the clay samples measure 0,5 to 0,6. The higher porosity in clays is typical, which indicates reliability. At this location, jet drilling is the method of choice, which results in smaller cuttings. Smaller cuttings are less reliable to measure as they are more contaminated by the drilling mud.

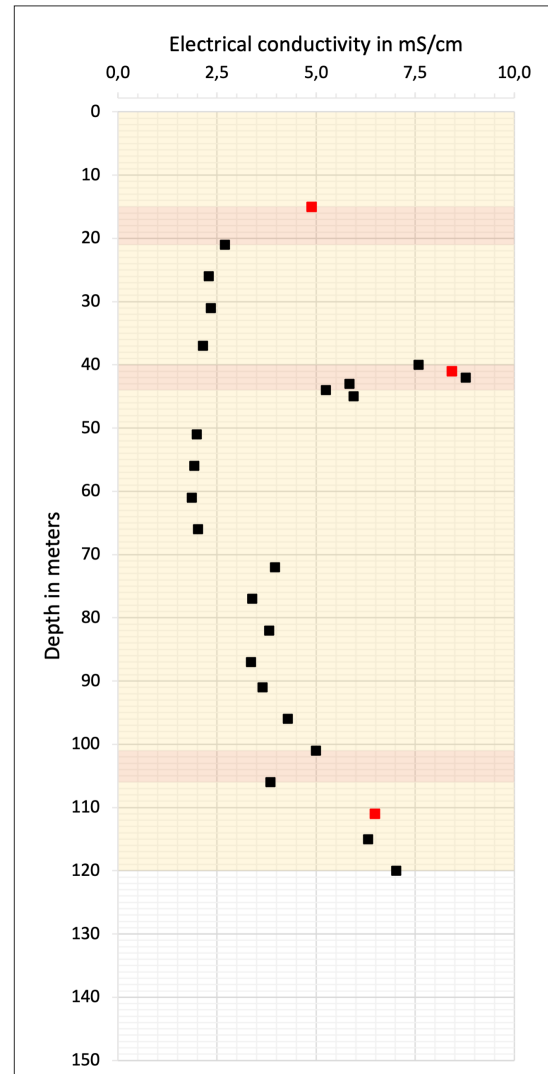
The electrical conductivity curve shows the most apparent increase in salinity towards deeper parts of the Peize and Waalre formation.

### **3.2.4 Results interpretation**

The three sampling locations cannot be compared based on their porosity or conductivity due to their different handling method during drilling. It is, however, possible to just compare the location of the clays and sands as they are recognisable by geologists and are visualised in the graphs. Figure 16a shows how WC1 is missing in the Rijswijk samples as these are contaminated too much to be categorised as either clay or sand. WC2 is way more pronounced but is not as recognisable in the other two locations. WC1 shows a thickness of >20 meter in Rotterdam but does pinch towards the south resulting in only 5 meter of clay in Delft, about 15km away. This pinching of 1m/km can be very common and might imply that the WC1's observed at different locations are not the



(a) Porosity



(b) Porewater electrical conductivity

Figure 15: Obtained values for the Delft samples

same continuous layer. These fluvial clays have likely been formed as floodplains during river overflowing filling a sedimentary basin. Sedimentary basins represent accumulations of clastic and evaporite materials in a geologically depressed area (Tiab & Donaldson, 2016). Due to this nature the sedimentary layers thin toward the edges. Depending on the size of these floodplains, the Waalre clays connect or are separate strata. This is hard to prove without a seismic study which has not been done for this area.

If, in the past, more saline water was present in the aquifers, this would have diffused into the clays. The clays show a delayed response to subsurface salinity changes. Rotterdam WC1, WC2 (80m) and WC3 (90m) show a bell-shaped conductivity increase indicating a salinity drop. Another explanation could be that the process of drilling and sampling has flushed the sands; this would, however, not clarify the clay's internal tracer profile. Most curious is the conductivity profile observed in WC1, which shows from the bottom up a continuous pore water salinity of about 5 mS/cm. The top 10 meter, however,

shows a different profile comparable to the clay layers WC2 and WC3. This, compared to Rijswijk, seems to be a more clear and better comprehensible system.

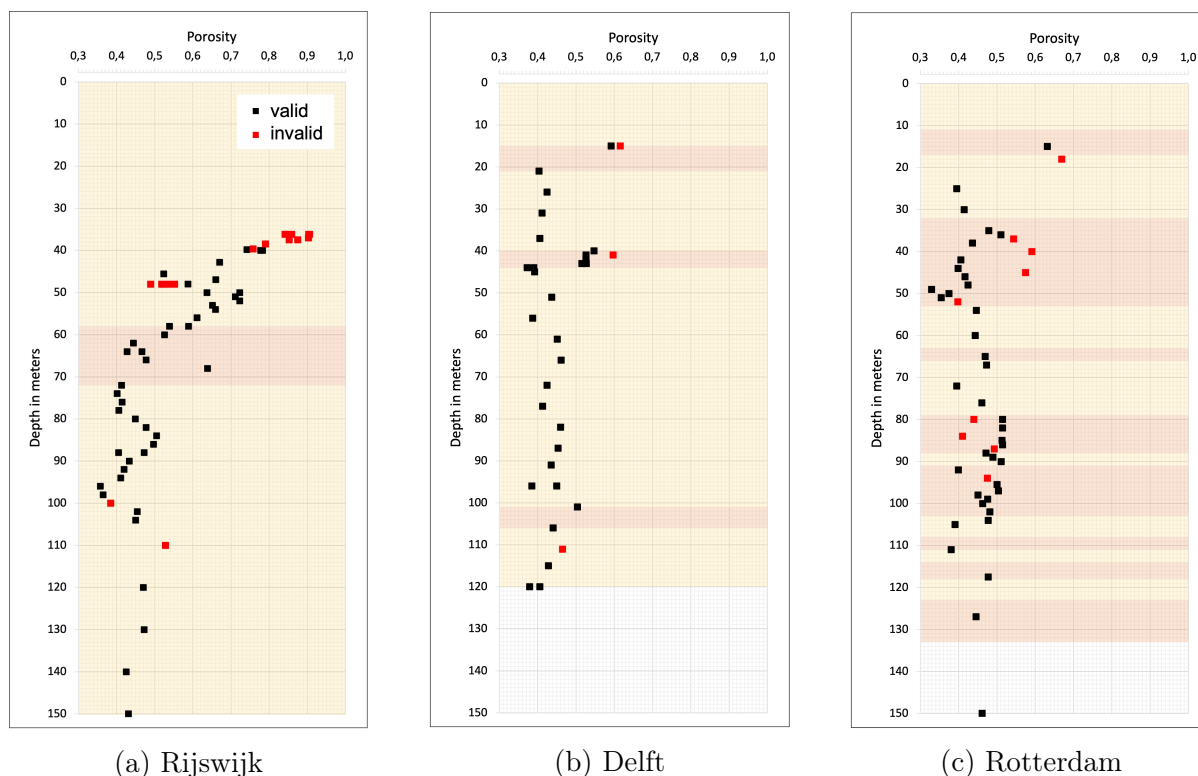


Figure 16: Calculated sample porosity per site

Correlating on the conductivity shown in Figure 17a, 17b and 17c it is clear that almost all clays show higher conductivity than their neighbouring sands. Especially WC1 in Rotterdam and Delft show similarities in conductivity peaks. Their thickness is of another order, but the process they have been subject to can be very similar. The increase in salinity towards the deeper parts is visible in both Rotterdam and Delft. Rijswijk does not show this curve which can be explained by the drilling mud contamination with the KCl-mixture.

Interpreting the three conductivity curves, the choice has to be made in which location to invest valuable modelling time. Reliability, validity, efficiency, and relevance must be weighed to make this decision. The Rotterdam case WC1 scores best on all these criteria as it features;

- The most sample points;
- Is the only location drilled with the better suction drilling method;
- Drilled with very low salt content in the mud;
- Most relevant due to its thickness

The Delft location shows the most natural curve with the influence of meteoric water being lower towards deeper aquifers. WC1 at 40-meter depth stands out in its porosity and conductivity. This indicates, just as the Rotterdam graphs do, that the adjacent aquifers used to be more saline. The salinity of the clay aquitards observed in Delft is 2 to 3 times higher than their surrounding aquifers. The anomaly might be explained by

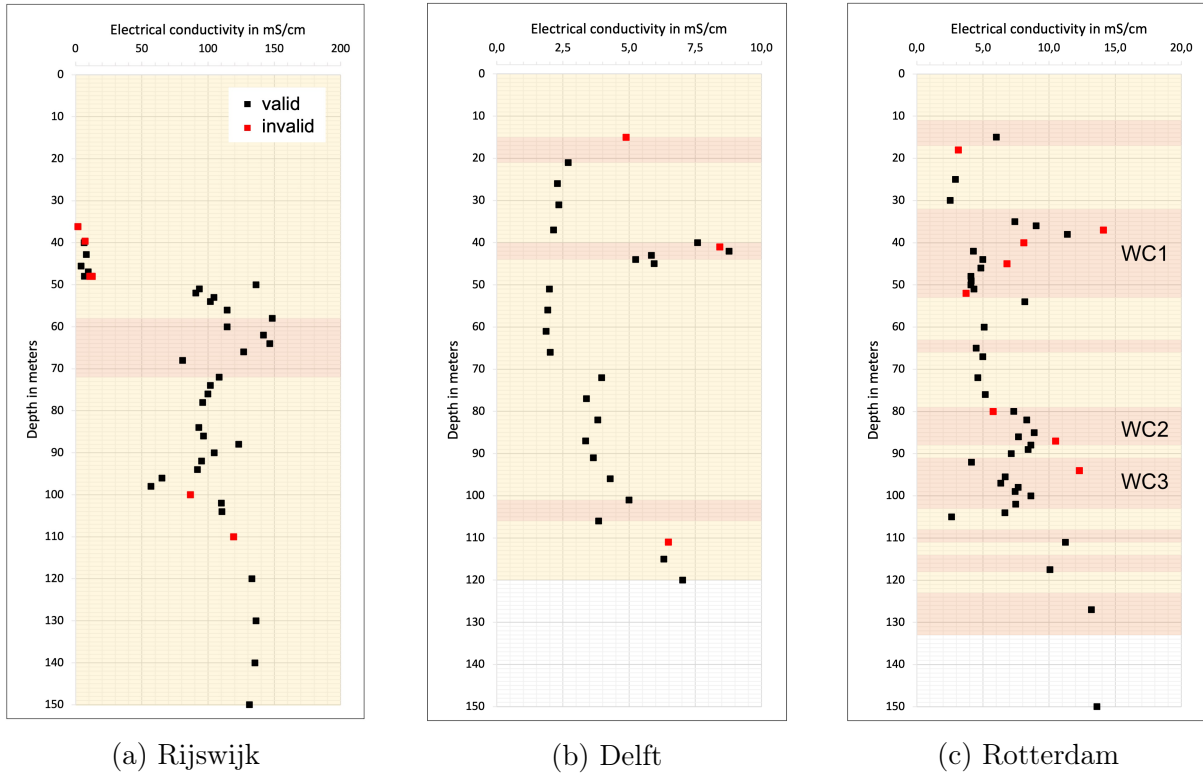


Figure 17: Electrical conductivity of laboratory pore water | Please note different  $x$ -axis scales

the flushing of the sands. This flushing is expected to be of higher influence on smaller cuttings (sands) than it is on lumps (clays).

From these results the conclusion can be drawn that the sampling locations provided very distinctive results. The Rijswijk measurements unfortunately prove to be too contaminated. The Delft measurements showed so little clay that an actual gradient is not distinguishable. The Rotterdam measurements, and especially WC1, are picked to be fitted by the model constructed in the next chapter. This location has the best chance to be a fitting natural analogue that can broaden the knowledge on poorly indurated clays in the Netherlands

## 4 Model

### 4.1 Methodology

By creating a model of Rotterdam WC1 and alternating boundary conditions it is attempted to fit the measured conductivity curves. Literature has been widely consulted, most from Somsen (2015), Visser et al. (2015), Griffioen (2015), TNO DINOloket (2019), Rijdsdijk et al. (2005), Hydreco (2014), Hummelman et al. (2019) and ten Veen et al. (2013).

#### 4.1.1 Modelling method

A multiphysics simulation is employed to investigate several subsurface evolutions. The model allows for a conventional physics-based user interface and coupled partial differential equations (PDEs) systems. Transport of Diluted Species is the main package employed which is based on equation (4.1) described in 2.2.1 Diffusion.

When a model is described, the steady-state model is the final state in which no net flux is observed. Time does not influence the steady-state model, but it can take infinite time to reach that point. In this research, a total time of 1 million years is a given, which allows for a transient model. Such a model takes time (among others) as an input, from where the solver continues each calculation based on the final time-steps outcome. Equation 4.1, Fick's second law, is used to determine the one-dimensional concentration for each timestep and depth.

$$\frac{\partial C(z, t)}{\partial t} = D \cdot \frac{\partial^2 C(z, t)}{\partial z^2} \quad (4.1)$$

where concentration input values are given in  $mol/m^3$ , the unit for depth  $z$  is meter and time is calculated in seconds.  $D$  is the diffusion coefficient described in subsection 2.2.1 in  $m^2/s$ . As the model is one-dimensional, the direction of advection or diffusion can only be vertical. To simplify the model, the vertical accretion of strata is considered; at year zero, all layers are present. A base model is constructed and visualised to get a first impression and set a standard.

#### 4.1.2 Base model

The base model is constructed using the acquired boundary conditions and initial values to set a standard for all other models. The Rotterdam location shows the most promising and accessible clay layer and will serve as the base model. The second clay layer at a depth of 32 to 53 meter is the first Waalre clay (WC1). The base model's initial values and boundary conditions are listed in Table 6

The concentration input of  $mol/m^3$  is a standard model input. During lab work, the standard of miliSiemens/cm has been used. Therefore all model results are expressed in mS/cm via Equation 3.5.

Table 6: Base model boundary conditions and input

Boundary conditions	Value	Unit	Source
Top clay layer	-32	<i>m</i>	3.2.2 Rotterdam
Bottom clay layer	-53	<i>m</i>	"
NaCl concentration top	10	<i>mol/m<sup>3</sup></i>	"
NaCl concentration bottom	28	<i>mol/m<sup>3</sup></i>	"
<b>Input</b>			
Diffusion coefficient clay ( $D_c$ )	7,5e-12	<i>m<sup>2</sup>/s</i>	2.2.1 Diffusion
Initial NaCl concentration clay ( $C$ )	0,5	<i>mol/m<sup>3</sup></i>	2.3.5 Hydrogeology
Advection velocity field ( $u$ )	0	<i>m/s</i>	
Number of time-steps	11	-	
Time per step ( $\delta t$ )	100.000	a	
Total time (T)	1	Ma	2.5 Natural Analogues

### 4.1.3 Boundary conditions and input values

The boundary conditions for the base model described in Table 6 are listed below.  $C(z, t)$  is varied throughout this research, i.e. the concentration as a function of space and time;

$$C(z, t) = c \text{ mol/m}^3 \quad (4.2)$$

where the diffusion coefficient of both the sands and clays greatly influences the model results. The unit of this coefficient is  $m^2/s$ . The diffusion coefficient of NaCl in clays differs per clay. As described in subsection 4.1.7 the diffusion coefficient for NaCl in demineralised water is about  $1,8e - 9m^2/s$  (Nimdeo et al., 2014). This is the highest diffusion observed in any soil without advection. Clays retard this diffusion due to their tortuosity and constrictivity (Chou et al., 2012). The geometric factor for Helium in clay obtained from Pearson et al. (2003) is used as a reference to the base model.  $D$  is determined by multiplying the factor with the diffusion coefficient for NaCl in water (Equation 4.3).

$$D_{clay} = 7,5e - 12 \text{ m}^2/s \quad (4.3)$$

where the diffusion coefficient for the sandy layers in between is much higher as its geometric factor is of less influence. On top of this faster diffusion, there is a measurable advection in most sand aquifers of several meters per year, which makes them subject to sea level salinity changes (van der Molen & van Ommen, 1985)

### 4.1.4 Model variances

The number of variables in a model built to imitate reality is endless. For this one-dimensional model, for example, porosity, permeability, heterogeneity, particle size, temperature, pressure, pH and a great deal more could have been varied. This would, however, not fit the size of this research and introduce uncontrollable uncertainties. Three

variables are adjusted to fit the measured lab results: bottom salt concentration, vertical advection and diffusion coefficient. In the following subsections, these choices made will be exemplified.

#### 4.1.5 Bottom salt concentration

The WC1 base salt concentration has been assumed to be higher than the concentration on top. In exceptional circumstances, such as by (Bath et al., 1989), meteoric water may flow underneath a saltwater aquifer. It is assumed that this is not the case in the West Netherlands, as the geology differs significantly from the described case.

In subsection 2.3.6 the variation in sea level and accompanying groundwater salinity has been described. Introducing a sinusoid in the bottom concentration can be simulated over the run time of one million years. Figure 6 shows 8 cycles over a 900ky averaging 110ky per cycle (9 over 1Ma). During ice ages, the bottom of the top Waalre clay is positioned >50 meter above sea level, which implies meteoric water is present in both the top and bottom aquifer; this will be modelled as such. During some of these peaks, the sea level rose a few meters above today's levels. As it is currently right on the threshold, the peak of the sinusoid will be set to twice the salinity at the bottom of WC1.

Table 7: WC1 bottom concentration sinusoid

Input	Value	Unit	Variable
Concentration minimum	0,5	$mol/m^3$	
Concentration average	14	$mol/m^3$	$C_a$
Concentration maximum	27,5	$mol/m^3$	
Number of cycles	9	-	
Years per cycle	110	ky	
Seconds in cycle	3,46896e12	s	P
Thickness clay	20	m	
Depth bottom	-53	m	$z_{bot}$
Current sea level	high	-	

This assumptions stated in Table 7 are inserted in bottom concentration (Equation 4.4 to form a sinusoid. This equation results in a varying input that is visualised in Figure 18 (code in Code).

$$C(z_{bot}, t) = C_a \cdot (1 + \sin(\frac{2\pi t}{P} + \frac{\pi}{2})) \quad mol/m^3 \quad (4.4)$$

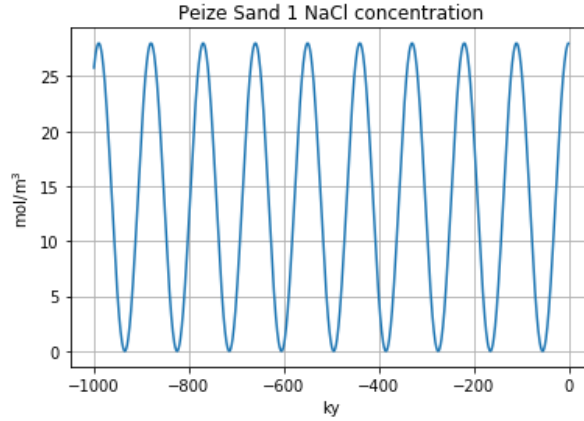


Figure 18: Peize Sand 1 fluctuating NaCl concentration over 1Ma

#### 4.1.6 Vertical advection

One-dimensional advection either transports bulk up or down. The model's input is a flux in meters per second which is acquired via Equation 2.6. The input values for this formula are shown in Table 8 which describes the substantiated variables acquired from literature.

Table 8: Minimum and maximum values Rotterdam WC1 Darcy's law

Variable	unit	Minimum	Maximum	source
$k$	$m^2$	$10^{-19}$	$5 * 10^{-17}$	Philip (1973) & Javadi et al. (2017)
$\mu$	$Pa \cdot s$		0,0013	10 °C (Engineering Toolbox, 2022)
$\Delta P$	$Pa$	0	5000	50 cm pressure head
$L$	$m$		21	Physical dimensions

Table 8 shows the values collected from literature. Both  $L$  and  $\Delta P$  are extracted from the clay dimensions. The thickness of the clay layer is 21 meter assumed to be homogeneous. TNO GDN (2022) provides insight into the pressure head measured in the clays and sands, both in the top and bottom aquifer. The bottom aquifers (second Peize sand) hydraulic head is averaged at 1,1 meter below ground level. The top aquifer measurements are between 1,5 to 1,6 below ground level, resulting in a hydraulic head difference of 50 cm. In case of heavy meteoric influx, the head of the top aquifer would increase, lowering the difference between the top and bottom aquifer. Using this data, the maximum pressure head is set to be 5000 Pascal ( 0,5m \* 9800 (Pa\*mH<sub>2</sub>O))

Table 9: Model input values advection

$q$ (m/s)	$q$ (m/ky)	$q$ (m/My)	description
1E-11	0,31	310	Maximum upward flux
1E-12	0,03	31	Low upwards flux
0	0	0	No advection
-1E-12	-0,03	-31	Medium downward flux

The values described in Table 8 describe a vast range of possible flux. If the pressure head at Rotterdam WC1 is 0 Pascal, there will be no advection. On the opposite, Darcy's law shows a potential flux of  $1E - 11m/s$  (0,3m/ky) for the maximum values. Since the input values differ in orders of magnitude, three flux ( $q$ ) values are chosen (see Table 9) to represent the possible circumstances Rotterdam WC1 endured. These values will be part of the scenario study elaborated on in subsection 4.1.8.

#### 4.1.7 Diffusion coefficient

The diffusion coefficient ( $D_c$ ) in the base case scenario is  $7.5e-12$  m<sup>2</sup>/s. This is based on the diffusion of Helium in pure water multiplied with its retardation factor in clays. As the ion size is a big influence on the retardation factor, it is expected that NaCl has transported slower than Helium. Therefore, the different input values for  $D_c$  in the model are fractions 1/2 and 1/10 of the original  $D_c$ .

#### 4.1.8 Scenario study

Combining the three different types of models described attempts to model a fit to the acquired lab curves. The natural subsurface system experiences advection, diffusion, salinity changes and numerous other external factors. By combining different sets of  $D_c$ , sea-level cycle and advection, the total number of combinations is  $3 * 2 * 4 = 24$ . These scenarios have been listed in Table 10 and are run over a time of 1 million years.

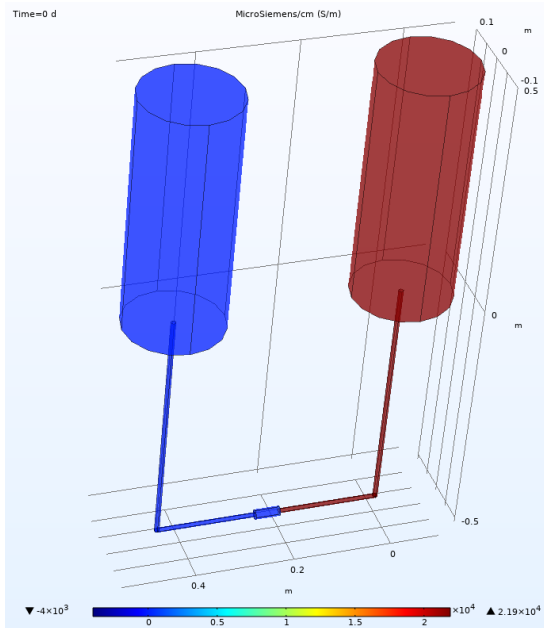
Table 10: Correlation scenarios

Scenario	$D_c$ ( $m^2/s$ )	Advection ( $m/s$ )	Sea-level cycle
A	7,5E-12	1E-11	yes
B	7,5E-12	1E-12	yes
C	7,5E-12	0	yes
D	7,5E-12	-1E-12	yes
E	7,5E-12	1E-11	no
F	7,5E-12	1E-12	no
G	7,5E-12	0	no
H	7,5E-12	-1E-12	no
I	3,75E-12	1E-11	yes
J	3,75E-12	1E-12	yes
K	3,75E-12	0	yes
L	3,75E-12	-1E-12	yes
M	3,75E-12	1E-11	no
N	3,75E-12	1E-12	no
O	3,75E-12	0	no
P	3,75E-12	-1E-12	no
Q	7,5E-13	1E-11	yes
R	7,5E-13	1E-12	yes
S	7,5E-13	0	yes
T	7,5E-13	-1E-12	yes
U	7,5E-13	1E-11	no
V	7,5E-13	1E-12	no
W	7,5E-13	0	no
X	7,5E-13	-1E-12	no

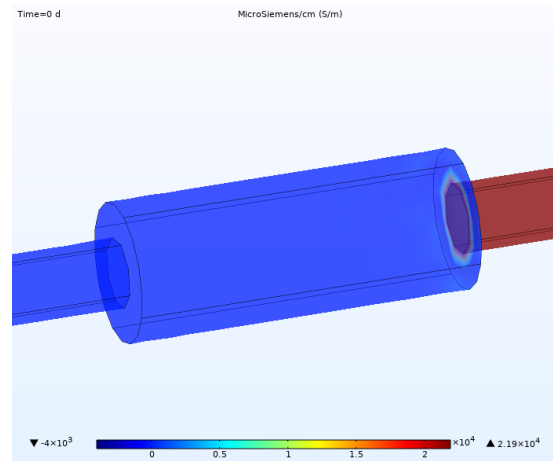
#### 4.1.9 Lab-testing diffusion coefficient and sensitivity study

The influence of the diffusion coefficient cannot be understated. It is, therefore, crucial to have a good understanding of this property. The scientific community does not agree on the best approach to estimate the coefficient for transport in porous media (see subsection 2.2.1). A model is constructed to test whether it is possible to measure the diffusion coefficient experienced by sodium chloride in the sampled clays. If the outcome of this model suggests results within a reasonable timeframe, the modelled setup will be tested in the lab.

A setup with two containers containing respectively fresh and saltwater are connected by a tube. A clay sample can be placed in the middle of this tube (Figure 19a). This setup has been extensively described and used by Das and Parvesh (2016). By measuring the change in salinity in the two containers, the diffusion coefficient for the clay cylinder can be calculated. All variables are known, area, concentrations and time. A model has been created to investigate whether it is possible to measure the coefficient in the lab within a given time frame. Figure 19 shows the created model on the left and a close-up of the



(a) Full modelled system at  $t=0$



(b) Close up clay container at  $t=0$

Figure 19: Lab setup modelled

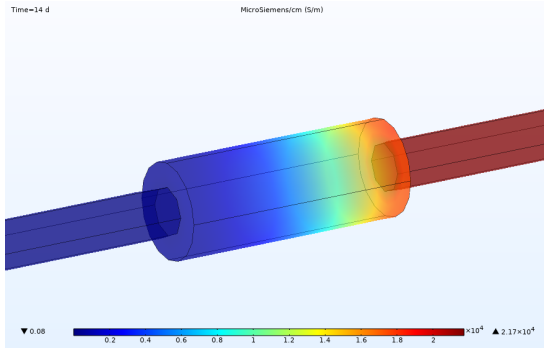
clay tube on the right. The setup is modelled in three dimensions to include the influence volume has on the dilution of NaCl in the water reservoirs.

Suppose this model proves that it is possible to measure a significant increase in the salinity of the freshwater container. In that case, this experiment can be done on actual clay samples from either Rotterdam, Rijswijk or Delft. Inputs, shown in Table 13 are chosen on the highest plausible dimension to observe any transfer of ions.

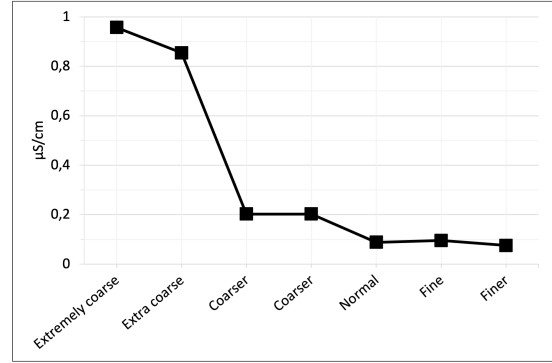
Table 11: Diffusion coefficient lab model dimensions

Input	Value	Unit	Source
$D_c$	$2e - 11$	$m^2/s$	Highest $D_c$ of NaCl in clay
Saline $C_{NaCl}$	1000	$mol/m^3$	Double salinity of North-sea
Fresh $C_{NaCl}$	0	$mol/m^3$	Demineralised water
Volume reservoirs	1, 5	l	Workable dimension
Length connecting tube	1	m	Per side / Allow room for setup
Clay container volume	4	ml	Standard tube / Radius = 0,5cm
Clay container length	5	cm	Standard tube
Total time	14	days	Experiment time

The most influential factors are the saline reservoir concentration and diffusion coefficient. The salinity of the reservoir is chosen to be twice the North-Sea salinity and a multiple of any observed salt concentration at WC1-depth (TNO GDN, 2022). The diffusion coefficient is a factor 50 higher than the  $D_c$  expected in subsection 4.1.7 and based on comparable experiments conducted by González (2007).



(a) Close up clay container at t=14d



(b) Mesh size sensitivity

Figure 20: Result and sensitivity

After running the experiment for 14 model days, the salinity increase in the fresh container was  $< 1\text{microS/cm}$ . This is below the threshold measurable by the conductivity probe. Demineralised water has a conductivity of 2 to 10  $\text{microS/cm}$ , making the increase immeasurable. The results are shown in Figure 20 visualise the inflow of ions into the clay sample.

This model can be used to test the influence of the mesh size. It might be that when increasing the mesh size, the result would show a reason to perform this test in the lab. Calculation times rose exponentially with an increase in mesh size. Figure 20b shows the modelled conductivity of the fresh container with an increase in mesh size. The result did not significantly improve after the 'coarser' mesh size. However, the calculation time increases exponentially towards mesh size 'finer'. After 70 days the measurable threshold of  $10\text{mS/cm}$  in the freshwater reservoir is reached. Based on the modelling results, the decision has been made not to perform the physical lab test as the runtime would be too high before the results would show.

## 4.2 Results

### 4.2.1 Base model results

The lab results show curves that prove once again that the environment is always more complex than any predictive model. As described in the methodology, the modelling target is to find a proper fit to the measured pore water salt concentration in the Rotterdam WC1 (Figure 14b). The boundary conditions and input summed up in Table 6 result in the plot shown in Figure 21, for clarity only five timesteps are visualised. On the right side of the figures the formations are labelled, being the Kreftenheye sandy aquifer (KH), the first Waalre clay aquitard (WC1) and the first Peize sand (PS1).

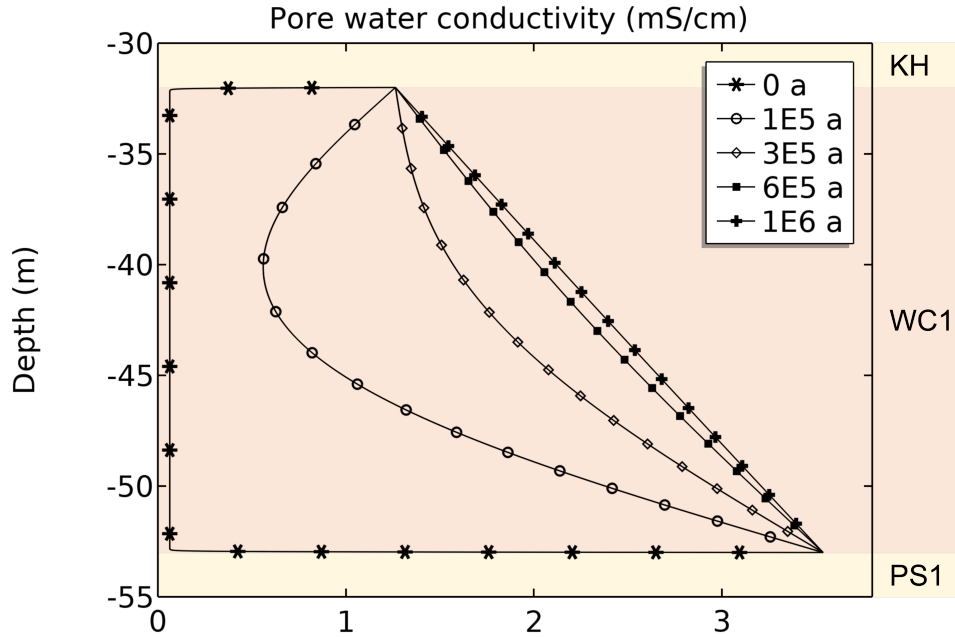


Figure 21: Model porewater conductivity | Total time 1My, showing five moments in time | Waalre clay 1 (WC1) aquitard between Kreftenheye (KH) and Peize Sand 1 (PS1) |  $D_c = 7.5E-12 \text{ m}^2/\text{s}$ , no advection, no sea level cycle

At  $t=0$ , the NaCl concentration in WC1 is lower than the concentration above and below the layer. With diffusion taking place, the clay is modelled to be intruded by NaCl ions from both sides. After less than 100ky, every part of the clay has been influenced by the NaCl above and below. Halfway through the model duration, after 600ky, a steady-state is almost reached, and the straight line indicates no more net concentration flux over depth.

### 4.2.2 Bottom salt concentration

The clay acts as a memory of past salinity by varying the bottom salt concentration. As the bottom salinity increases, the diffusion flux increases. This is because the  $\delta C$  in Equation 4.1 increases. When the bottom salinity drops again during an ice age, the

salinity of the clay pore-water is higher than that of the bottom aquifer. In that case, the direction of diffusion alters, and there is an ion flux away from the concentration peak.

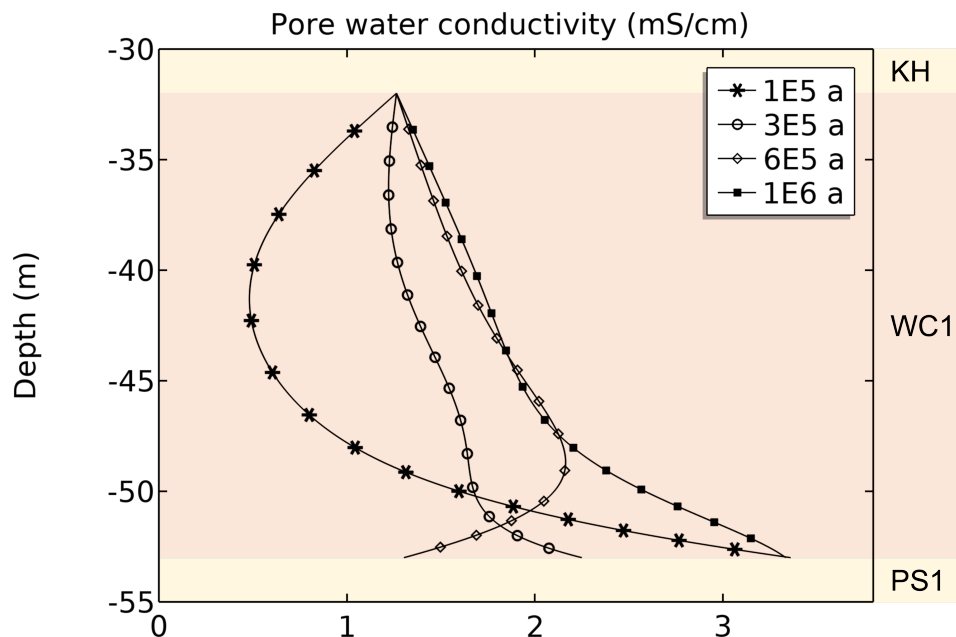


Figure 22: Model porewater conductivity | Total time 1My, showing four moments in time | Waalre clay 1 (WC1) aquitard between Kreftenheye (KH) and Peize Sand 1 (PS1) |  $D_c = 7.5E-12 \text{ m}^2/\text{s}$ , no advection, including sea level cycle from Table 7

Figure 22 is shown with a resolution of 4 timesteps illustrating the alternating high and low sea level and bottom salinity. The effect of this wave is best measurable in the bottom section and slowly diminishes towards the less saline top, which is more influenced by the fresher top aquifer. It clearly shows that the clay-'memory' shows a past peak, for instance, after 300ky. This can be useful when trying to find a fit for the WC1 Rotterdam results, especially combined with the other observed phenomena.

### 4.2.3 Vertical advection

Advection in a one-dimensional system can only influence the flow in the vertical direction; in this case, positive advection is in the upwards direction towards the surface. The advection modelled Figure 23 shows the upwards advection on the left and downwards on the right. The influence of both is significant compared to the base case (Figure 21)

In both cases, the steady-state is approached as the 100ky lines increasingly approach each other. The positive advection variant (Figure 23a) shows an apparent deviation from the base case, with the 300ky plot comparable to the base case steady state. The salinity of the bottom aquifer intrudes the clay almost halfway due to the advection. This is interesting when fitting the Rotterdam WC1 lab case as the bottom half of this clay layer appears to be as saline as the lower aquifer. Negative advection shows an apparent curve with a similar influence of the top aquifer on the salinity up to about half the modelled clay.

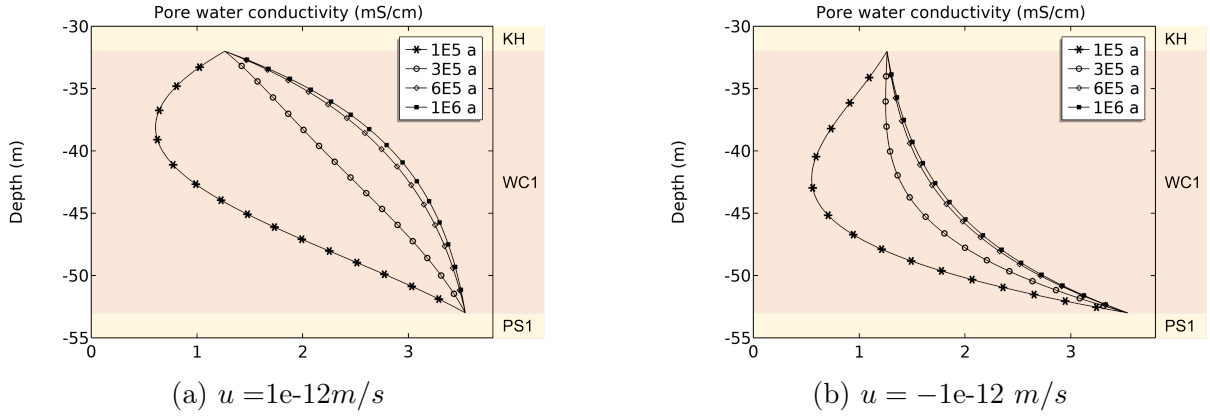


Figure 23: WC1 base model (Figure 21) + advection

#### 4.2.4 Diffusion coefficient

Figure 24 shows the base case and the influence of an increase or decrease in the value for diffusion. The standard coefficient is chosen as that of the base case being  $7,5e-12 \text{ m}^2/\text{s}$ . An increase of this  $D_c$ , visible in Figure 24a, results in a faster approach to the steady-state. On the contrary, a decrease in diffusion coefficient, especially in Figure 24b, results in a steady-state situation not being reached in 1Ma.

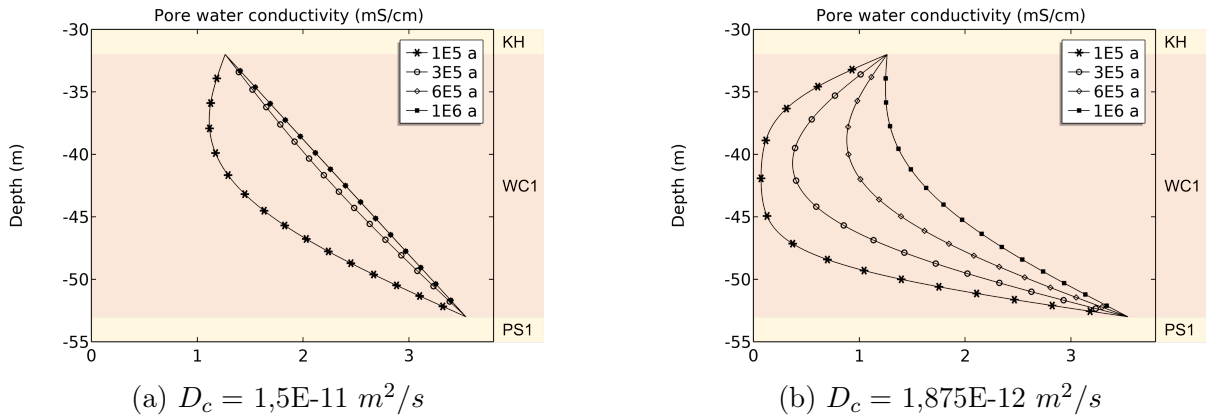


Figure 24: WC1 base model (Figure 21) with varying  $D_c$

The variations modelled and shown in Figure 24 are illustrating the effect of increasing and decreasing diffusion rates. The diffusion coefficient variations that are used in the scenario study are a  $1/2$  and  $1/10^{th}$  fraction of the diffusion coefficient determined based on helium diffusion (2.2.1 Diffusion).

#### 4.2.5 Scenario study

24 scenario's are modelled based the dimensions shown in Table 10. The results of every run are plotted in A Graphs. The following observations are made;

- The simulations that involve the sea-level cycle show the most dynamic results. This was to be expected as they feature three variables. Especially scenarios A, B, I, J,

Q and R show the 'clay-memory' described before. This indicates a part of the clay featuring a higher salinity than its top and the bottom. This can have two causes, either the original salt content of the clay was higher, or the past concentration boundary conditions have been higher. For all these scenarios, positive advection was modelled. This indicates that a changing bottom salinity and positive (upward) advection are mechanisms that work complementing.

- For the other scenarios involving a changing bottom salinity (C, D, K, L, S and T), this memory is not observable. These six scenarios feature either no advection or negative, downward advection. A cyclic pore water salinity and lack of or downward advection suppress each other's effect resulting in less influence. When comparing scenarios L and P, there is little difference in the conductivity curve even though scenario L is influenced by the salinity cycle.
- The influence of advection is more substantial and better observable when the  $D_c$  is lower. Scenario U, with a low  $D_c$  and a high upward advection, shows a uniform salt concentration throughout the WC1. Scenario E, same upward advection, higher  $D_c$  shows lower salinity towards the top due to diffusion into the top aquifer.
- Only in scenarios S and W, the original clay salinity of  $0,5 \text{ mol}/m^3$  is significant. These scenarios with meagre diffusion rates preserve original clay salinity, even after 1My of diffusion.

The relation between different variables is clear; the connection can be made to the laboratory fit. The scenarios that show the most similarity to the laboratory fit are Q and R, of which only R shows a great dip. Scenario R has been fitted to the laboratory measurements in Figure 25.

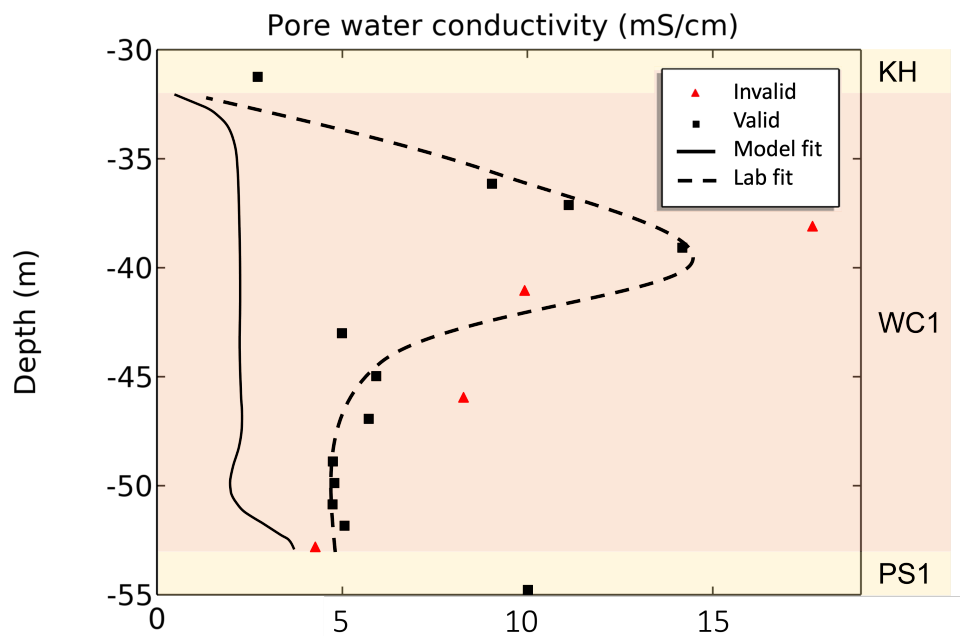


Figure 25: Laboratory conductivity measurements including fit compared to scenario R

Visible is the fact that nowhere in the clay the pore water salinity is high enough to reach the lab observed 15 mS/cm. The positive advection combined with the cyclic bottom

salinity curve results in the characteristic dip observed in the lab. Given the approach and known pore water salinity, it is impossible to recreate the laboratory observations with measured results. Adjusting the input of the model, not to based values but to achieve a fit, a more similar curve can be constructed. The result of that approach is a fit that shows more resemblance to the laboratory observations. The variables that achieve this fit are listed in Table 12.

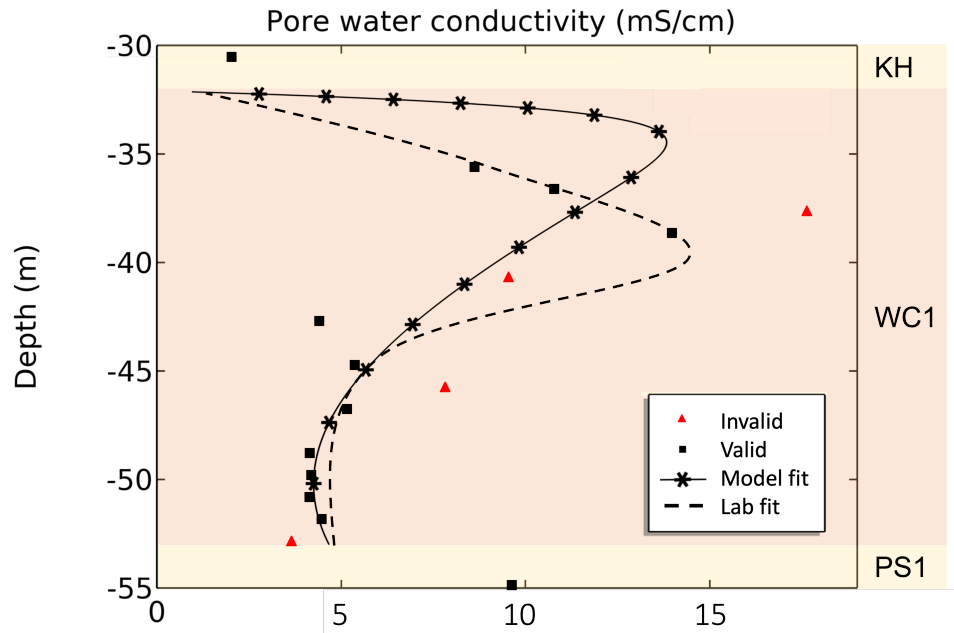


Figure 26: Laboratory conductivity measurements including fit compared to best fitting model

Table 12: Model dimensions that achieve best fit on laboratory measurements

Input	Value	Unit
Advection ( $u$ )	$2e-11$	$m^2/s$
PS1 $C_{NaCl}$ minimum	40	$mol/m^3$
PS1 $C_{NaCl}$ average	140	$mol/m^3$
PS1 $C_{NaCl}$ maximum	240	$mol/m^3$
$D_c$	1.5 – 11	$m^2/s$
phase	1.05	$Ma$

The way to achieve this better fitting is with salinity levels that are not measured, either above or below WC1. The fit is better in the bottom 10 meter than in the top.

#### 4.2.6 Model Results Interpretation

The combining laboratory and model results showed a model that hardly fit the measured results. The curve does show similarities to the laboratory results. The model can therefore expose the mechanisms underlying this curve. The simulated fit visualised in

Figure 26 outperformed the scenario study but would not have been constructed without it. The scenario study created a toolbox that allowed for pulling the right levers. The eventual fit shows how significant the influence of the salinity cycle is; there has not been any other variable found that was able to influence the curve similarly.

The model best fitting the laboratory data includes high aquifer salinity and positive advection. Based on this model advection is a contributing transporting mechanism together with diffusion.

## 5 Discussion

The main research objective was to find an ion gradient in the Peize-Waalre Formation that could prove the assumption of diffusion-dominant transport in poorly indurated Dutch clays. Based on the investigated clay layers ion gradients have been demonstrated. Especially the higher quality Rotterdam location proves to show several clay members with a higher ion concentration than its surrounding sand members. This higher clay ion concentration can be interpreted in three ways;

1. Its depositional salinity was higher than the current groundwater salinity and not all ions have been transported out of the clay.
2. The present groundwater salinity is lower than the clays salinity but over the course of the past million years the salinity of the groundwater has been higher, forcing ions into the clays via diffusion or advection. Remainder of this higher concentration is still visible in the clays while it has been lost in the sands, due to higher transport speeds through sands.
3. The cutting sampling method preserves porewater ions in clays better than in sands, resulting in a relatively higher ion concentration in clays than in sands.

A literature study partially based on (Knox et al., 2010) concluded that the depositional salinity was very low. Therefore the most probable interpretation is either past higher aquifer salinity or a measurement bias, both are discussed below.

### 5.1 Hydrogeology Analysis

The first half of this research focused on the porewater analysis of the Peize and Waalre Formation at three separate locations in the West-Netherlands.

#### 5.1.1 Continuity

For this research the assumption has been made that the clay layers are continuous and there is no communication between the sand bodies. It is known that in a fluvial depositional environment there is a possibility that the (channel sand) aquifers are connected (Slatt, 2013). The scale of continuity is crucial as, obviously, no formation is endless. The results in this research, partially from REGIS models and partially from cutting analysis, suggest that not every Waalre Clay layer is continuous between the sampling locations. The sampling locations are Delft, Rijswijk are about 10 kilometres apart. The measurements show a difference in salinity between sand bodies which is implausible when they communicate. The difference in thickness and number of Waalre and Peize bodies between the sampling locations does imply that the clay bodies cannot be assumed to be endless. The models provided by TNO as shown in Figure 9 suggest the first Waalre clay to terminate slightly north of the RCSG sampling location. This data suggests variable Peize sand formations inter-fingering with the Waalre clays without clear evidence that the separate observed clay members are part of the same strata. To be a proper natural analogue the conditions should be that the environment above and below the observed

clay is separated only by that particular clay. If the physical path from top to bottom of the clay exists in another form than through that clay, it cannot be a natural analogue. If the clay body is continuous for only a few kilometres the research timescale of one million years is too high. In such a case the advection speeds in the surround sand aquifers would transport NaCl around the clay member disqualifying it as a natural analogue.

To improve the knowledge on continuity of the Waalre clay the REGIS II V2.2 model that is part of the TNO Dinoloket allows for manual interpretation of member continuity. Borehole data is abundant in the west-Netherlands. The appearance of a certain layer in two separate boreholes, especially when they are in close proximity, suggest the continuity of that layer. It does however not guarantee that continuity which may lead to a faulty interpretation. A seismic study could be done to (dis)prove the continuity of the measured clays. Seismic imagery provides continuous data on a layers presence where models that are based on borehole data (such as REGIS II) interpolate between boreholes.

### 5.1.2 Location differences

The Rotterdam sampling location proved to be the most valuable due to the usage of suction drilling. In retrospect the Rijswijk location served as a pilot location to improve methods as the samples were too contaminated with drilling mud. The combination of using a soft-soil-drill, reverse circulation, and little to no drilling mud is important when cuttings are sampled. Especially the more sandy parts of formations were flushed substantially but how much has not been quantified in this research. Cutting gathering is a cheap and broadly applicable method to investigate subsurface conditions. If pore water measurements need to be done with high precision these can only be applied to intact clay lumps as other types of smaller cuttings tend to dilute or are contaminated by drilling mud. Jet drilling proved to be too destructive for cutting analysis. Jet drilling does come with more disadvantages, such as caving and transport delay, which leads to reverse (suction) drilling being the preferred method. It is advised to select sampling locations based on the drilling method and mud composition. If the mud contains too many ions, comparable to the Rijswijk location, it is unsuitable for laboratory conductivity analysis. It would, however, still be interesting to seek any natural tracers in these 'contaminated' samples. Portable XRF could be a method to do geochemical measurements to flushed cuttings. By using such devices tracer elements can be analysed as is proposed by (Ravansari et al., 2020).

It is unlikely that the concentration gradient is an anomaly that is caused by the sampling handling. Drilling, flushing, storing, preparing and measuring all influence a sample. Especially the flushing of the soils with drilling fluid can cause - and has caused - alterations in the sample salinity. This is the reason to exclude the Rijswijk drill site results from the main conclusion. It could be that the drilling mud has also influenced the other two locations. By sampling three locations and observing their differences, the decision has been made to model only the least disturbed. The problems with contamination experienced in Rijswijk enforce the conclusion that the Rotterdam samples are relatively clean. Another gradient origin can be depositional. The gradient, however, shows higher salinity in the clays implying that these have been deposited in a more saline environment than

it is today. Geological evidence does exclude this as their depositional environment has been proven to be fluvial.

### 5.1.3 Data acquisition

When aiming to gather information on porewater salinity cutting sampling is a method that comes with imperfections. When attempting to analyse pore water contents, especially of sands, cutting analyses are deemed less accurate than in-situ measurements. Cuttings are present wherever the subsurface is perforated compared to cores that always need special equipment to be taken. Squeezing of pore water outperforms cutting sampling in terms of accuracy as it has been successively improved and became the standard for obtaining porewater samples (Wersin et al., 2022). If cores are available, this is the preferred conductivity measuring approach. For future research, it is recommended only to analyse cuttings that have come to the surface so that the pore contents are unaltered. This is the case for the bigger clay lumps, but it is impossible for loose sands.

Cutting analyses is the preferred approach as a pre-study to justify future further investigation of a particular formation. This does not have to be the specific formations investigated in this research, as a natural analogue is the research target. The trade-off between quantity and quality is a hard one but this research has demonstrated that both are needed to understand a system's dynamics. Quantity came in the Rijswijk measurements but the quality proved to be too low to draw well-founded conclusions. The Rotterdam samples were of much higher quality but the WC1 could have been sampled more on a smaller interval to increase the certainty of the measurements. Coring subsequently squeezing of a targeted shallow poorly indurated clay would result in both the quality and quantity desired, albeit more expensive. When doing conventional coring, part or the excess soil comes up as drill cutting (AAPG Wiki, 2022). To quantify the accuracy of porewater cutting sampling analysis this could be a opportunity to compare these methods. By both squeezing the core-sample and analysing the same depth cuttings the error can be determined.

### 5.1.4 Laboratory observations

Lower water content is measured in laboratory sand samples then there is in measured in clay. This can partially be explained by the higher porosity of clay compared to sands. However, the influence of ex situ measurements is expected to be higher on sands than it is on clays. Uncompacted sands such as the Peize sands appear to loosen when dug up as their packing is disturbed. Even for the relatively small pressure experienced at 50 meters depth the sand is compacted, releasing this pressure and mixing increases the porosity (Mahmoodlu et al., 2016). This alters the ratio between solids and fluids. The porosity determined ex-situ has not been compared to the in-situ porosity. When the logs are available, it would be valuable to check whether porosity ratios are comparable. This would increase the value of cuttings. If there is a direct relationship between the in-situ and ex-situ measurements, that confirms the protocol followed in this research.

The laboratory porosity is higher than the soils shown in-situ as unconsolidated sands show porosity from .25 to .5 according to Yu et al. (1993). This can be explained by the disturbance the soil has experienced during drilling, transport, sieving and sampling. Clays can show porosity up to .7, but high numbers are found in only one measurement. The shallow depth of these sediments allows for some densification, but one cannot speak of proper compaction. It is unknown whether the porosity ratio between the different samples is present both in the lab and in-situ. If that is the case, the 10% rise in porosity between 80- and 90-meter depth could still indicate a deviation. The measured porosity could also be related to the sorting of the soil; better-sorted soil shows higher porosity as the gaps cannot be filled with other smaller particles.

The influence of organics on samples, their water content and salinity has not been investigated. All samples containing organics visually have been declared invalid for laboratory studies. Some have been tested and they all showed extremely high conductivities which would result in outliers that would not be of any contribution. Ponziani et al. (2011) describe the knowledge gap there is on the influence of organics on the electrical conductivity of porewater. The potential leaching of organic ions into porewater need further investigation to increase accuracy. This to prevent the (unknown) presence of organics result in incorrect interpretation of the conductivity measurements.

### **5.1.5 Data possibilities**

The hydraulic head between the Kreftenheye (KH) and Peize sand 1 (PS1) has been determined based on external data by TNO. This is the driver behind advection and crucial in further determining the ratio between diffusion and advection in the Peize and Waalre formations in transporting ions. Pressure (mud) logs provided by the drilling operators could contribute to this.

Most of the assumptions done on salinity, hydraulic head, meteoric influx and ground water levels are done based on a geologic timescale. However, current day water-management such as dikes, pumping stations, groundwater extraction and climate change alter this natural balance (Oude Essink et al., 2010). Further research should determine whether the current aquifer ion concentration is representative for the the past million years or that this balance has been disrupted by recent human intervention.

Drinking water companies measure the salinity of their aquifers to very high precision and regularity to determine where the fresh to brackish interface is located (FOSTER, 2022). The salinity these companies work with is generally lower than the salinity observed during this research. That does not exclude these aquifers and formations from being a potential natural analogue. Further research could, perhaps without gathering actual soil, gather data at these companies to see if there are aquifer-aquitard systems that might be of help. If so, this historical data could be analysed to investigate whether there are poorly indurated clays that could serve as a natural analogue.

### 5.1.6 Conductivity sample handling

The containers that hold the conductive fluid measured for all sampling locations were stand to leach for two days. After the planned measurements were taken the Rotterdam samples have been left to leach for another two months. These aged samples have been re-measured following the methodology used before. The ratio between the original - 2 day - conductivity and the aged - 2 month - conductivity is plotted in (Figure 27).

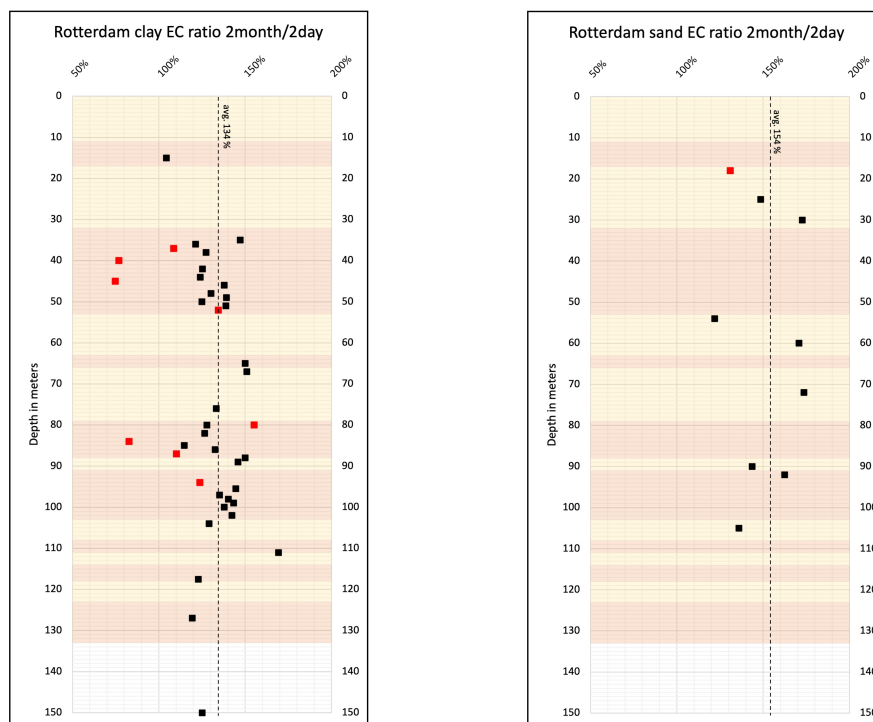


Figure 27: Rotterdam samples increase of conductivity over 2months time

What is striking is the increase of about 140% over this timespan. Supposed is that there is no significant influence on the result of this research as every sample has been treated the same way to prevent any discrepancies. An accepted explanation has not been found but a suggestions is the influence of temperature on the samples. Temperature and conductivity are strongly related and the temperatures - of the climate controlled lab - have not been noted. If the temperature influence proves not to be the origin of this discrepancy the influence of organics should be investigated Ponziani et al. (2011).

### 5.1.7 pXRF

Part of this research focused on the elements and minerals that were part of the total dissolved solids in the pore water. By measuring the dried samples using a portable X-ray Fluorescence device (*Niton XL5 plus*) these contents could be investigated over depth. The focus has been on *NaCl* which proved to be more conveniently measured using a conductivity probe. Other elements could however prove to be good tracer elements. Tracers described by Gimmi (2010) and Mazurek et al. (2009) can be found in Dutch

poorly indurated clays and can therefore contribute to natural analogue studies. Portable X-ray fluorescence is a well suited technique for cutting analysis. If uncontaminated cuttings can be measured, natural tracer elements that would otherwise go undetected can be measured. Further research could seek to find tracers in the Peize and Waalre clays or others. These tracers can help determining the elements specific diffusion coefficient through observed formation which can give insights in the retardation capacity of the clay. It should be considered that the limits of detection (LoD) of specific machines can vary significantly.

## 5.2 Hydrogeology Modelling

The empirical conductivity data does not fit the model directly. The curve does however show similarities to the laboratory results. This implied that the mechanisms underlying this curve could be exposed. The scenario study created a toolbox that allowed for pulling the right levers. The eventual fit showed how significant the influence of the salinity cycle is; there has not been any other variable found that was able to influence the curve similarly. No other variable could model the Rotterdam WC1 conductivity curve observed in the laboratory. The model best fitting the laboratory data includes high aquifer salinity and positive advection. Based on this model advection is a contributing transporting mechanism together with diffusion.

The variables that were used as input are chosen based on their expected influence. Especially the salinity cycle proved to be of high impact to the modelled clay layer. The laboratory results showed clay packages that were thinner than originally anticipated. The sampling resolution of one sample per meter therefore resulted in 20 samples for the WC1 and <10 for each underlying Waalre clay (WC2, WC3). The amount of observed, suitable curves was therefore restricted to one. If either the resolution is increased or the observed clay layers are thicker the certainty increases and the model could be verified by comparing different sites.

The model is a one dimensional single clay layer imitation of reality which is, self-evidently, a simplification. To fathom the dynamics of shallow poorly indurated Dutch clays the model could be expanded to be two- or three-dimensional. The one-dimensional model will be a starting point from where additions can be made after which they can be verified based on empirical research. When input values are not based on experimental data it is hard to verify the outcome of a model. To determine whether the response of the modelled environment is consistent with reality it is advised to complicate the model one property at the time. For this research three variables were investigated which broadened knowledge on their dynamics but did therefore contain a less exact quantification of each variable.

A solution not investigated in this research, may be in the heterogeneity of the first Waalre clay. For this research the simplifying assumption has been done that the entire clay is assigned with the same physical properties. However, it is possible, if not likely, that the properties vary over depth. If the bottom half of WC1 has a higher diffusion coefficient then the top half this could partially explain the conductivity curve. Differences

in advection cannot be modelled heterogeneously since the one dimensional model would not allow for only one single advection velocity. If the advection velocities would differ per layer the amount of water would increase in certain locations which is not possible. Every layer observed in this research has been assumed to be homogeneous. It would be interesting to see future research that models clay properties varied over depth. A coarsening upward or downward formation is common in geology and would significantly improve the model's accuracy.

The determine hydraulic head difference that causes advection is determined based on nearby measurements provided by TNO. The mud logs of the sampled drilling locations where not publicly available at the moment of this research. These mud logs can help determine the difference in pressure between different formations which is directly related to the hydraulic head.

The (physical) experiment discussed in 4.1.9 Lab-testing diffusion coefficient and sensitivity study was calculated to run for 70 days before conclusions could be drawn. It is advised to perform this test on several intact clay cuttings to accurately determine the diffusion coefficient for *NaCl* in Waalre clays. If this is proven empirically, that would significantly improve the model's validity.

### 5.3 Research Footprint

This research has been done while taking its footprint into consideration. Drilling, sampling and testing can have a big impact on the environment and it is important to try and minimise this within reason. Table 13 lists the materials used and steps taken to mitigate the consumption of this research.

Table 13: Material consumption and waste mitigation

Material	# used	Waste mitigation measures	Point of improvement
500ml Plastic jars	50	Rinsed and re-used	Share with follow-up researchers. Use glass jars
2L Freezer bags	200	-	Use glass jars
50ml Polypropylene lab containers	75	Rinsed and re-used. Recycled for non-academic purposes	-

## 6 Conclusions and Outlook

This research aimed to identify an ion concentration gradient in shallow, poorly indurated Dutch clays as a natural analogue for radionuclide transport. Based on an experimental analysis of the pore water content of drill cuttings, there can be concluded that such a gradient is observable and significant. Sampled locations show several clay layers with a pore-water conductivity gradient. The measured subsurface data and external information allowed for a model fitting the empirical data. The results of this model suggest that this gradient originates from adjacent aquifer salinity, the clays' physical properties and the difference in hydraulic head. The best-fitting model employs a high diffusion coefficient and positive (upward) advection of  $2e-11$  m/s or 0,6m/ky. The mechanics of this model are a heavily simplified simulation of the Waalre clays. Conclusions drawn based on this model are subject to the uncertainties experienced during the soil sampling. The modelled clays transport ions through diffusion and advection, implying that the transport method is not diffusion-dominated. The uncertainties in the sampling method do oblige further research before the Peize and Waalre clays transport mechanics can be understood.

The desired rock property for nuclear waste disposal is the ability to retard radionuclides and withhold them from the biosphere. Based on literature and laboratory results of this research, the Peize and Waalre formation is not sufficiently continuous. Due to the difference in depth and number of sand/clay alternations, this research cannot state the Peize and Waalre formation as representative of deeper, poorly indurated clays. This does not mean that research into these shallow transport mechanics does not contribute to understanding deeper poorly indurated clays.

### 6.1 Research Question

*Is there an ion concentration gradient in the Peize-Waalre Formation that confirms the assumption that transport of radionuclides in poorly indurated clays in the Netherlands takes place predominantly by diffusion?*

With reasonable certainty, there can be stated that there is an ion concentration gradient in the Peize-Waalre formation. Using this gradient to assume that transport of these ions occurs predominantly by diffusion is a step too far. However, modelling showed that a very low advection rate of cm/ky, either positive or negative, results in very distinctive salinity gradients. These gradients have not been observed in Rotterdam WC2 and WC3 as they show dome-shaped gradients. WC1 shows a unique curve that has been fitted by investigating several different scenarios. The most likely scenario this research found fitting the WC1 salinity curve is combined transport by diffusion and advection.

Suppose upward advection rates influence WC1; this clay formation can still be a natural analogue for poorly indurated clays in the Netherlands. While serving as a natural analogue, it can show the impact of advection on ion concentrations and the possible dilution that takes place while being transported. This is, however, something to be investigated in subsequent research.

## 6.2 Sub-questions

- *Is there an ion concentration gradient in the Peize-Waalre formation?*

There is a measurable gradient visible in both several clay layers measured in this research. These include the Rotterdam and Delft WC1 and the Rotterdam WC2 and WC3. This Rotterdam WC1 gradient does not have the typical bell curve observed. The Rotterdam WC2 and WC3 show a more typical curve, albeit of much lower intensity. The salinity difference in the deeper parts of the Waalre clays is lower, which results in a lower gradient.

- *Could an ion concentration gradient originate from another mechanism than transport processes?*

The observed gradient in the Rotterdam Waalre clay most probably originates from transport processes, diffusion and advection. The measurements show consistency, and there are no inexplicable outliers in the lab results. On top of that, the empirical results can be fit using a model that only employs transport mechanisms. The fluvial origin excludes high original pore-water salinity amplifying the conclusion that the ion gradient is based on transport processes.

- *Are there properties or characteristics that prevent the Peize-Waalre from being a natural analogue for the Paleogene clays?*

The salinity of the aquifers above and below the research first Waalre clay formation is not as constant as previously expected. Literature research shows a variation in meteoric influx, sea level and salinity. The continuity of the observed Peize clay formation cannot be proven. What is observed is the change in observed clay 'fingers' of the Waalre clay between different sampling locations. This change in number and thickness indicates a depositional environment that alternates locally. WC1 in Rotterdam and Delft significantly differ in size, and it might be possible that this is not the same continuous formation. If these plains are unconnected clay lobes, the sand aquifers are connected. This connection would complicate the model where the assumption has been made that the sands are unconnected. The concentration difference will be negligible when the top and bottom aquifers are connected. In such a case, the Peize-Waalre formations cannot be a natural analogue for the Paleogene clays.

- *Is it possible to model the measured ion profiles and apply that to poorly indurated clays in the Netherlands?*

It is possible to model ion profiles in poorly indurated Dutch clays. The three different properties investigated in this research, diffusion coefficient, advection rate and bottom aquifer salinity, all behaved as expected based on other research. The input values of the model were initially based on values observed in the field and

data acquired from literature; this did not result in a fit to the laboratory data. By alternating input to data to fit the laboratory observations, a potential history of WC1 was constructed.

### 6.3 Outlook

This study researched the possibility of the Peize and Waalre clay being a natural analogue for deeper, poorly indurated clays. Analysing cuttings and subsequently using that data to construct a model proved to be a tortuous track. Considering that this study is the first to look at these formations in this aspect, a highly simplified model was used. The limitations and consequences of this simplified model are described the discussion above, the recommendations done there are listed below;

- Seismic study to evaluate continuity of Waalre clays
- Select new sampling based on suction drilling method
- Compare cutting porewater to same depth squeezed core-sample porewater
- Check in-situ porosity logs to evaluate ex-situ porosity determination
- Determine influence of human water-management interference in aquifer system
- Check sample location borehole logs when available to compare in-situ measurements with ex-site laboratory data. Mud pressure logs could help determine pressure head differences between the Kreftenheye and Peize Sands, driving advection through the Waalre clays.
- Perform >2 month physical lab test described in 4.1.9 Lab-testing diffusion coefficient and sensitivity study
- Perform X-ray fluorescence measurements on cuttings to investigate tracer elements and determine their specific diffusion coefficient
- Acquire drinkwater companies salinity data to look for potential natural analogues
- Sample sieved drilling fluid to determine its salinity separate from the cuttings



## References

- AAPG Wiki. (2022). Conventional coring. [https://wiki.aapg.org/Conventional\\_coring](https://wiki.aapg.org/Conventional_coring)
- Abels, H. A., Van Simaey, S., Hilgen, F. J., De Man, E., & Vandenberghe, N. (2007). Obliquity-dominated glacio-eustatic sea level change in the early Oligocene: Evidence from the shallow marine siliciclastic Rupelian stratotype (Boom Formation, Belgium). *Terra Nova*, 19(1), 65–73. <https://doi.org/10.1111/j.1365-3121.2006.00716.x>
- Alexander, W. R., Reijonen, H. M., & McKinley, I. G. (2015). Natural analogues: studies of geological processes relevant to radioactive waste disposal in deep geological repositories. *Swiss Journal of Geosciences*, 108(1), 75–100. <https://doi.org/10.1007/s00015-015-0187-y>
- Bath, A., Ross, C., Entwisle, D., Cave, M., & Green, K. (1989). Hydrochemistry of porewaters from London Clay, Lower London Tertiaries and Chalk at the Bradwell Site, Essex. *British Geological Survey Report WE/89/26*.
- Bini, F., Pica, A., Marinozzi, A., & Marinozzi, F. (2019). A 3D Model of the Effect of Tortuosity and Constrictivity on the Diffusion in Mineralized Collagen Fibril. *Scientific Reports*, 9(1), 1–14. <https://doi.org/10.1038/s41598-019-39297-w>
- Canul-Macario, C., Salles, P., Hernández-Espriú, A., & Pacheco-Castro, R. (2020). Empirical relationships of groundwater head–salinity response to variations of sea level and vertical recharge in coastal confined karst aquifers. *Hydrogeology Journal*, 28(5), 1679–1694. <https://doi.org/10.1007/s10040-020-02151-9>
- Carslaw, H., & Jaeger, J. (1946). *Conduction of Heat in Solids* ISBN: 9780198533689.
- Castellazzi, P., Mercier, G., & Blais, J. F. (2012). Study of an amphoteric surfactant in a soil decontamination process using ANS enhanced fluorescence: Micellar behavior and dosing in synthetic and soil solutions. *Water, Air, and Soil Pollution*, 223(1), 337–349. <https://doi.org/10.1007/s11270-011-0862-1>
- Chou, H., Wu, L., Zeng, L., & Chang, A. (2012). Evaluation of solute diffusion tortuosity factor models for variously saturated soils. *Water Resources Research*, 48(10), 1–11. <https://doi.org/10.1029/2011WR011653>
- COMSOL. (2017). Diffusion Coefficient. <https://www.comsol.com/multiphysics/diffusion-coefficient>
- Croisé, J., Schlickenrieder, L., Marschall, P., Boisson, J. Y., Vogel, P., & Yamamoto, S. (2004). Hydrogeological investigations in a low permeability claystone formation: The Mont Terri Rock Laboratory. *Physics and Chemistry of the Earth*, 29(1), 3–15. <https://doi.org/10.1016/j.pce.2003.11.008>
- Das, P., & Parvesh, M. (2016). Salt Diffusion in Compacted Plastic Clay : Experimental and Theoretical. (July), 1–8.
- Department of Sustainable Natural Resources. (1990). Soil Survey Standard Test Method Soil Moisture Content. *Standards Association of Australia*, 1–5. <https://www.environment.nsw.gov.au/resources/soils/testmethods/mc.pdf>
- Engineering Toolbox. (2022). Water - Dynamic (absolute) and kinematic viscosity. [https://www.engineeringtoolbox.com/water-dynamic-kinematic-viscosity-d\\_596.html](https://www.engineeringtoolbox.com/water-dynamic-kinematic-viscosity-d_596.html)
- Faul, H. (2018). Geologic time scale ISBN: 9780444594259. *Bulletin of the geological society of america* (pp. 637–644). [https://doi.org/10.1130/0016-7606\(1960\)71\[637:GTS\]2.0.CO;2](https://doi.org/10.1130/0016-7606(1960)71[637:GTS]2.0.CO;2)
- FOSTER. (2022). Unieke glasvezeltechnologie zorgt voor fijnmazig betrouwbare metingen van de zoutconcentratie. <https://fosterproject.nl/resultaten/>
- Gimmi, T., & Waber, H. (2004). TECHNICAL REPORT 04-05. (December).
- Gimmi, T. (2010). Natural tracer profiles. (December).
- González, F. (2007). Water diffusion through compacted clays analyzed by neutron scattering and tracer experiments Fátima González Sánchez.
- Griffioen, J. (2015). The composition of deep groundwater in the Netherlands in relation to disposal of radioactive waste. *Opera-Pu-Tno-521-2*.
- Griffioen, J., Verweij, H., & Stuurman, R. (2016). The composition of groundwater in Palaeogene and older formations in the Netherlands. A synthesis. *Geologie en Mijnbouw/Netherlands Journal of Geosciences*, 95(3), 349–372. <https://doi.org/10.1017/njg.2016.19>
- Handbook of Chemistry & Physics. (2001). Standard KCl solutions for calibrating conductivity cells. *CRC Handbook of Chemistry & Physics-*, 2001–2001.

- Hasenpatt, R., Degen, W., & Kahr, G. (1989). Flow and diffusion in clays. *Applied Clay Science*, 4(2), 179–192. [https://doi.org/10.1016/0169-1317\(89\)90007-0](https://doi.org/10.1016/0169-1317(89)90007-0)
- Hummelman, J., Maljers, D., Menkovic, A., Reindersma, R., Vernes, R., & Stafleu, J. (2019). Totstandkomingsrapport Hydrogeologisch Model (REGIS II). *TNO Rapport 2019 R11654*, 95. [www.dinoloket.nl/regis-ii-het-hydrogeologische-model](http://www.dinoloket.nl/regis-ii-het-hydrogeologische-model)
- Hydreco. (2014). DAP Detailed Well Construction Design.
- Inspectie Leefomgeving en Transport. (2013). De kwaliteit van het drinkwater in Nederland in 2012, 1–17.
- Javadi, S., Ghavami, M., Zhao, Q., & Bate, B. (2017). Advection and retardation of non-polar contaminants in compacted clay barrier material with organoclay amendment. *Applied Clay Science*, 142, 30–39. <https://doi.org/10.1016/j.clay.2016.10.041>
- Knox, R., Bosch, J., Rasmussen, E.S., H.-C., C., M., Hiss, De Lugt, I., Kasiński, J., King, C., Köthe, A., Słodkowska, B., Standke, G., Vandenberghe, N., Doornenbal, J., & Stevenson, A. (2010). Petroleum Geological Atlas of the Southern Permian Basin Area, Chapter 12, 219.
- Leupin, O. X., Van Loon, L. R., Gimmi, T., Wersin, P., & Soler, J. M. (2017). Exploring diffusion and sorption processes at the Mont Terri rock laboratory (Switzerland): lessons learned from 20 years of field research. *Swiss Journal of Geosciences*, 110(1), 391–403. <https://doi.org/10.1007/s00015-016-0254-z>
- Mahmoodlu, M., Raof, A., Sweijen, T., & van Genuchten, M. T. (2016). Effects of Sand Compaction and Mixing on Pore Structure and the Unsaturated Soil Hydraulic Properties. *Vadose Zone Journal*, 15(8), vzj2015.10.0136. <https://doi.org/10.2136/vzj2015.10.0136>
- Mazurek, M., Alt-Epping, P., Bath, A., Gimmi, T., & Waber, H. (2009). Natural tracer profiles across argillaceous formations: The CLAYTRAC project. OECD/NEA Rep. 6253, OECD Nuclear Energy Agency, Paris, France. *Organisation for Economic Co-operation and Development*, (6253), 251. [www.oecdbookshop.org](http://www.oecdbookshop.org)
- Mazurek, M., Gautschi, A., Marschall, P., Vigneron, G., Lebon, P., & Delay, J. (2008). Transferability of geoscientific information from various sources (study sites, underground rock laboratories, natural analogues) to support safety cases for radioactive waste repositories in argillaceous formations. *Physics and Chemistry of the Earth*, 33(SUPPL. 1). <https://doi.org/10.1016/j.pce.2008.10.046>
- Millington, R. J., & Quirk, J. P. (1961). Permeability of porous solids. *Transactions of the Faraday Society*, 57, 1200–1207. <https://doi.org/10.1039/TF9615701200>
- NAWG. (2021). What are natural analogues? <https://www.natural-analogues.com/background/what-are-natural-analogues>
- Niedrist, G. H., Cañedo-Argüelles, M., & Cauvy-Fraunié, S. (2021). Salinization of Alpine rivers during winter months. *Environmental Science and Pollution Research*, 28(6), 7295–7306. <https://doi.org/10.1007/s11356-020-11077-4>
- Nimdeo, Y. M., Joshi, Y. M., & Muralidhar, K. (2014). Measurement of mass diffusivity using interferometry through sensitivity analysis. *Industrial and Engineering Chemistry Research*, 53(49), 19338–19350. <https://doi.org/10.1021/ie502601h>
- NOAA. (2016). Eustatic sea level curve for the last million years. [https://serc.carleton.edu/integrate/teaching\\_materials/coastlines/student\\_materials/907](https://serc.carleton.edu/integrate/teaching_materials/coastlines/student_materials/907)
- Oude Essink, G. H., Van Baaren, E. S., & De Louw, P. G. (2010). Effects of climate change on coastal groundwater systems: A modeling study in the Netherlands. *Water Resources Research*, 46(10), 1–16. <https://doi.org/10.1029/2009WR008719>
- Overeem, I., Veldkamp, A., Tebbens, L., & Kroonenberg, S. B. (2003). Modelling Holocene stratigraphy and depocentre migration of the Volga delta due to Caspian Sea-level change. *Sedimentary Geology*, 159(3-4), 159–175. [https://doi.org/10.1016/S0037-0738\(02\)00257-9](https://doi.org/10.1016/S0037-0738(02)00257-9)
- Pearson, F., Arcos, D., Bath, A., Boisson, J., Fernández, A., Gäbler, H., Gaucher, E., Gautschi, A., Griffault, L., Hernán, P., & Waber, H. (2003). *Mont Terri Project – Geochemistry of Water in the Opalinus Clay Formation at the Mont Terri Rock Laboratory ISBN 3931995984* (tech. rep. No. 12). Bundesamt für Wasser und Geologie, BWG.
- Philip, J. R. (1973). Dynamics of Fluids in Porous Media. *Journal of Fluid Mechanics*, 61(1), 206–208. <https://doi.org/10.1017/S0022112073210662>

- Phillips, F., & Castro, M. (2014). Groundwater Dating and Residence-Time Measurements ISBN: 9780080983004. *Treatise on geochemistry* (pp. 361–400). Elsevier. <https://doi.org/10.1016/B978-0-08-095975-7.00513-1>
- Ponziani, M., Slob, E., Ngan-Tillard, D., & Vanhala, H. (2011). Influence of water content on the electrical conductivity of peat. *International Water Technology Journal*, 1.
- Quante, M., & Colijin, F. (2016). North Sea Region Climate Assessment (NOSCCA) ISBN 9783319397436. <https://doi.org/10.1007/978-3-319-39745-0>
- Ravansari, R., Wilson, S. C., & Tighe, M. (2020). Portable X-ray fluorescence for environmental assessment of soils: Not just a point and shoot method. *Environment International*, 134 (November 2019), 105250. <https://doi.org/10.1016/j.envint.2019.105250>
- Rijsdijk, K. F., Passchier, S., Weerts, H. J., Laban, C., van Leeuwen, R. J., & Ebbing, J. H. (2005). Revised Upper Cenozoic stratigraphy of the Dutch sector of the North Sea Basin: Towards an integrated lithostratigraphic, seismostratigraphic and allostratigraphic approach. *Geologie en Mijnbouw/Netherlands Journal of Geosciences*, 84(2), 129–146. <https://doi.org/10.1017/S0016774600023015>
- Safetyatsea. (2008). Information about the North Sea Region. <https://web.archive.org/web/20081209095426/http://www.safetyatsea.se/index.php?section=northsea>
- Schultz van Haegen, M. (2017). Kamerbrief ANVS 2017/4927.
- Shackelford, C. D. (1991). Laboratory diffusion testing for waste disposal - A review. *Journal of Contaminant Hydrology*, 7(3), 177–217. [https://doi.org/10.1016/0169-7722\(91\)90028-Y](https://doi.org/10.1016/0169-7722(91)90028-Y)
- Slatt, R. M. (2013). Fluvial Deposits and Reservoirs ISBN: 978-0-444-56365-1. <https://doi.org/10.1016/B978-0-444-56365-1.00007-9>
- Smet Group. (2022). *Smet Group Technology Vertical borings* (tech. rep.).
- Somsen, O. J. G. (2015). VU Research Portal. *Journals.Sagepub.Com*, 47(3), 220–243. <https://doi.org/10.1177/0095399713509530>
- Stuyfzand, P. (1991). Sporenelementen in grondwater in Nederland - deel 1. *H20*, 1. <https://edepot.wur.nl/375349>
- ten Veen, J., de Bruin, G., & TNO Utrecht. (2013). De Eridanosdelta : een begraven wereld tot leven gewekt. *GEA*, (3), 68–71.
- Thomas, H. R., Sedighi, M., & Vardon, P. J. (2012). Diffusive Reactive Transport of Multicomponent Chemicals Under Coupled Thermal, Hydraulic, Chemical and Mechanical Conditions. *Geotechnical and Geological Engineering*, 30(4), 841–857. <https://doi.org/10.1007/s10706-012-9502-9>
- Tiab, D., & Donaldson, E. C. (2016). Introduction to Petroleum Geology. *Petrophysics* (pp. 23–66). Elsevier. <https://doi.org/10.1016/B978-0-12-803188-9.00002-4>
- TNO. (2019). Formatie naar ouderdom. <https://www.dinoloket.nl/stratigrafische-nomenclator/via-diagram/formatie-naar-ouderdom>
- TNO DINoloket. (2019). Kwaliteitstoetsingsdocument Hydrogeologisch Inhoudsopgave.
- TNO DINoloket. (2022). DINoloket. [www.dinoloket.nl/ondergrondmodellen](http://www.dinoloket.nl/ondergrondmodellen)
- TNO – GDN. (2021). Rupel Formatie. *Stratigrafische nomenclator van nederland* (6-12-2021). <http://www.dinoloket.nl/stratigrafische-nomenclator/rupel-formatie>
- TNO GDN. (2022). Grondwatertool, Geologische Dienst Nederland. <https://www.grondwatertools.nl/thema-grondwater-projecten/zoet-en-zout-grondwater>
- van der Molen, W., & van Ommen, H. (1985). Waterkwaliteit in Grondwater-stromingsstelsels. *Landbouwniversiteit Wageningen*.
- Vanýsek, P. (2012). Handbook of Chemistry and Physics: 93rd Edition; ISBN:9781439880494. *Electrochemical series* (p. 20). <http://books.google.com/books?id=-BzP7Rk17WkC&pg=SA5-PA80>
- Verhoef, E., Neeft, E., Bartol, J., Scholten, C., Buitenhuis, A., Van Der Veen, G., Vuorio, M., Chapman, N., & McCombie, C. (2020). Long-term research programme for disposal of radioactive waste (tech. rep. November). [www.covra.nl](http://www.covra.nl)
- Verhoef, E., Neeft, E., Chapman, N., & McCombie, C. (2017). COVRA: OPERA Safety Case. *COVRA publications*, (December), 1–147.
- Vis, G. J., Verweij, H., & Koenen, M. (2016). The Rupel Clay Member in the Netherlands: Towards a comprehensive understanding of its geometry and depositional environment. *Geologie en Mijn-*

- bouw/Netherlands Journal of Geosciences*, 95(3), 221–251. <https://doi.org/10.1017/njg.2016.25>
- Vis, G. J., & Verweij, J. (2014). Geological and geohydrological characterization of the Boom Clay and its overburden. *Technical report OPERA- PU- TNO411*, 91.
- Visser, P. W., Kooi, H., & Stuyfzand, P. J. (2015). The thermal impact of aquifer thermal energy storage (ATES) systems: a case study in the Netherlands, combining monitoring and modeling. *Hydrogeology Journal*, 23(3), 507–532. <https://doi.org/10.1007/s10040-014-1224-z>
- Vreedenburg, E., & van Zanten, Y. (1991). De gevolgen van de te zoute Rijn.
- Wersin, P., Mazurek, M., & Gimmi, T. (2022). Porewater chemistry of Opalinus Clay revisited: Findings from 25 years of data collection at the Mont Terri Rock Laboratory. *Applied Geochemistry*, 138(November 2021), 105234. <https://doi.org/10.1016/j.apgeochem.2022.105234>
- WKOtool. (2022). <https://wkotool.nl>
- Wong, T. E., De Jager, J., & Batjes, D. (2007). The geology of the Netherlands. ISBN 9789069844817. *Mededelingen Rijks Geologische Dienst*.
- Yu, C., Loureiro, C., Cheng, J. J., Jones, L. G., Wang, Y. Y., Chia, Y. P., & Faillace, E. (1993). Data Collection Handbook to Support Modeling Impacts of Radioactive Material In Soil. (April), 158. <https://doi.org/10.2172/10162250>

# A Graphs

This appendix shows the graphs that are produced either as porewater analysis result or as model output. Figure A.2 to Figure A.25 are the modelled scenario variations as described in Table 10. Their captions describe the variations modelled in the following order; Scenario, Diffusion coefficient ( $D_c$ ) in  $m^2/s$ , Advection (Adv) in  $m/s$ , sea level cycle, active or inactive, as described in subsection 4.2.2.

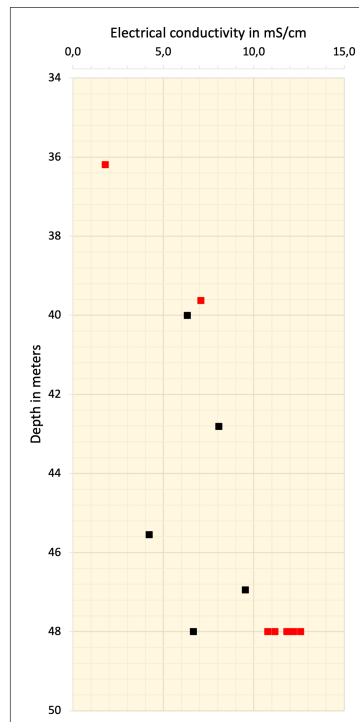


Figure A.1: Rijswijk conductivity with focus on first drilling session with tapwater as drilling fluid

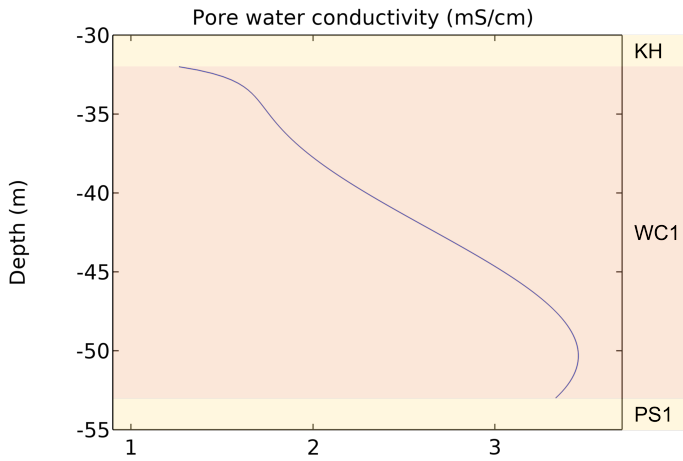


Figure A.2: Sc.A,  $D_c=7,5E-12 \text{ m}^2/s$ ,  $Adv= 1E-11 \text{ m/s}$ , sea level cycle = active

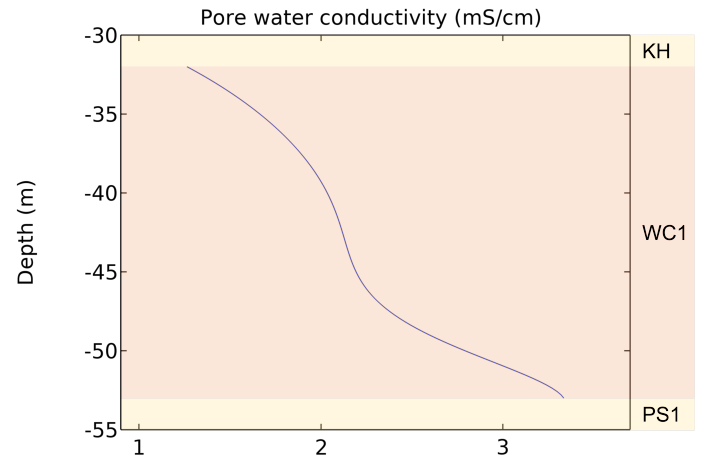


Figure A.3: Sc.B,  $D_c=7,5E-12 \text{ m}^2/s$ ,  $Adv=1E-12 \text{ m/s}$ , sea level cycle = active

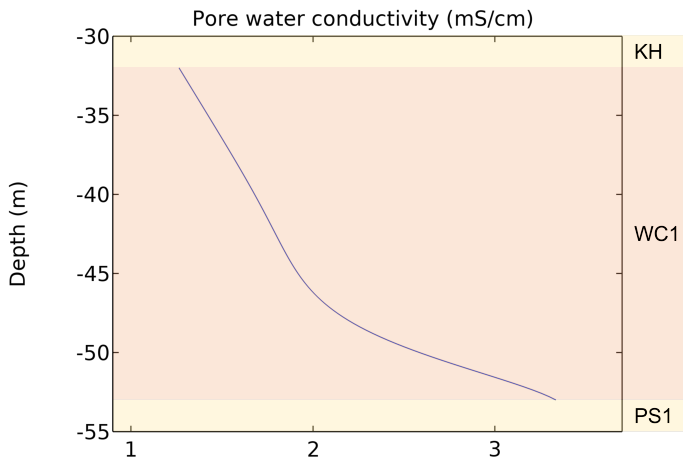


Figure A.4: Sc.C,  $D_c=7,5E-12 \text{ m}^2/s$ ,  $Adv=0 \text{ m/s}$ , sea level cycle = active

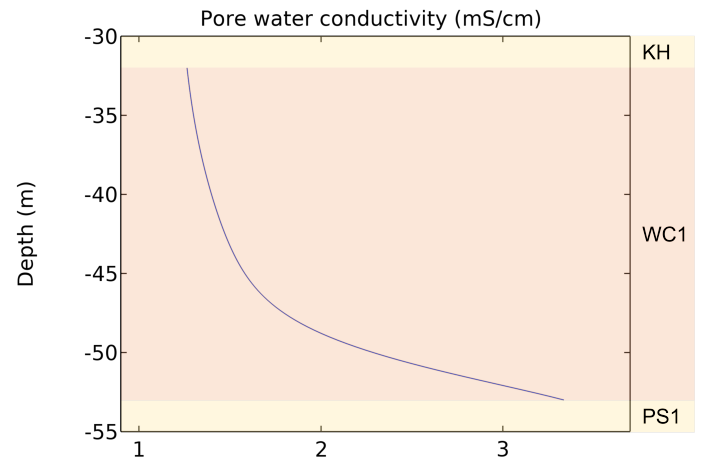


Figure A.5: Sc.D,  $D_c=7,5E-12 \text{ m}^2/s$ ,  $Adv=-1E-12 \text{ m/s}$ , sea level cycle = active

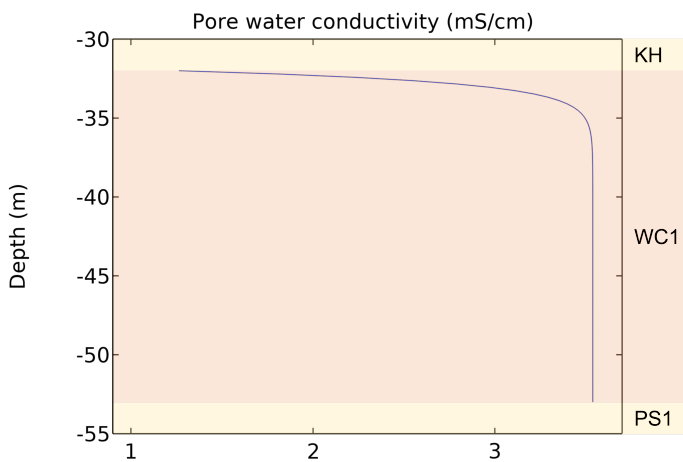


Figure A.6: Sc.E,  $D_c=7,5E-12 \text{ m}^2/s$ ,  $Adv=1E-11 \text{ m/s}$ , sea level cycle = inactive

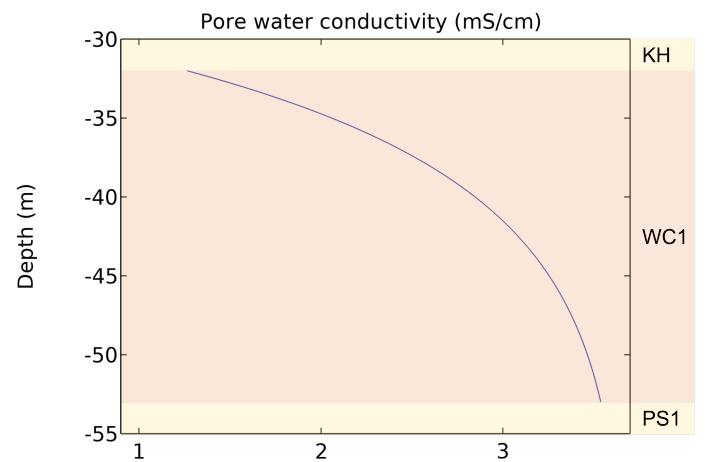


Figure A.7: Sc.F,  $D_c=7,5E-12 \text{ m}^2/s$ ,  $Adv=1E-12 \text{ m/s}$ , sea level cycle = inactive

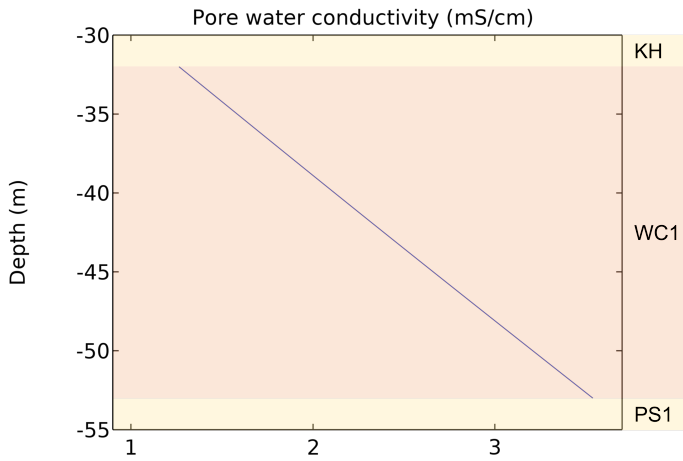


Figure A.8: Sc.G,  $D_c=7,5E-12 \text{ m}^2/s$ ,  $Adv=0 \text{ m/s}$ , sea level cycle = inactive

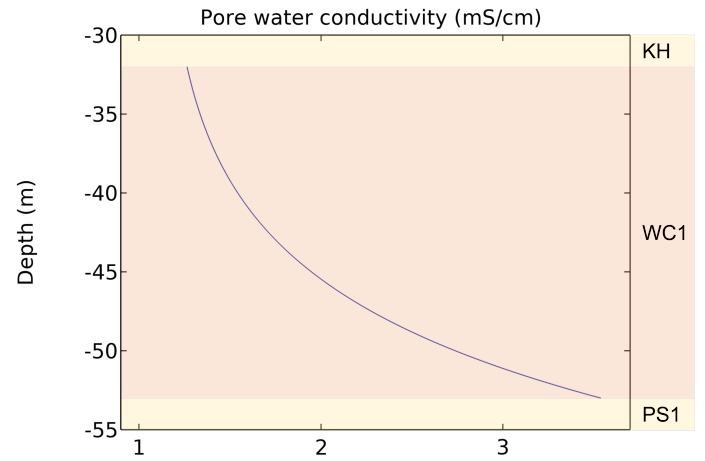


Figure A.9: Sc.H,  $D_c=7,5E-12 \text{ m}^2/s$ ,  $Adv=-1E-12 \text{ m/s}$ , sea level cycle = inactive

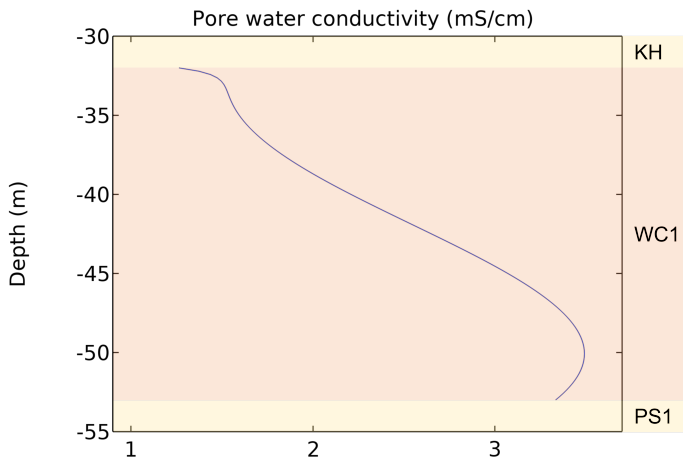


Figure A.10: Sc.I,  $D_c = 3,75E-12 \text{ m}^2/s$ ,  $Adv=1E-11 \text{ m/s}$ , sea level cycle = active

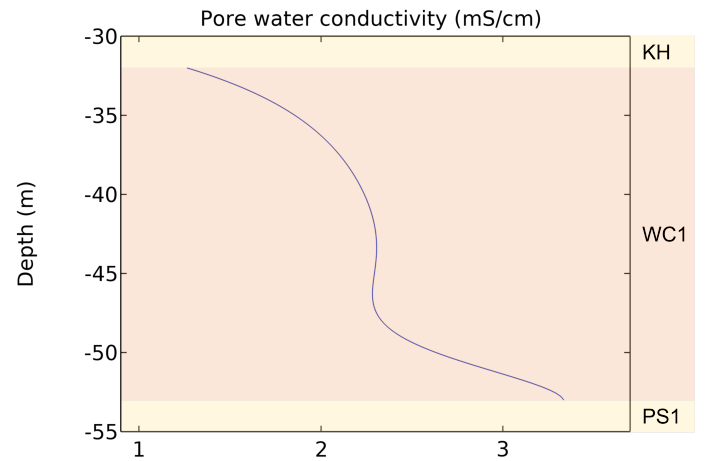


Figure A.11: Sc.J,  $D_c = 3,75E-12 \text{ m}^2/s$ ,  $Adv=1E-12 \text{ m/s}$ , sea level cycle = active

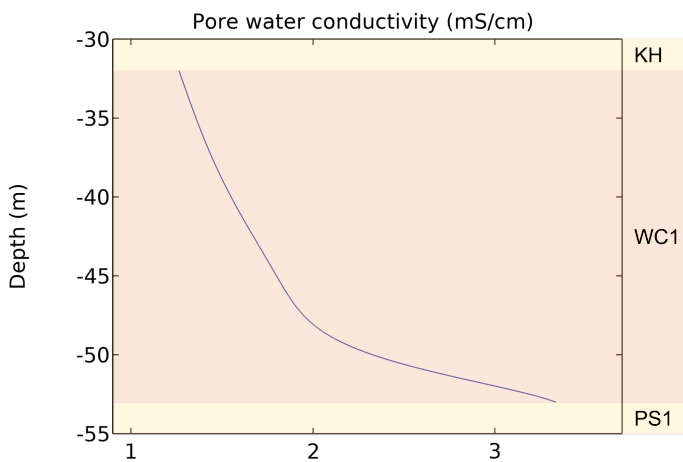


Figure A.12: Sc.K,  $D_c = 3,75E-12 \text{ m}^2/s$ ,  $Adv=0 \text{ m/s}$ , sea level cycle = active

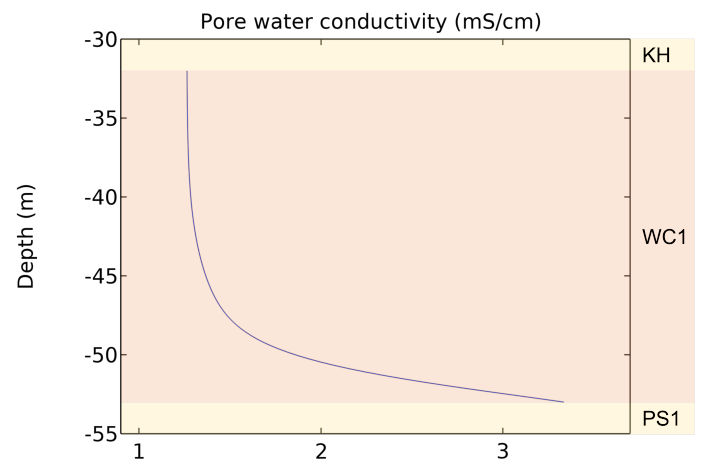


Figure A.13: Sc.L,  $D_c = 3,75E-12 \text{ m}^2/s$ ,  $Adv=-1E-12 \text{ m/s}$ , sea level cycle = active

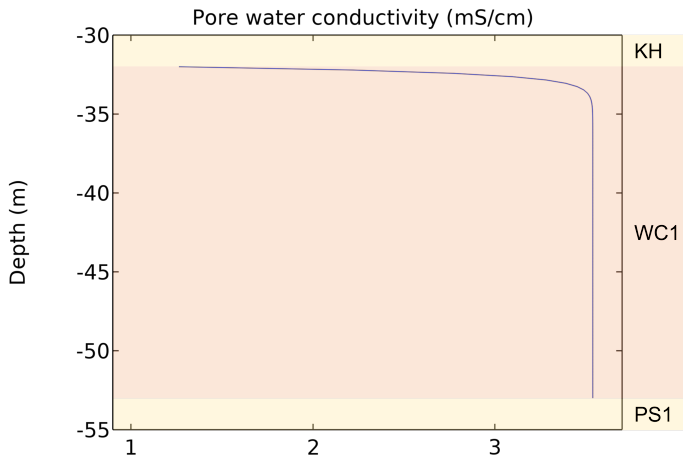


Figure A.14: Sc.M,  $D_c = 3,75E-12 \text{ m}^2/s$ ,  $Adv=1E-11 \text{ m/s}$ , sea level cycle = inactive

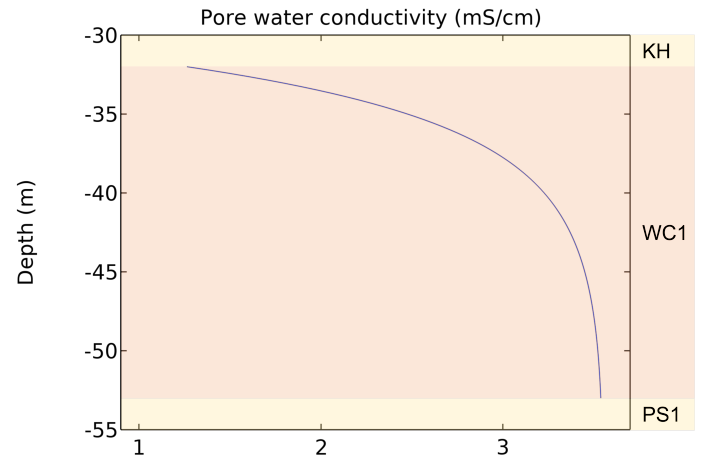


Figure A.15: Sc.N,  $D_c = 3,75E-12 \text{ m}^2/s$ ,  $Adv=1E-12 \text{ m/s}$ , sea level cycle = inactive

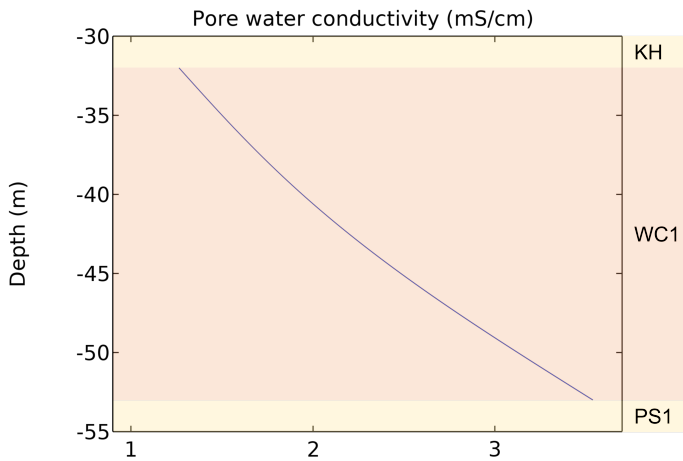


Figure A.16: Sc.O,  $D_c = 3,75E-12 \text{ m}^2/s$ ,  $Adv=0 \text{ m/s}$ , sea level cycle = inactive

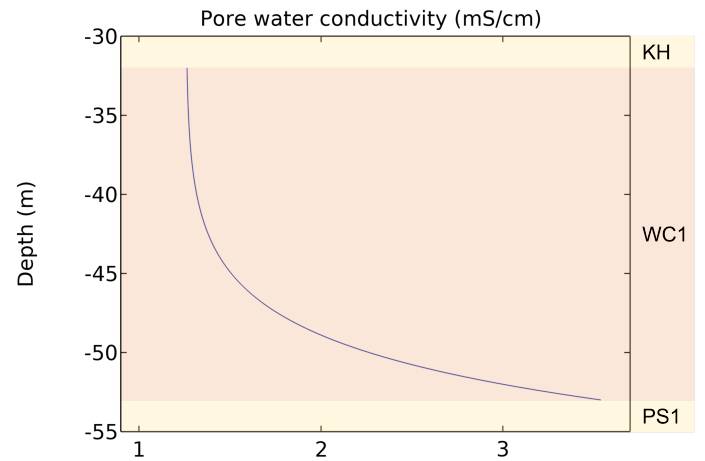


Figure A.17: Sc.P,  $D_c = 3,75E-12 \text{ m}^2/s$ ,  $Adv=-1E-12 \text{ m/s}$ , sea level cycle = inactive

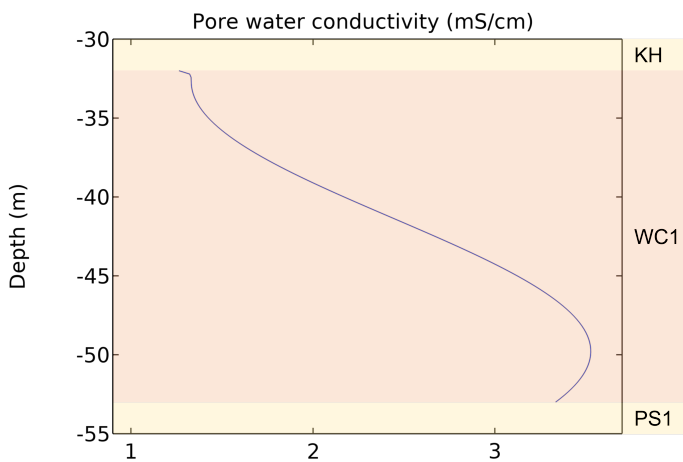


Figure A.18: Sc.Q,  $D_c = 7,5E-13 \text{ m}^2/s$ ,  $Adv=1E-11 \text{ m/s}$ , sea level cycle = active

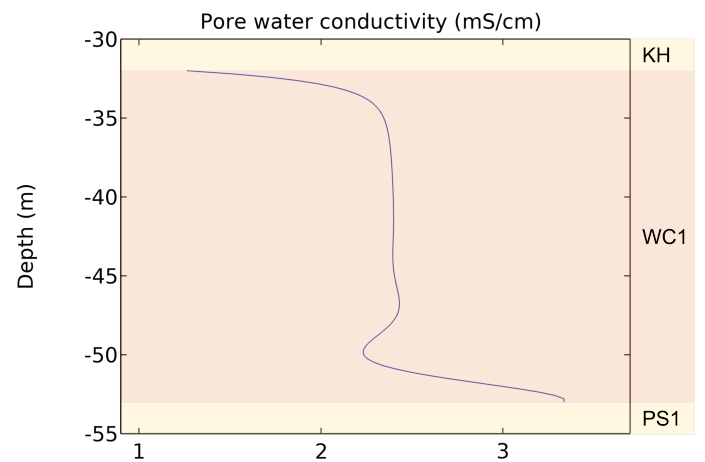


Figure A.19: Sc.R,  $D_c = 7,5E-13 \text{ m}^2/s$ ,  $Adv=1E-12 \text{ m/s}$ , sea level cycle = active

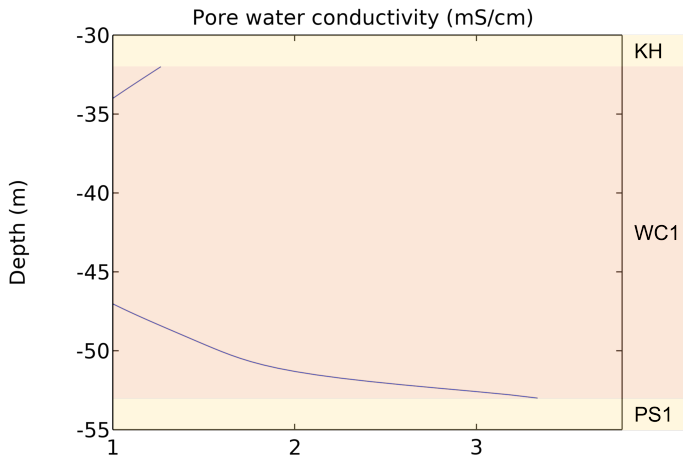


Figure A.20: Sc.S,  $D_c = 7,5E-13 \text{ m}^2/s$ ,  $Adv=0 \text{ m/s}$ , sea level cycle = active

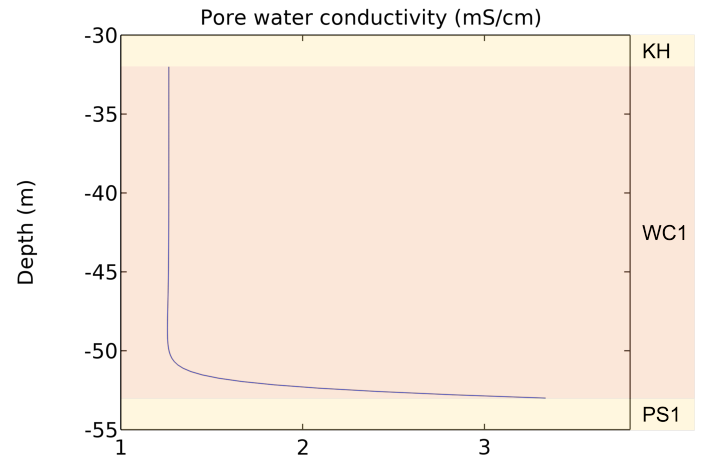


Figure A.21: Sc.T,  $D_c = 7,5E-13 \text{ m}^2/s$ ,  $Adv=-1E-12 \text{ m/s}$ , sea level cycle = active

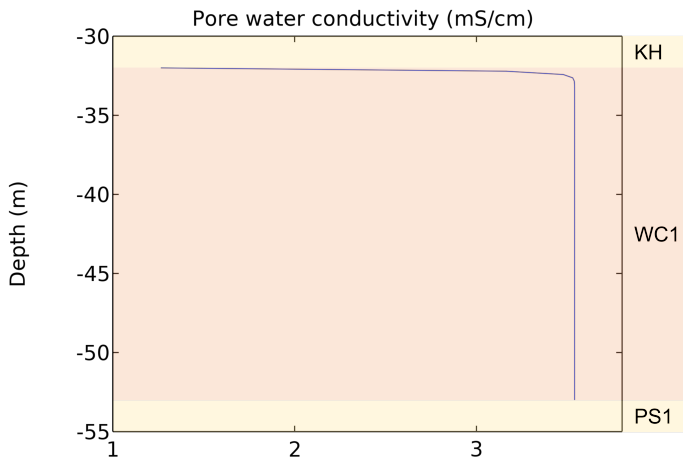


Figure A.22: Sc.U,  $D_c = 7,5E-13 \text{ m}^2/s$ ,  $Adv=1E-11 \text{ m/s}$ , sea level cycle = inactive

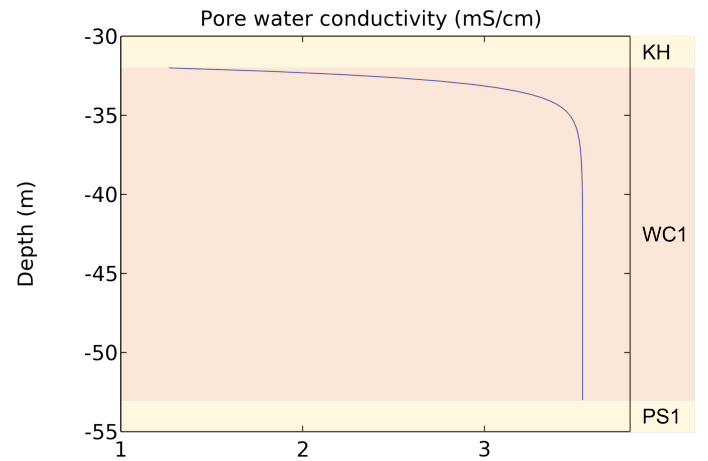


Figure A.23: Sc.V,  $D_c = 7,5E-13 \text{ m}^2/s$ ,  $Adv=1E-12 \text{ m/s}$ , sea level cycle = inactive

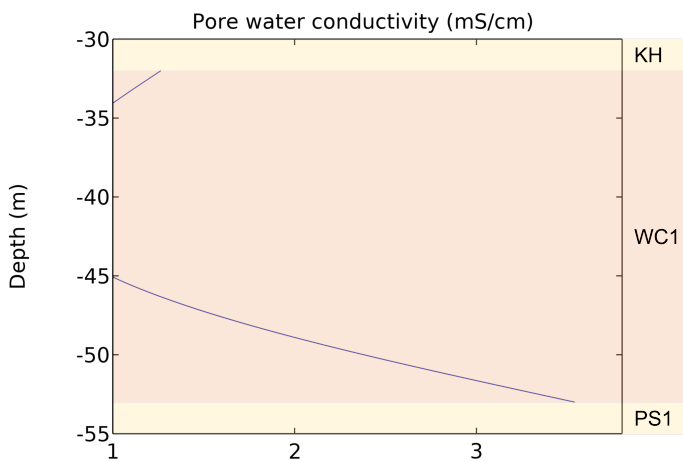


Figure A.24: Sc.W,  $D_c = 7,5E-13 \text{ m}^2/s$ ,  $Adv=0 \text{ m/s}$ , sea level cycle = inactive

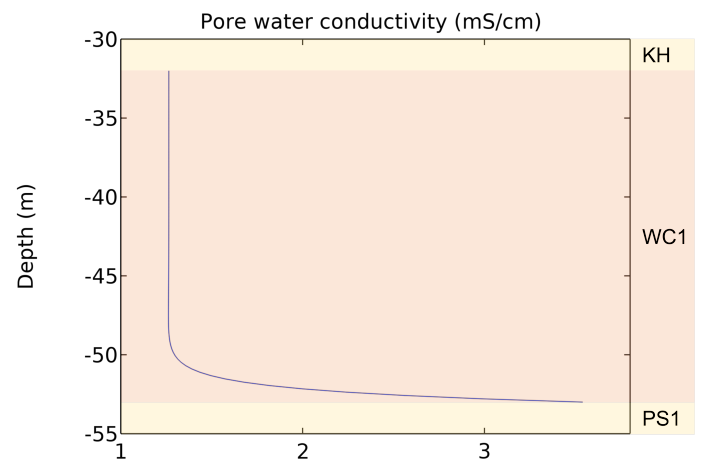


Figure A.25: Sc.X,  $D_c = 7,5E-13 \text{ m}^2/s$ ,  $Adv=-1E-12 \text{ m/s}$ , sea level cycle = inactive

## B Images

*All images shown in this appendix have been compressed to maintain a workable file size. If you are interested in the full resolution version please contact the author (b.t.m.vanesser@tudelft.nl).*



Figure B.1: RCSG facilities



Figure B.2: Push core used at the RCSG location



Figure B.3: Sample bin in Rotterdam showing big clay lumps

## C Data

This appendix shows laboratory porewater sample data.

Series	Sample #	depth in m	moment in oven	weight before	sample weight	weight after	weight water (g and ml)	weight clay (g)	volume clay (ml)	disk weight	water content (weight%)	water content / porosity (volume%)	ml pore water in dry 5g sample	Resistivity (kOhm/cm)	capillary resistivity (kOhm/cm) standard	EC (µS/cm) 1/5 (after 2 months)	EC undiluted (µS/cm)	Resistivity (mS/cm)	bulk resistivity kOhm/cm	brongdoort geleidend	NOTES	NOTES 2
B	B	0	26/Jan	12,4	11,3	11,2	1,1 10,2	3,8	1,1	10%	23%	0,56								0	bentonite	
B	B	0	05/Apr	7,4	6,3	6,8	0,6 5,7	2,2	1,1	10%	22%	0,53	1160	3,50						0		
DAPm	4344	44	05/Apr	16,9	15,9	14,0	2,9 13,0	4,9	1,1	18%	37%	1,12	17,8	3,00						1		
DAPm	1E+05	##	05/Apr	18,1	17,1	14,9	3,2 13,9	5,2	1,1	19%	38%	1,15	30,1	5,40						1		
DAPm	9596	96	05/Apr	16,6	15,6	13,6	3,0 12,6	4,7	1,1	19%	38%	1,18	29,8	4,90						1		
DAPm	4041	41	05/Apr	16,5	15,5	11,9	4,6 10,9	4,1	1,1	30%	53%	2,09	21,9	4,50						1		
DAPm	4142	42	05/Apr	32,0	31,0	22,9	9,1 21,8	8,2	1,1	30%	53%	2,10	24,5	4,00						1		
DAPm	4243	43	05/Apr	32,0	31,0	22,9	9,2 21,8	8,2	1,1	30%	53%	2,10	25,2	4,60						1		
DAPm	1415	15	05/Apr	14,3	13,3	9,6	4,7 8,6	3,2	1,1	35%	59%	2,74	25,4	8,00						1		
DAPm	N	61	07/Apr	36,6	34,9	28,4	8,3 26,6	10,0	1,8	24%	45%	1,55			1870	1,9				zand	1	
DAPm	M	56	07/Apr	29,4	27,6	24,1	5,3 22,3	8,4	1,8	19%	39%	1,19			1932	1,9				zand	1	overgedaan, ongewogen in oven
DAPm	L	51	07/Apr	41,4	39,7	32,5	9,0 30,7	11,6	1,8	23%	44%	1,46			2001	2,0				zand	1	overgedaan, ongewogen in oven
DAPm	O	66	07/Apr	34,7	33,0	26,7	8,1 24,9	9,4	1,8	24%	46%	1,62			2028	2,0				zand	1	
DAPm	E	37	07/Apr	35,7	34,6	28,6	7,1 27,5	10,4	1,1	20%	41%	1,29			2154	2,2				zand	1	grof zand
DAPm	C	26	07/Apr	28,0	27,0	22,2	5,9 21,1	8,0	1,1	22%	42%	1,39			2302	2,3				zand	1	sandy
DAPm	D	31	07/Apr	27,4	26,3	21,9	5,5 20,8	7,9	1,1	21%	41%	1,32			2350	2,4				zand	1	sandy
DAPm	B	21	07/Apr	23,3	22,2	18,8	4,5 17,7	6,7	1,1	20%	40%	1,28			2704	2,7				zand	1	sandy
DAPm	S	87	07/Apr	37,8	36,0	29,2	8,6 27,4	10,4	1,8	24%	45%	1,56			3361	3,4				zand	1	
DAPm	Q	77	07/Apr	37,0	35,3	29,6	7,4 27,9	10,5	1,8	21%	41%	1,33			3393	3,4				zand	1	
DAPm	T	91	07/Apr	43,0	41,3	33,7	9,3 32,0	12,1	1,8	23%	44%	1,46			3658	3,7				zand	1	
DAPm	R	82	07/Apr	34,0	32,3	26,2	7,8 24,4	9,2	1,8	24%	46%	1,61			3830	3,8				zand	1	
DAPm	W	##	07/Apr	36,2	34,4	28,3	7,9 26,5	10,0	1,8	23%	44%	1,48			3860	3,9				zand	1	
DAPm	P	72	07/Apr	33,8	32,1	26,8	7,0 25,1	9,5	1,8	22%	42%	1,39			3969	4,0				zand	1	
DAPm	U	96	07/Apr	37,1	35,3	28,7	8,3 27,0	10,2	1,8	24%	45%	1,54			4298	4,3				zand	1	
DAPm	A	15	07/Apr	33,9	32,8	21,5	12,4 20,5	7,7	1,1	38%	62%	3,03			4900	4,9				klei	0	organics
DAPm	V	##	07/Apr	40,8	39,0	29,9	10,8 28,2	10,6	1,8	28%	50%	1,92			5007	5,0				klei	1	
DAPm	J	44	07/Apr	38,8	37,0	31,6	7,2 29,9	11,3	1,8	19%	39%	1,20			5252	5,3				zand	1	overgedaan, ongewogen in oven

DAPm I	43	07/Apr	45,8	44,1	33,2	12,6	31,5	11,9	1,8	29%	52%	2,01	5852	5,9	klei	1	overgedaan, ongewogen in oven				
DAPm K	45	07/Apr	38,0	36,3	30,9	7,1	29,2	11,0	1,8	20%	39%	1,22	5953	6,0	zand	1	overgedaan, ongewogen in oven				
DAPm Y	##	07/Apr	43,5	41,8	34,3	9,2	32,6	12,3	1,8	22%	43%	1,41	6323	6,3	zand	1					
DAPm X	##	07/Apr	44,9	43,2	34,3	10,7	32,5	12,3	1,8	25%	46%	1,64	6496	6,5	zand	0	laten vallen, geschud, meting kan kloppen				
DAPm Z	##	07/Apr	29,3	27,6	23,7	5,6	21,9	8,3	1,8	20%	41%	1,29	7031	7,0	zand	1					
DAPm F	40	07/Apr	29,4	28,4	20,5	8,9	19,5	7,4	1,1	31%	55%	2,28	7596	7,6	klei	1	kleilig				
DAPm G	41	07/Apr	30,3	29,2	19,8	10,5	18,8	7,1	1,1	36%	60%	2,79	8430	8,4	klei	0	organics				
DAPm H	42	07/Apr	36,3	34,6	26,1	10,2	24,4	9,2	1,8	30%	53%	2,10	8783	8,8	klei	1					
MEENT 6737	84	08/Feb	23,3	22,3	18,7	4,6	17,6	6,7	1,1	21%	41%	1,31	2500	57530	57,5	klei	0	sand / ruikt chemisch	X24		
MEENT 6724	37	08/Feb	27,9	26,8	19,5	8,3	18,5	7,0	1,1	31%	54%	2,25	1380	14112	14,1	klei	0	zwarte klei (organisch) , of	X40		
MEENT 5607	##	08/Feb	31,4	30,4	24,0	7,4	22,9	8,7	1,1	24%	46%	1,62	1101	13622	13,6	klei	1	klei	X2		
MEENT 5619	94	08/Feb	36,2	35,2	27,3	9,0	26,2	9,9	1,1	25%	48%	1,71	1040	12295	12,3	klei	0	zwarte en grijze klei	X17		
MEENT 5608	##	08/Feb	22,3	21,3	17,4	4,9	16,3	6,2	1,1	23%	45%	1,51	955	13215	13,2	klei	1	klei	X7		
MEENT 5622	89	08/Feb	30,6	29,5	22,7	7,9	21,7	8,2	1,1	27%	49%	1,81	890	8427	8,4	11,00	38,87	klei	1		X19
MEENT 5610	##	08/Feb	16,9	15,8	13,9	3,0	12,8	4,8	1,1	19%	38%	1,16	880	11240	11,2	13,70	48,41	klei	1	klei	X11
MEENT 6732	88	08/Feb	38,8	37,8	29,3	9,5	28,3	10,7	1,1	25%	47%	1,68	870	8627	8,6			klei	1		X28
MEENT 6725	36	08/Feb	43,2	42,1	31,3	11,9	30,2	11,4	1,1	28%	51%	1,96	860	9021	9,0			klei	1		X48
MEENT 5609	##	08/Feb	28,8	27,7	21,7	7,1	20,6	7,8	1,1	26%	48%	1,72	853	10073	10,1			klei	1	klei	X1
MEENT 6731	87	08/Feb	23,2	22,1	17,2	5,9	16,2	6,1	1,1	27%	49%	1,83	848	10505	10,5			klei	0		X15
MEENT 4515	38	08/Feb	36,6	35,5	28,5	8,0	27,5	10,4	1,1	23%	44%	1,46	847	11393	11,4	6,40	22,61	klei	1		X37
MEENT 6736	82	08/Feb	23,8	22,7	17,3	6,5	16,2	6,1	1,1	29%	51%	2,00	844	8327	8,3	12,60	44,52	klei	1		X22
MEENT 6733	86	08/Feb	22,9	21,9	16,7	6,3	15,6	5,9	1,1	29%	51%	2,00	815	7685	7,7			klei	1		X26
MEENT 4520	15	08/Feb	29,1	28,1	18,1	11,0	17,0	6,4	1,1	39%	63%	3,24	813	6019	6,0	6,40	22,61	klei	1	zachte klei	X47
MEENT 6738	85	08/Feb	26,6	25,6	19,3	7,3	18,3	6,9	1,1	28%	51%	1,99	811	8889	8,9			klei	1		X25
MEENT 5621	90	08/Feb	29,7	28,7	21,6	8,1	20,6	7,8	1,1	28%	51%	1,97	810	7146	7,1	11,50	40,63	zand	1	zandige klei	X27
MEENT 5614	##	08/Feb	38,8	37,8	29,6	9,3	28,5	10,8	1,1	25%	46%	1,62	772	8627	8,6	16,60	58,65	klei	1		X16
MEENT 6726	35	08/Feb	38,1	37,0	28,6	9,5	27,5	10,4	1,1	26%	48%	1,73	756	7419	7,4			klei	1	nat en zandig	X38
MEENT 6735	80	08/Feb	41,8	40,8	30,2	11,7	29,1	11,0	1,1	29%	51%	2,00	752	7346	7,3			klei	1	zandige klei, erg nat, overq	X20
MEENT 5613	##	08/Feb	31,2	30,1	23,4	7,8	22,3	8,4	1,1	26%	48%	1,75	747	7489	7,5			klei	1		X8
MEENT 5615	99	08/Feb	29,0	28,0	21,9	7,1	20,8	7,9	1,1	26%	48%	1,71	731	7446	7,4			klei	1		X13
MEENT 5618	96	08/Feb	26,8	25,7	19,7	7,0	18,7	7,0	1,1	27%	50%	1,89	730	6693	6,7			klei	1		X12
MEENT 4516	40	08/Feb	24,8	23,7	16,4	8,4	15,4	5,8	1,1	35%	59%	2,73	680	8105	8,1			klei	0	organics	X35
MEENT 5616	98	08/Feb	23,3	22,2	18,0	5,3	17,0	6,4	1,1	24%	45%	1,55	666	7672	7,7			klei	1		X9
MEENT 5617	97	08/Feb	28,7	27,6	21,0	7,7	20,0	7,5	1,1	28%	50%	1,92	658	6348	6,3			klei	1		X14
MEENT 6728	18	08/Feb	33,6	32,6	19,5	14,1	18,5	7,0	1,1	43%	67%	3,81	630	3156	3,2			zand	0	plantenresten	X39
MEENT 6742	54	08/Feb	34,5	33,5	26,7	7,8	25,7	9,7	1,1	23%	45%	1,52	605	8168	8,2			zand	1		X33
MEENT 5612	##	08/Feb	29,7	28,7	22,4	7,3	21,3	8,0	1,1	26%	48%	1,72	594	6678	6,7			klei	1		X10

MEENT 6735	80	08/Feb	12,7	11,7	10,1	2,7	9,0	3,4	1,1	23%	44%	1,48	532	5787	5,8				klei	0	x20 = x21, harde korrel	X21
MEENT 4521	60	08/Feb	31,3	30,2	24,3	7,0	23,3	8,8	1,1	23%	44%	1,50	524	5106	5,1	10,70	37,81		zand	1	nat / zandig	X29
MEENT 5606	45	08/Feb	28,1	27,0	19,0	9,1	17,9	6,8	1,1	34%	57%	2,54	520	6828	6,8				klei	0	zwarte klei (organisch), m:	X4
MEENT 4522	67	08/Feb	42,6	41,5	32,1	10,5	31,0	11,7	1,1	25%	47%	1,69	510	4991	5,0				klei	1	natte klei	X43
MEENT 6723	65	08/Feb	40,1	39,1	30,3	9,8	29,3	11,1	1,1	25%	47%	1,67	450	4497	4,5				klei	1	fijn zand / zandige klei	X45
MEENT 6734	76	08/Feb	22,2	21,2	17,1	5,2	16,0	6,0	1,1	24%	46%	1,61	445	5188	5,2				klei	1	wet / discoloured	X23
MEENT 6727	72	08/Feb	33,7	32,6	27,2	6,4	26,2	9,9	1,1	20%	39%	1,23	394	4614	4,6				zand	1	zandig / niet nat	X30
MEENT 4519	46	08/Feb	37,4	36,3	29,7	7,7	28,6	10,8	1,1	21%	42%	1,35	360	4847	4,8	15,30	54,06		klei	1	zakje open	X42
MEENT 5620	92	08/Feb	22,9	21,9	18,6	4,4	17,5	6,6	1,1	20%	40%	1,25	338	4146	4,1				zand	1	zand	X18
MEENT 4518	44	08/Feb	28,7	27,7	23,2	5,5	22,1	8,4	1,1	20%	40%	1,25	310	5005	5,0				klei	1	mooie blauwgrijze klei	X36
MEENT 6739	48	08/Feb	38,4	37,4	30,3	8,1	29,2	11,0	1,1	22%	42%	1,39	297	4097	4,1				klei	1		X34
MEENT 4517	42	08/Feb	35,5	34,4	28,4	7,1	27,4	10,3	1,1	20%	41%	1,29	277	4290	4,3	12,80	45,23		klei	1		X44
MEENT 5604	51	08/Feb	34,2	33,2	28,5	5,7	27,5	10,4	1,1	17%	35%	1,04	250	4341	4,3	14,00	49,47		klei	1		X3
MEENT 6741	52	08/Feb	37,8	36,7	30,5	7,3	29,4	11,1	1,1	20%	40%	1,24	250	3735	3,7	13,00	45,93		klei	0	grote klont	X46
MEENT 6730	30	08/Feb	35,3	34,3	28,1	7,2	27,0	10,2	1,1	21%	41%	1,34	233	2527	2,5				zand	1	grof zand / nat	X41
MEENT 6740	50	08/Feb	41,3	40,2	33,9	7,4	32,8	12,4	1,1	18%	37%	1,13	231	4094	4,1				klei	1	mooie klei	X32
MEENT 6729	25	08/Feb	34,9	33,8	28,2	6,7	27,1	10,2	1,1	20%	39%	1,23	214	2924	2,9				zand	1	nat / grof zand	X31
MEENT 5605	49	08/Feb	17,9	16,9	15,3	2,6	14,3	5,4	1,1	16%	33%	0,93	213	4129	4,1				klei	1		X6
MEENT 5611	##	08/Feb	28,4	27,4	23,1	5,3	22,0	8,3	1,1	19%	39%	1,21	174	2644	2,6				zand	1	zand	X5
RW1 4510	43	14/Jan	9,4	8,4	5,8	3,6	4,7	1,8	1,1	43%	67%	3,84		8079	8,1					1		4510/1
RW1 b4	48	14/Jan	20,4	19,4	14,3	6,1	13,2	5,0	1,1	32%	55%	2,33	12196	12,2						0		b4/1
RW1 kern2	36	14/Jan	6,6	5,6	2,3	4,4	1,2	0,5	1,1	78%	91%	###			0,0					0		kern2/1
RW1 4514	48	14/Jan	37,2	36,2	24,6	12,6	23,5	8,9	1,1	35%	59%	2,69	6663	6,7						1		4514/1
RW1 4512	46	14/Jan	32,9	31,8	23,5	9,3	22,5	8,5	1,1	29%	52%	2,08	4215	4,2						1		4512/1
RW1 4505	37	14/Jan	95,1	94,1	30,6	64,5	29,5	11,1	1,1	69%	85%	###			0,0					0	geen EC, geen soil	4505/2
RW1 4508	40	14/Jan	7,7	6,6	4,2	3,4	3,2	1,2	1,1	52%	74%	5,41			0,0					1		4508/1
RW1 4509	40	14/Jan	7,8	6,7	3,9	3,9	2,8	1,1	1,1	58%	78%	6,79			0,0					1		4509/1
RW1 4506	38	14/Jan	12,1	11,1	5,6	6,5	4,6	1,7	1,1	59%	79%	7,12			0,0					0	geen EC, geen soil	4506/1
RW1 kern4	36	14/Jan	8,1	7,1	3,4	4,7	2,4	0,9	1,1	67%	84%	###			0,0					0		kern4/1
RW1 kern3	36	14/Jan	26,8	25,7	9,2	17,6	8,1	3,1	1,1	68%	85%	###			0,0					0		kern3/1
RW1 4505	37	14/Jan	15,7	14,7	5,1	10,6	4,0	1,5	1,1	73%	88%	###			0,0					0	geen EC, geen soil	4505/1
RW1 4504	37	14/Jan	14,9	13,8	4,1	10,8	3,1	1,2	1,1	78%	90%	###			0,0					0	geen EC, geen soil	4504/1
RW1 kern1	36	14/Jan	15,9	14,9	4,3	11,6	3,3	1,2	1,1	78%	90%	###			0,0					0		kern1/1
RW1 4503	36	14/Jan	13,2	12,2	4,7	8,5	3,7	1,4	1,1	70%	86%	###	1787	1,8						0		4503/1
RW1 4511	40	14/Jan	17,9	16,8	8,3	9,6	7,2	2,7	1,1	57%	78%	6,62	6325	6,3						1		4511/1
RW1 4507	40	14/Jan	11,5	10,5	5,8	5,7	4,8	1,8	1,1	54%	76%	5,90	7075	7,1						0	geen soil	4507/1
RW1 4513	47	14/Jan	25,9	24,9	15,4	10,5	14,3	5,4	1,1	42%	66%	3,67	9541	9,5						1		4513/1

RW1	b3	48	14/Jan	24,2	23,2	18,1	6,2	17,0	6,4	1,1	27%	49%	1,81	10780	10,8	0		b3/1	
RW1	b1	48	14/Jan	24,6	23,6	17,8	6,8	16,8	6,3	1,1	29%	52%	2,03	11183	11,2	0		b1/1	
RW1	b5	48	14/Jan	22,6	21,6	16,1	6,5	15,0	5,7	1,1	30%	54%	2,17	11841	11,8	0		b5/1	
RW1	b2	48	14/Jan	20,2	19,1	14,6	5,6	13,5	5,1	1,1	29%	52%	2,07	12594	12,6	0		b2/1	
RW2	80	80	26/Jan	25,4	24,3	19,6	5,7	18,6	7,0	1,1	24%	45%	1,54		0,0	1			
RW2	64	64	26/Jan	20,9	19,8	15,9	4,9	14,9	5,6	1,1	25%	47%	1,65		0,0	1		klei	
RW2	88	88	26/Jan	26,3	25,3	19,9	6,4	18,9	7,1	1,1	25%	47%	1,69		0,0	1			
RW2	82	82	26/Jan	16,4	15,4	12,5	3,9	11,4	4,3	1,1	26%	48%	1,72		0,0	1			
RW2	58	58	26/Jan	18,0	16,9	12,0	5,9	11,0	4,1	1,1	35%	59%	2,70		0,0	1		meer kleiig	
RW2	50	50	26/Jan	11,7	10,7	6,4	5,3	5,4	2,0	1,1	50%	72%	4,92		0,0	1			
RW2	98	98	26/Jan	22,1	21,0	18,3	3,7	17,3	6,5	1,1	18%	36%	1,08	56830	56,8	1		grof	
RW2	96	96	26/Jan	25,0	24,0	20,8	4,2	19,8	7,5	1,1	17%	36%	1,05	65174	65,2	1		grof	
RW2	68	68	26/Jan	14,2	13,2	9,0	5,3	7,9	3,0	1,1	40%	64%	3,33	80652	80,7	1		klei	
RW2	100	##	26/Jan	18,1	17,1	14,9	3,3	13,8	5,2	1,1	19%	38%	1,18	86630	86,6	0	organics	grof	
RW2	52	52	26/Jan	15,0	14,0	8,1	6,9	7,0	2,7	1,1	50%	72%	4,93	90791	90,8	1			
RW2	94	94	26/Jan	19,4	18,3	15,5	3,8	14,5	5,5	1,1	21%	41%	1,32	91985	92,0	1			
RW2	84	84	26/Jan	15,5	14,5	11,5	4,0	10,5	3,9	1,1	28%	50%	1,92	93062	93,1	1			
RW2	51	51	26/Jan	17,5	16,5	9,6	8,0	8,5	3,2	1,1	48%	71%	4,65	93295	93,3	1			
RW2	92	92	26/Jan	19,9	18,9	15,9	4,1	14,8	5,6	1,1	21%	42%	1,37	95022	95,0	1			
RW2	78	78	26/Jan	24,3	23,3	19,6	4,8	18,5	7,0	1,1	20%	41%	1,29	95991	96,0	1			
RW2	86	86	26/Jan	14,9	13,8	11,1	3,8	10,1	3,8	1,1	27%	50%	1,87	96614	96,6	1			
RW2	76	76	26/Jan	15,3	14,3	12,3	3,0	11,3	4,2	1,1	21%	41%	1,34	99881	99,9	1			
RW2	74	74	26/Jan	18,4	17,3	14,9	3,5	13,8	5,2	1,1	20%	40%	1,27	#####	###	1			
RW2	54	54	26/Jan	14,0	12,9	8,5	5,5	7,5	2,8	1,1	42%	66%	3,65	#####	###	1			
RW2	53	53	26/Jan	14,5	13,5	8,9	5,6	7,9	3,0	1,1	41%	65%	3,53	#####	###	1			
RW2	90	90	26/Jan	18,3	17,3	14,5	3,9	13,4	5,1	1,1	22%	43%	1,44	#####	###	1			
RW2	72	72	26/Jan	15,8	14,8	12,7	3,1	11,7	4,4	1,1	21%	41%	1,33	#####	###	1	kleiig als 58		
RW2	102	##	26/Jan	16,7	15,6	12,9	3,7	11,9	4,5	1,1	24%	45%	1,57	#####	###	1			
RW2	104	##	26/Jan	17,8	16,8	13,9	4,0	12,8	4,8	1,1	24%	45%	1,54	#####	###	1			
RW2	56	56	26/Jan	16,1	15,1	10,5	5,6	9,5	3,6	1,1	37%	61%	2,97	#####	###	1			
RW2	60	60	26/Jan	16,9	15,9	12,2	4,7	11,2	4,2	1,1	30%	53%	2,09	#####	###	1	klei		
RW2	66	66	26/Jan	14,0	13,0	10,7	3,3	9,7	3,6	1,1	26%	48%	1,72	#####	###	1	klei		
RW2	62	62	26/Jan	16,2	15,1	12,7	3,5	11,6	4,4	1,1	23%	44%	1,51	#####	###	1	klei		
RW2	88	88	05/Apr	17,8	16,8	14,4	3,4	13,3	5,0	1,1	20%	41%	1,29	3,6	2,60	#####	###	1	
RW2	50	50	05/Apr	13,2	12,2	8,4	4,8	7,3	2,8	1,1	40%	64%	3,31	2,7	5,60	#####	###	1	
RW2	64	64	05/Apr	17,4	16,4	13,8	3,6	12,8	4,8	1,1	22%	43%	1,41	#####	###	1			
RW2	58	58	05/Apr	14,8	13,8	10,6	4,2	9,5	3,6	1,1	31%	54%	2,21	3,5	6,50	#####	###	1	

RW3	180	##	26/Jan	48,8	47,8	38,4	10,4	37,3	14,1	1,1	22%	43%	1,40
RW3	110	##	26/Jan	27,2	26,1	19,4	7,8	18,4	6,9	1,1	30%	53%	2,11
RW3	150	##	26/Jan	36,0	35,0	28,2	7,8	27,2	10,3	1,1	22%	43%	1,43
RW3	120	##	26/Jan	29,6	28,6	22,4	7,2	21,4	8,1	1,1	25%	47%	1,67
RW3	140	##	26/Jan	31,2	30,2	24,6	6,6	23,6	8,9	1,1	22%	43%	1,40
RW3	130	##	26/Jan	26,1	25,1	19,8	6,3	18,7	7,1	1,1	25%	47%	1,69
RW3	170	##	26/Jan	36,6	35,6	29,0	7,7	27,9	10,5	1,1	22%	42%	1,37
RW3	160	##	26/Jan	39,1	38,1	29,8	9,4	28,7	10,8	1,1	25%	46%	1,63

##### ###  
##### ###  
##### ###  
##### ###  
##### ###  
##### ###  
##### ###  
##### ###

1  
0 smelly / plastics  
1  
1  
1  
1  
1  
1

## D Code

This appendix shows the code used to plot figures in this report.

```
1 import numpy as np
2 import matplotlib.pyplot as plot
3
4 A=14
5
6 # Get x values of the sine wave
7 time = np.arange(-1000, 0, 1);
8
9 # Amplitude of the sine wave is sine of a variable like time
10 amplitude = A*(1+np.sin(((2*np.pi*time)/110)+np.pi/2))
11
12 # Plot a sine wave using time and amplitude obtained for the sine wave
13 plot.plot(time, amplitude)
14
15 # Give a title for the sine wave plot
16 plot.title('Peize Sand 1 NaCl concentration')
17
18 # Give x axis label for the sine wave plot
19 plot.xlabel('kya')
20
21 # Give y axis label for the sine wave plot
22 plot.ylabel('mol/m3;$')
23
24 plot.grid(True, which='both')
25 plot.show()
```

Figure D.1: code to plot Figure 18

